

Enter Web Address: [Adv. Search](#) [Compare Arch](#)Searched for <http://www.ec-nantes.fr/>**78** ResultsNote some duplicates are not shown. [See all.](#)

* denotes when site was updated.

Search Results for Jan 01, 1996 - Dec 12, 2005

1996	1997	1998	1999	2000	2001	2002
1 pages	5 pages	3 pages	4 pages	10 pages	8 pages	8 pages
Dec 19, 1996 *	Feb 03, 1997 *	Feb 08, 1998 *	Feb 08, 1999 *	Feb 29, 2000 *	Feb 02, 2001	May 28, 2002 *
	Apr 12, 1997 *	Apr 15, 1998 *	Feb 18, 1999	Mar 03, 2000	Feb 04, 2001	Jun 01, 2002
	Jul 19, 1997	Jun 28, 1998 *	Apr 17, 1999 *	May 10, 2000	Mar 01, 2001	Jun 05, 2002
	Oct 11, 1997 *		Apr 24, 1999	May 11, 2000	Mar 02, 2001	Aug 02, 2002 *
	Dec 10, 1997 *			Jun 18, 2000 *	Apr 01, 2001	Sep 26, 2002
				Jun 19, 2000 *	Jul 11, 2001 *	Sep 27, 2002
				Oct 15, 2000 *	Jul 20, 2001	Oct 16, 2002
				Oct 19, 2000	Sep 22, 2001	Nov 25, 2002 *
				Nov 09, 2000		
				Dec 05, 2000 *		

[Home](#) | [Help](#)[Internet Archive](#) | [Terms of Use](#) | [Privacy Policy](#)



Enter Web Address: [Adv. Search](#)

Robots.txt Query Exclusion.

We're sorry, access to <http://www.ec-nantes.fr/Fr/> has been blocked by the site owner via robots.txt.

[Read more about robots.txt](#)

[See the site's robots.txt file.](#)

Try another request or [click here](#) to search for all pages on [ec-nantes.fr/Fr/](http://www.ec-nantes.fr/Fr/)

See the [FAQs](#) for more info and help, or [contact us](#).

[Home](#) | [Help](#)

[Internet Archive](#) | [Terms of Use](#) | [Privacy Policy](#)



Enter Web Address: [Adv. Search](#)

Robots.txt Query Exclusion.

We're sorry, access to <http://www.ec-nantes.fr/Fr/Recherche> has been blocked by the site owner via robots.txt.

[Read more about robots.txt](#)

[See the site's robots.txt file.](#)

Try another request or click here to search for all pages on [ec-nantes.fr/Fr/Recherche](http://www.ec-nantes.fr/Fr/Recherche)

See the [FAQs](#) for more info and help, or [contact](#) us.

[Home](#) | [Help](#)

[Internet Archive](#) | [Terms of Use](#) | [Privacy Policy](#)



Enter Web Address: [Adv. Search](#)

Robots.txt Query Exclusion.

We're sorry, access to <http://www.ec-nantes.fr/Fr/Recherche/DEE> has been blocked by the site owner via robots.txt.

[Read more about robots.txt](#)

[See the site's robots.txt file.](#)

Try another request or click here to search for all pages on [ec-nantes.fr/Fr/Recherche/DEE](http://www.ec-nantes.fr/Fr/Recherche/DEE)

See the [FAQs](#) for more info and help, or [contact](#) us.

[Home](#) | [Help](#)

[Internet Archive](#) | [Terms of Use](#) | [Privacy Policy](#)



Enter Web Address: [Adv. Search](#)

Robots.txt Query Exclusion.

We're sorry, access to <http://www.ec-nantes.fr/Fr/Recherche/DEE/Dah> has been blocked by the site owner via robots.txt.

[Read more about robots.txt](#)

[See the site's robots.txt file.](#)

Try another request or [click here](#) to search for all pages on [ec-nantes.fr/Fr/Recherche/DEE/Dah](http://www.ec-nantes.fr/Fr/Recherche/DEE/Dah)

See the [FAQs](#) for more info and help, or [contact](#) us.

[Home](#) | [Help](#)

[Internet Archive](#) | [Terms of Use](#) | [Privacy Policy](#)



Enter Web Address: [Adv. Search](#)

Robots.txt Query Exclusion.

We're sorry, access to <http://www.ec-nantes.fr/Fr/Recherche/DEE/Dah/urbcap.htm> has been blocked by the site owner via robots.txt.

[Read more about robots.txt](#)

[See the site's robots.txt file.](#)

Try another request or click here to search for all pages on [ec-nantes.fr/Fr/Recherche/DEE/Dah/urbcap.htm](http://www.ec-nantes.fr/Fr/Recherche/DEE/Dah/urbcap.htm)

See the [FAQs](#) for more info and help, or [contact](#) us.

[Home](#) | [Help](#)

[Internet Archive](#) | [Terms of Use](#) | [Privacy Policy](#)

Enter Web Address: [Adv. Search](#) [Compare Arch](#)Searched for <http://fodok.tuwien.ac.at/>**41** ResultsNote some duplicates are not shown. [See all.](#)

* denotes when site was updated.

Search Results for Jan 01, 1996 - Dec 12, 2005

1996	1997	1998	1999	2000	2001	2002	2003
0 pages	0 pages	1 pages	3 pages	2 pages	9 pages	5 pages	14 pages
		Dec 12, 1998 *	Jan 25, 1999	Oct 25, 2000 *	Feb 05, 2001 *	Jan 21, 2002	Jan 26, 2003 * Feb 05, 2003
			Feb 08, 1999 *	Dec 01, 2000 *	Mar 01, 2001 *	Aug 02, 2002	Mar 20, 2003 Mar 25, 2003
			Feb 24, 1999		Mar 02, 2001	Sep 22, 2002	Mar 25, 2003 Apr 26, 2003
					Apr 05, 2001 *	Oct 16, 2002 *	Apr 26, 2003 May 22, 2003
					Apr 18, 2001	Nov 28, 2002 *	May 22, 2003 Jun 19, 2003
					May 16, 2001 *		Jun 19, 2003 Jul 30, 2003
					Jul 22, 2001		Jul 30, 2003 Aug 08, 2003
					Sep 27, 2001 *		Aug 08, 2003 Sep 21, 2003
					Nov 28, 2001		Sep 21, 2003 Oct 09, 2003
							Oct 09, 2003 Oct 17, 2003
							Oct 17, 2003 Nov 23, 2003
							Nov 23, 2003 Dec 15, 2003
							Dec 15, 2003 Dec 25, 2003

[Home](#) | [Help](#)[Internet Archive](#) | [Terms of Use](#) | [Privacy Policy](#)



Enter Web Address:

[Adv. Search](#)

0 pages found for <http://fodok.tuwien.ac.at/online-bin/>

Sorry, no matches.

Keep in mind...

- **There is no text search.** Enter a web address in the box above.
- Click here to search for all pages on fodok.tuwien.ac.at/
- [See the FAQs](#) for more info and help, or [contact us](#).

[Home](#) | [Help](#)

[Internet Archive](#) | [Terms of Use](#) | [Privacy Policy](#)



Enter Web Address: [Adv. Search](#)

0 pages found for <http://fodok.tuwien.ac.at/online-bin/run?function=document&id=E360-04-09>

Sorry, no matches.

Keep in mind...

- **There is no text search.** Enter a web address in the box above.
- Click here to search for all pages on fodok.tuwien.ac.at/
- [See the FAQs](#) for more info and help, or [contact us](#).

[Home](#) | [Help](#)

[Internet Archive](#) | [Terms of Use](#) | [Privacy Policy](#)

Enter Web Address: [Adv. Search](#) [Compare Arch](#)Searched for http://www.mitre.org/work/best_papers/best_papers_01/**5 Results**

* denotes when site was updated.

Search Results for Jan 01, 1996 - Dec 12, 2005

1996	1997	1998	1999	2000	2001	2002	2003	2004	2005
0 pages	0 pages	0 pages	0 pages	0 pages	0 pages	0 pages	1 pages	4 pages	0 pages
							Oct 03, 2003 *	May 17, 2004 *	
								Jun 18, 2004 *	
								Oct 22, 2004	
								Nov 25, 2004	

[Home](#) | [Help](#)[Internet Archive](#) | [Terms of Use](#) | [Privacy Policy](#)

Enter Web Address: [Adv. Search](#)

0 pages found for http://www.mitre.org/work/best_papers/best_papers_01/calpin_paradigm/

Sorry, no matches.

Keep in mind...

- **There is no text search.** Enter a web address in the box above.
- Click here to search for all pages on [mitre.org/](http://www.mitre.org/)
- See the [FAQs](#) for more info and help, or [contact us](#).

[Home](#) | [Help](#)

[Internet Archive](#) | [Terms of Use](#) | [Privacy Policy](#)



Enter Web Address: [Adv. Search](#)

0 pages found for

http://www.mitre.org/work/best_papers/best_papers_01/calpin_paradigm/calpin_paradigm.pdf

Sorry, no matches.

Keep in mind...

- **There is no text search.** Enter a web address in the box above.
- Click here to search for all pages on [mitre.org/](http://www.mitre.org/)
- [See the FAQs](#) for more info and help, or [contact us](#).

[Home](#) | [Help](#)

[Internet Archive](#) | [Terms of Use](#) | [Privacy Policy](#)

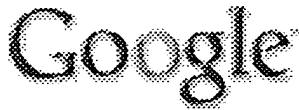
Enter Web Address: [Adv. Search](#)Searched for <http://ai.eecs.umich.edu/people/laird/papers/ML99-2.pdf>**1 Results**

* denotes when site was updated.

Search Results for Jan 01, 1996 - Dec 12, 2005

1996	1997	1998	1999	2000	2001	2002	2003	2004	2005
0 pages	0 pages	0 pages	0 pages	0 pages	0 pages	0 pages	1 pages	0 pages	0 pages
							Apr 12, 2003 *		

[Home](#) | [Help](#)[Internet Archive](#) | [Terms of Use](#) | [Privacy Policy](#)

[Sign in](#)
[Web](#)
[Images](#)
[Groups](#)
[News](#)
[Froogle](#)
[Local](#)
[New!](#)
[more »](#)

+"~simulation ~domain" +"~simulation ~task" +

Search

[Advanced Search](#)
[Preferences](#)

Web Results 1 - 10 of about 62 for +"~simulation ~domain" +"~simulation ~task" +~aspect +~matching. (0

[PDF] [Learning by Observation in a Tactical Air Combat Domain](#)

File Format: PDF/Adobe Acrobat - [View as HTML](#)

aspects of behavioral cloning is its effectiveness in a complex domain. ...
simulation domain similar to the domains used in behavioral cloning and ...
 ai.eecs.umich.edu/people/laird/papers/ML99-2.pdf - [Similar pages](#)

[PDF] [XUEQIN HUANG XML-Based Messaging in the JSIM Simulation ...](#)

File Format: PDF/Adobe Acrobat - [View as HTML](#)

the reuse and interoperability problems in the **simulation domain**. ... more challenging
simulation task, such as the design of a spacecraft, would require ...
 chief.cs.uga.edu/~jam/home/theses/huang_thesis/writeup/xhuangms.pdf - [Similar pages](#)

[DOC] [ACKNOWLEDGEMENTS](#)

File Format: Microsoft Word - [View as HTML](#)

A far more challenging **simulation task**, such as the design of a spacecraft, would
 require even ... <xsl:template **match**="/message/agentInfo/replicationSize"> ...
 chief.cs.uga.edu/~jam/home/theses/huang_thesis/writeup/xhuangms.doc - [Similar pages](#)

[PDF] [Center for the Simulation of Accidental Fires & Explosions](#)

File Format: PDF/Adobe Acrobat - [View as HTML](#)

technique will be extended to other modeling **aspects** within C-SAFE. ... the emphasis
 in formulating surrogates will be on **matching** volatility and soot ...
 www.csafe.utah.edu/documents/FY99AnnualReport.pdf - [Similar pages](#)

[PS] [To appear in Computer Generated Forces and Behavioral ...](#)

File Format: Adobe PostScript - [View as HTML](#)

... problem spaces and a local portion that is local combat **simulation task**. ...
 o owncomputation of "target **aspect**" from its ownsubstantial overhead. ...
 www.isi.edu/soar/papers/cgf/94/Event/PRfinal.ps - [Similar pages](#)

[PDF] [Cluster Simulation in Time-Triggered Real-Time Systems](#)

File Format: PDF/Adobe Acrobat - [View as HTML](#)

simulation task states and annihilating of already sent messages. ... to the
simulation domain, by simulation distribution and by the simulation type. Ad- ...
 www.decomsys.com/publications/tg_Dissertation.pdf - [Similar pages](#)

[PDF] [Enabling interactive and collaborative oil reservoir simulations ...](#)

File Format: PDF/Adobe Acrobat - [View as HTML](#)

These models are coupled across interfaces by a set of **matching** or ... To construct
 the set of Grid elements constituting the **simulation domain**, ...
 www.caip.rutgers.edu/TASSL/Papers/discover-ipars-ccpe-si-05.pdf - [Similar pages](#)

[LABORATOIRE DE MECANIQUE DES FLUIDES - UMR CNRS 2698](#)

Since spatial resolution and **simulation domain** extent are two antagonist factors
 in the ... Here follow some elements proposed to the **Simulation Task Group**. ...
 www.ec-nantes.fr/Fr/Recherche/DEE/Dah/urbcap.htm - 141k - [Cached](#) - [Similar pages](#)

[PDF] QUANTUM ELECTRONIC DEVICE SIMULATION

File Format: PDF/Adobe Acrobat - View as HTML

regions must be included in the **simulation domain** in order that the assumed classical ... In fact, this device and **simulation task** have been the ...

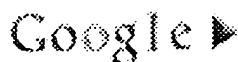
www.nas.nasa.gov/~biegel/pubs/thesis.pdf - Similar pages

[PDF] lcg.web.cern.ch/LCG/tdr/drafts/lcg_tdr_v384.pdf

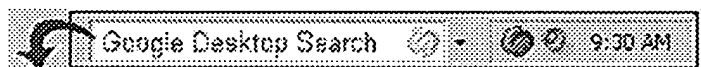
File Format: PDF/Adobe Acrobat - View as HTML

Supplemental Result - Similar pages

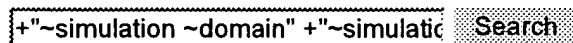
Try your search again on [Google Book Search](#)



Result Page: 1 2 **Next**



Free! Instantly find your email, files, media and web history. Download now.



[Search within results](#) | [Language Tools](#) | [Search Tips](#) | [Dissatisfied? Help us improve](#)

[Google Home](#) - [Advertising Programs](#) - [Business Solutions](#) - [About Google](#)

©2005 Google

[Sign in](#)
[Web](#)
[Images](#)
[Groups](#)
[News](#)
[Froogle](#)
[Local](#)
[New!](#)
[more »](#)

[Advanced Search](#)
[Preferences](#)
Web Results 1 - 10 of about 79 for "~simulation ~domain" "~simulation ~task" ~aspect. (0.52 seconds)

[PDF] 1998: TRAFFIC SIMULATION BASED ON THE HIGH LEVEL ARCHITECTURE

File Format: PDF/Adobe Acrobat - [View as HTML](#)

in section 5.4, which show different **aspects** of the goals, reusability and interoperability. ... In the civil **simulation domain**, we face a different ...

www.informs-sim.org/wsc98papers/149.PDF - [Similar pages](#)

[PDF] TRAFFIC SIMULATION BASED ON THE HIGH LEVEL ARCHITECTURE

File Format: PDF/Adobe Acrobat - [View as HTML](#)

aspects of interoperability and reusability become the. main goals in using distributed ... traffic **simulation domain** in particular (refer to figure ...

www.docs.iff.fhg.de/documents/hla/WSC98HLATraffic.pdf - [Similar pages](#)

Enabling Technology for Simulation Science V

9:10 am: The Economics of **Simulation Task** Force, S. Gordon, ... This now includes modeling **aspects** of human behavior under contract to the Army Research ...

www.rl.af.mil/tech/conferences/ModSim/ETConfProgV.html - 217k - [Cached](#) - [Similar pages](#)

[PDF] Learning by Observation in a Tactical Air Combat Domain

File Format: PDF/Adobe Acrobat - [View as HTML](#)

aspects of behavioral cloning is its effectiveness in a complex domain. ... **simulation domain** similar to the domains used in behavioral cloning and ...

ai.eecs.umich.edu/people/laird/papers/ML99-2.pdf - [Similar pages](#)

[PDF] XUEQIN HUANG XML-Based Messaging in the JSIM Simulation ...

File Format: PDF/Adobe Acrobat - [View as HTML](#)

the reuse and interoperability problems in the **simulation domain**. ... more challenging **simulation task**, such as the design of a spacecraft, would require ...

chief.cs.uga.edu/~jam/home/theses/huang_thesis/writeup/xhuangms.pdf - [Similar pages](#)

[PDF] Extending the High Level Architecture Paradigm to Economic Simulation

File Format: PDF/Adobe Acrobat - [View as HTML](#)

the tools and capabilities to the economic **simulation domain**. ... distributed **simulation task**: What new questions will be answered or what special problems ...

www.mitre.org/work/best_papers/best_papers_01/calpin_paradigm/calpin_paradigm.pdf - [Similar pages](#)

FoDok Online - Dokument E360-04-09

Another **aspect** when simulating process steps is the amount of time consumed by ... computation time is to split the **simulation task** into individual threads, ...

fodok.tuwien.ac.at/online-bin/run?function=document&id=E360-04-09 - 8k - [Cached](#) - [Similar pages](#)

[PDF] Center for the Simulation of Accidental Fires & Explosions

File Format: PDF/Adobe Acrobat - [View as HTML](#)

technique will be extended to other modeling **aspects** within C-SAFE. Preliminary work has ... 3.3.5 Polymer MD **simulation**, Task CD-5. ...

www.csafe.utah.edu/documents/FY99AnnualReport.pdf - [Similar pages](#)

[PS] To appear in Computer Generated Forces and Behavioral ...

Ref #	Hits	Search Query	DBs	Default Operator	Plurals	Time Stamp
L1	338510	simulat\$4	US-PGPUB; USPAT; EPO; JPO; DERWENT; IBM_TDB	OR	ON	2005/12/12 09:43
L2	341224	rule\$1	US-PGPUB; USPAT; EPO; JPO; DERWENT; IBM_TDB	OR	ON	2005/12/12 09:44
L3	1007763	match\$4	US-PGPUB; USPAT; EPO; JPO; DERWENT; IBM_TDB	OR	ON	2005/12/12 09:44
L4	324	1 same 2 same 3	US-PGPUB; USPAT; EPO; JPO; DERWENT; IBM_TDB	OR	ON	2005/12/12 09:45

L5	83	("4622013", "4874784", "4981766", "4931950", "4964077", "4977529", "5002491", "5170464", "5189402", "5208745", "5208898", "5239617", "5259766", "5267865", "5310349", "5311422", "5317688", "5326270", "5359701", "5372507", "5395243", "5441415", "5491743", "5533903", "5535422", "5537141", "5539869", "5566291", "5576844", "5577186", "5597312", "5616033", "5644686", "5644727", "5673369", "5690496", "5696885", "5701400", "5720007", "5727161", "5727950", "5745652", "5772446", "5779468", "5788508", "5791907", "5799151", "5799292", "5806056", "5810747", "5822745", "5823781", "5823788", "5835683", "5868575", "5870768", "5875437", "5889845", "5893123", "5911581", "5974446", "5987443", "6003021", "6015348", "6016486", "6018730", "6018731", "6018732", "6023691", "6023692", "6026386", "6029156", "6029158", "6029159", "6032141", "6064998", "6067537", "6067538", "6073127", "6085184", "6101489", "6125358", "6134539").pn.	USPAT	OR	ON	2005/12/12 09:50
----	----	--	-------	----	----	------------------

L6	86	("5987443", "6003021", "6134539", "6067537", "6032141", "6535861", "6073127", "6023691", "6101489", "6026386", "6067538", "6542880", "6085184", "6016486", "6023692", "6029158", "6029156", "6018732", "6018731", "6125358", "6064998", "6018730", "6029159", "6622003", "6591256", "6282362", d372435, "6658398", "6549893", "6493690", "6452070", "6284947", "20020035478", "20010016839", "20030172082", "20020171982", "20030163361", "20030041040", "20020090595", "20020067822", "20030106040", "20020161777", "20030093831", "20030041343", wo-9744766-a1, wo-9832109-a1).did.	US-PGPUB; USPAT; EPO; JPO; DERWENT; IBM_TDB	OR	ON	2005/12/12 09:50
L7	148	L5 xor L6 L5 and L6	US-PGPUB; USPAT; EPO; JPO; DERWENT; IBM_TDB	OR	ON	2005/12/12 09:50
L8	84	("5987443", "6003021", "6134539", "6067537", "6032141", "6535861", "6073127", "6023691", "6101489", "6026386", "6067538", "6542880", "6085184", "6016486", "6023692", "6029158", "6029156", "6018732", "6018731", "6125358", "6064998", "6018730", "6029159", "6622003", "6591256", "6282362", d372435, "6658398", "6549893", "6493690", "6452070", "6284947", "20020035478", "20010016839", "20030172082", "20020171982", "20030163361", "20030041040", "20020090595", "20020067822", "20030106040", "20020161777", "20030093831", "20030041343", wo-9744766-a1, wo-9832109-a1).did.	US-PGPUB; USPAT; DERWENT	OR	ON	2005/12/12 09:50

L9	46	("5987443", "6003021", "6134539", "6067537", "6032141", "6535861", "6073127", "6023691", "6101489", "6026386", "6067538", "6542880", "6085184", "6016486", "6023692", "6029158", "6029156", "6018732", "6018731", "6125358", "6064998", "6018730", "6029159", "6622003", "6591256", "6282362", d372435, "6658398", "6549893", "6493690", "6452070", "6284947", "20020035478", "20010016839", "20030172082", "20020171982", "20030163361", "20030041040", "20020090595", "20020067822", "20030106040", "20020161777", "20030093831", "20030041343", wo-9744766-a1, wo-9832109-a1).did.	US-PGPUB; USPAT; EPO	OR	ON	2005/12/12 09:50
L10	86	L8 xor L9 L8 and L9	US-PGPUB; USPAT; EPO; JPO; DERWENT; IBM_TDB	OR	ON	2005/12/12 09:50
L11	49	("5987443", "6003021", "6134539", "6067537", "6032141", "6535861", "6073127", "6023691", "6101489", "6026386", "6067538", "6542880", "6085184", "6016486", "6023692", "6029158", "6029156", "6018732", "6018731", "6125358", "6064998", "6018730", "6029159", "6622003", "6591256", "6282362", d372435, "6658398", "6549893", "6493690", "6452070", "6284947", "20020035478", "20010016839", "20030172082", "20020171982", "20030163361", "20030041040", "20020090595", "20020067822", "20030106040", "20020161777", "20030093831", "20030041343", "5694601", "5701400", "5827070", wo-9744766-a1, wo-9832109-a1). did.	US-PGPUB; USPAT; EPO	OR	ON	2005/12/12 09:50

L12	90	("5987443", "6003021", "6134539", "6067537", "6032141", "6535861", "6073127", "6023691", "6101489", "6026386", "6067538", "6542880", "6085184", "6016486", "6023692", "6029158", "6029156", "6018732", "6018731", "6125358", "6064998", "6018730", "6029159", "6622003", "6591256", "6282362", d372435, "6658398", "6549893", "6493690", "6452070", "6284947", "20020035478", "20010016839", "20030172082", "20020171982", "20030163361", "20030041040", "20020090595", "20020067822", "20030106040", "20020161777", "20030093831", "20030041343", "5694601", "5701400", "5827070", wo-9744766-a1, wo-9832109-a1). did.	US-PGPUB; USPAT; DERWENT	OR	ON	2005/12/12 09:50
L13	92	L11 xor L12 L11 and L12	US-PGPUB; USPAT; EPO; JPO; DERWENT; IBM_TDB	OR	ON	2005/12/12 09:50
L14	97	("5274572", "5542024", "5561760", "5673369", "5819248", "4803641", "4920499", "4965742", "5182793", "5263126", "5295230", "5307446", "5317677", "5333237", "5337320", "5388189", "5493729", "5566092", "5617514", "5630025", "5696884", "5704018", "6098061", "6240329", "4763277", "4783752", "4809219", "4816994", "4847784", "4866634", "4870591", "4872122", "4884218", "4916633", "4918620", "4922432", "4931951", "4939668", "4949278", "4967368", "5005143", "5019992", "5067099", "5197016", "5253184", "5283895", "5301260", "5301314", "5353384", "5394543").pn.	US-PGPUB; USPAT; EPO; JPO; DERWENT; IBM_TDB	OR	ON	2005/12/12 09:50

L15	50	("5274572", "5542024", "5561760", "5673369", "5819248", "4803641", "4920499", "4965742", "5182793", "5263126", "5295230", "5307446", "5317677", "5333237", "5337320", "5388189", "5493729", "5566092", "5617514", "5630025", "5696884", "5704018", "6098061", "6240329", "4763277", "4783752", "4809219", "4816994", "4847784", "4866634", "4870591", "4872122", "4884218", "4916633", "4918620", "4922432", "4931951", "4939668", "4949278", "4967368", "5005143", "5019992", "5067099", "5197016", "5253184", "5283895", "5301260", "5301314", "5353384", "5394543").pn.	USPAT	OR	ON	2005/12/12 09:50
L16	97	L14 xor L15 L14 and L15	US-PGPUB; USPAT; EPO; JPO; DERWENT; IBM_TDB	OR	ON	2005/12/12 09:50
L17	97	("5274572", "5542024", "5561760", "5673369", "5819248", "4803641", "4920499", "4965742", "5182793", "5263126", "5295230", "5307446", "5317677", "5333237", "5337320", "5388189", "5493729", "5566092", "5617514", "5630025", "5696884", "5704018", "6098061", "6240329", "4763277", "4783752", "4809219", "4816994", "4847784", "4866634", "4870591", "4872122", "4884218", "4916633", "4918620", "4922432", "4931951", "4939668", "4949278", "4967368", "5005143", "5019992", "5067099", "5197016", "5253184", "5283895", "5301260", "5301314", "5353384", "5394543").pn.	US-PGPUB; USPAT; EPO; JPO; DERWENT; IBM_TDB	OR	ON	2005/12/12 09:51

L18	7	(expert adj system\$1 and (("5274572", "5542024", "5561760", "5673369", "5819248", "4803641", "4920499", "4965742", "5182793", "5263126", "5295230", "5307446", "5317677", "5333237", "5337320", "5388189", "5493729", "5566092", "5617514", "5630025", "5696884", "5704018", "6098061", "6240329", "4763277", "4783752", "4809219", "4816994", "4847784", "4866634", "4870591", "4872122", "4884218", "4916633", "4918620", "4922432", "4931951", "4939668", "4949278", "4967368", "5005143", "5019992", "5067099", "5197016", "5253184", "5283895", "5301260", "5301314", "5353384", "5394543").pn.)) and 706/46.ccls.	US-PGPUB; USPAT; EPO; JPO; DERWENT; IBM_TDB	OR	ON	2005/12/12 09:51
L19	97	L17 xor L18 L17 and L18	US-PGPUB; USPAT; EPO; JPO; DERWENT; IBM_TDB	OR	ON	2005/12/12 09:51

L20	52	("5987443", "6003021", "6134539", "6067537", "6032141", "6535861", "6073127", "6023691", "6101489", "6026386", "6067538", "6542880", "6085184", "6016486", "6023692", "6029158", "6029156", "6018732", "6018731", "6125358", "6064998", "6018730", "6029159", "6622003", "6591256", "6282362", d372435, "6658398", "6549893", "6493690", "6452070", "6284947", "6611822", "20020035478", "20010016839", "20030172082", "20020171982", "20030163361", "20030041040", "20020090595", "20020067822", "20030106040", "20020161777", "20030093831", "20030041343", "20030084015", "20030023686", "5694601", "5701400", "5827070", wo-9744766-a1, wo-9832109-a1).did.	US-PGPUB; USPAT; EPO	OR	ON	2005/12/12 09:51
L21	149	17 xor L20 17 and L20	US-PGPUB; USPAT; EPO; JPO; DERWENT; IBM_TDB	OR	ON	2005/12/12 09:52

L22	53	("5987443", "6003021", "6134539", "6067537", "6032141", "6535861", "6073127", "6023691", "6101489", "6026386", "6067538", "6542880", "6085184", "6016486", "6023692", "6029158", "6029156", "6018732", "6018731", "6125358", "6064998", "6018730", "6029159", "6622003", "6591256", "6282362", d372435, "6658398", "6549893", "6493690", "6452070", "6284947", "6611822", "20020035478", "20010016839", "20030172082", "20020171982", "20030163361", "20030041040", "20020090595", "20020067822", "20030106040", "20020161777", "20030093831", "20030041343", "20030084015", "20030023686", "5694601", "5701400", "5827070", wo-9744766-a1, wo-9832109-a1, "5170464").did.	US-PGPUB; USPAT; EPO	OR	ON	2005/12/12 09:52
L23	98	("5987443", "6003021", "6134539", "6067537", "6032141", "6535861", "6073127", "6023691", "6101489", "6026386", "6067538", "6542880", "6085184", "6016486", "6023692", "6029158", "6029156", "6018732", "6018731", "6125358", "6064998", "6018730", "6029159", "6622003", "6591256", "6282362", d372435, "6658398", "6549893", "6493690", "6452070", "6284947", "6611822", "20020035478", "20010016839", "20030172082", "20020171982", "20030163361", "20030041040", "20020090595", "20020067822", "20030106040", "20020161777", "20030093831", "20030041343", "20030084015", "20030023686", "5694601", "5701400", "5827070", wo-9744766-a1, wo-9832109-a1, "5170464").did.	US-PGPUB; USPAT; DERWENT	OR	ON	2005/12/12 09:52

L24	100	L22 xor L23 L23 and L23	US-PGPUB; USPAT; EPO; JPO; DERWENT; IBM_TDB	OR	ON	2005/12/12 09:52
L25	148	7 xor 10 7 and 10	US-PGPUB; USPAT; EPO; JPO; DERWENT; IBM_TDB	OR	ON	2005/12/12 09:52
L26	189	13 xor 16 13 and 16	US-PGPUB; USPAT; EPO; JPO; DERWENT; IBM_TDB	OR	ON	2005/12/12 09:53
L27	197	21 xor 24 21 and 24	US-PGPUB; USPAT; EPO; JPO; DERWENT; IBM_TDB	OR	ON	2005/12/12 09:53
L28	249	25 xor 26 25 and 26	US-PGPUB; USPAT; EPO; JPO; DERWENT; IBM_TDB	OR	ON	2005/12/12 09:53
L29	256	27 xor 28 27 and 28	US-PGPUB; USPAT; EPO; JPO; DERWENT; IBM_TDB	OR	ON	2005/12/12 09:56
L30	3	4 and 29	US-PGPUB; USPAT; EPO; JPO; DERWENT; IBM_TDB	OR	ON	2005/12/12 09:53
L31	0	30 and @ad<"19981222"	US-PGPUB; USPAT; EPO; JPO; DERWENT; IBM_TDB	OR	ON	2005/12/12 09:57
L32	172	706/60.ccls.	US-PGPUB; USPAT; EPO; JPO; DERWENT; IBM_TDB	OR	ON	2005/12/12 09:56
L33	157	706/59.ccls.	US-PGPUB; USPAT; EPO; JPO; DERWENT; IBM_TDB	OR	ON	2005/12/12 09:56

L34	289	706/50.ccls.	US-PGPUB; USPAT; EPO; JPO; DERWENT; IBM_TDB	OR	ON	2005/12/12 09:56
L35	450	706/47.ccls.	US-PGPUB; USPAT; EPO; JPO; DERWENT; IBM_TDB	OR	ON	2005/12/12 09:56
L36	495	706/46.ccls.	US-PGPUB; USPAT; EPO; JPO; DERWENT; IBM_TDB	OR	ON	2005/12/12 09:56
L37	838	706/45.ccls.	US-PGPUB; USPAT; EPO; JPO; DERWENT; IBM_TDB	OR	ON	2005/12/12 09:56
L38	245	706/11.ccls.	US-PGPUB; USPAT; EPO; JPO; DERWENT; IBM_TDB	OR	ON	2005/12/12 09:56
L39	393	434/219.ccls.	US-PGPUB; USPAT; EPO; JPO; DERWENT; IBM_TDB	OR	ON	2005/12/12 09:56
L40	560	434/118.ccls.	US-PGPUB; USPAT; EPO; JPO; DERWENT; IBM_TDB	OR	ON	2005/12/12 09:56
L41	633	434/322.ccls.	US-PGPUB; USPAT; EPO; JPO; DERWENT; IBM_TDB	OR	ON	2005/12/12 09:56
L42	537	434/362.ccls.	US-PGPUB; USPAT; EPO; JPO; DERWENT; IBM_TDB	OR	ON	2005/12/12 09:56
L43	333	715/503.ccls.	US-PGPUB; USPAT; EPO; JPO; DERWENT; IBM_TDB	OR	ON	2005/12/12 09:56

L44	79	715/504.ccls.	US-PGPUB; USPAT; EPO; JPO; DERWENT; IBM_TDB	OR	ON	2005/12/12 09:56
L45	9	715/904.ccls.	US-PGPUB; USPAT; EPO; JPO; DERWENT; IBM_TDB	OR	ON	2005/12/12 09:56
L46	5	715/903.ccls.	US-PGPUB; USPAT; EPO; JPO; DERWENT; IBM_TDB	OR	ON	2005/12/12 09:56
L47	1612	705/7.ccls.	US-PGPUB; USPAT; EPO; JPO; DERWENT; IBM_TDB	OR	ON	2005/12/12 09:56
L48	306	L32 xor L33 L32 and L33	US-PGPUB; USPAT; EPO; JPO; DERWENT; IBM_TDB	OR	ON	2005/12/12 09:56
L49	701	L34 xor L35 L34 and L35	US-PGPUB; USPAT; EPO; JPO; DERWENT; IBM_TDB	OR	ON	2005/12/12 09:56
L50	1170	L36 xor L37 L36 and L37	US-PGPUB; USPAT; EPO; JPO; DERWENT; IBM_TDB	OR	ON	2005/12/12 09:56
L51	638	L38 xor L39 L38 and L39	US-PGPUB; USPAT; EPO; JPO; DERWENT; IBM_TDB	OR	ON	2005/12/12 09:56
L52	1089	L40 xor L41 L40 and L41	US-PGPUB; USPAT; EPO; JPO; DERWENT; IBM_TDB	OR	ON	2005/12/12 09:56
L53	870	L42 xor L43 L42 and L43	US-PGPUB; USPAT; EPO; JPO; DERWENT; IBM_TDB	OR	ON	2005/12/12 09:56

L54	87	L44 xor L45 L44 and L45	US-PGPUB; USPAT; EPO; JPO; DERWENT; IBM_TDB	OR	ON	2005/12/12 09:56
L55	1617	L46 xor L47 L46 and L47	US-PGPUB; USPAT; EPO; JPO; DERWENT; IBM_TDB	OR	ON	2005/12/12 09:56
L56	930	L48 xor L49 L48 and L49	US-PGPUB; USPAT; EPO; JPO; DERWENT; IBM_TDB	OR	ON	2005/12/12 09:56
L57	1735	L50 xor L51 L50 and L51	US-PGPUB; USPAT; EPO; JPO; DERWENT; IBM_TDB	OR	ON	2005/12/12 09:56
L58	1703	L52 xor L53 L52 and L53	US-PGPUB; USPAT; EPO; JPO; DERWENT; IBM_TDB	OR	ON	2005/12/12 09:56
L59	1702	L54 xor L55 L54 and L55	US-PGPUB; USPAT; EPO; JPO; DERWENT; IBM_TDB	OR	ON	2005/12/12 09:56
L60	2310	L56 xor L57 L56 and L57	US-PGPUB; USPAT; EPO; JPO; DERWENT; IBM_TDB	OR	ON	2005/12/12 09:56
L61	3348	L58 xor L59 L58 and L59	US-PGPUB; USPAT; EPO; JPO; DERWENT; IBM_TDB	OR	ON	2005/12/12 09:56
L62	5535	L60 xor L61 L60 and L61	US-PGPUB; USPAT; EPO; JPO; DERWENT; IBM_TDB	OR	ON	2005/12/12 09:56
L63	12	4 and L62	US-PGPUB; USPAT; EPO; JPO; DERWENT; IBM_TDB	OR	ON	2005/12/12 09:56

L64	5	63 and @ad<"19981222"	US-PGPUB; USPAT; EPO; JPO; DERWENT; IBM_TDB	OR	ON	2005/12/12 09:57
-----	---	-----------------------	---	----	----	------------------


[Home](#) | [Login](#) | [Logout](#) | [Access Information](#) | [Alerts](#) |

Welcome United States Patent and Trademark Office

Search Results

[BROWSE](#)[SEARCH](#)[IEEE XPLORE GUIDE](#)

Results for "(((simulation<in>metadata) <and> (rule<in>metadata))<and> (match<i>..."

Your search matched 52 of 1282825 documents.

A maximum of 52 results are displayed, 25 to a page, sorted by Relevance in Descending order.



» Search Options

[View Session History](#)[New Search](#)

Modify Search

((((simulation<in>metadata) <and> (rule<in>metadata))<and> (match<in>metada

☐ Check to search only within this results setDisplay Format: ☒ Citation ☐ Citation & Abstract

» Key

IEEE JNL IEEE Journal or Magazine

IEE JNL IEE Journal or Magazine

IEEE CNF IEEE Conference Proceeding

IEE CNF IEE Conference Proceeding

IEEE STD IEEE Standard

Select Article Information

View: [1-](#)

- ☐ **51. The method to suppress radar clutter by selecting a filter based on product profile of clutter categorized by neural network**
Sugimoto, T.; Fujisaka, T.; Oh-Hashi, Y.; Kondoh, M.;
Circuits and Systems, 1992., Proceedings of the 35th Midwest Symposium on
9-12 Aug. 1992 Page(s):260 - 263 vol.1
Digital Object Identifier 10.1109/MWSCAS.1992.271385
[AbstractPlus](#) | Full Text: [PDF](#)(256 KB) IEEE CNF
- ☐ **52. On the development of a fuzzy model for nonlinear systems**
Lai, J.-Y.; Shieh, J.-J.; Lin, Y.-C.;
Intelligent Robots and Systems '93, IROS '93. Proceedings of the 1993 IEEE/F
Conference on
Volume 2, 26-30 July 1993 Page(s):943 - 949 vol.2
Digital Object Identifier 10.1109/IROS.1993.583260
[AbstractPlus](#) | Full Text: [PDF](#)(576 KB) IEEE CNF

View Selected Items

View: [1-](#)[Help](#) [Contact Us](#) [Privacy & ;](#)

© Copyright 2005 IEEE -




[Home](#) | [Login](#) | [Logout](#) | [Access Information](#) | [Alerts](#) |

Welcome United States Patent and Trademark Office

Search Results

BROWSE

SEARCH

IEEE XPLORE GUIDE

Results for "(((simulation<in>metadata) <and> (rule<in>metadata))<and> (match<i>i..."

Your search matched **52** of **1282825** documents.A maximum of **52** results are displayed, **25** to a page, sorted by **Relevance** in **Descending** order.

» Search Options

[View Session History](#)[New Search](#)

Modify Search

(((simulation<in>metadata) <and> (rule<in>metadata))<and> (match<in>metada

☐ Check to search only within this results setDisplay Format: ☒ Citation ☐ Citation & Abstract

» Key

IEEE JNL IEEE Journal or Magazine

IEE JNL IEE Journal or Magazine

IEEE CNF IEEE Conference Proceeding

IEE CNF IEE Conference Proceeding

IEEE STD IEEE Standard

Select Article Information

View: 1-

- ☐ **26. Adaptive transform domain interference suppression in a hybrid DS/FH-s**
 Pouttu, A.; Juntti, J.; Kumpumaki, T.;
 Spread Spectrum Techniques and Applications, 1998. Proceedings., 1998 IEE
 International Symposium on
 Volume 1, 2-4 Sept. 1998 Page(s):351 - 355 vol.1
 Digital Object Identifier 10.1109/ISSSTA.1998.726256
[AbstractPlus](#) | Full Text: [PDF](#)(512 KB) IEEE CNF
- ☐ **27. Convergence implementation of adaptive lattice algorithm with fuzzy bas**
 Geun-Taek Ryu; Dae-Sung Kim; Dea-Young Lee; Sung-Hwan Han; Ho-Seok \ Bae;
 Circuits and Systems, 1998. IEEE APCCAS 1998. The 1998 IEEE Asia-Pacific
 24-27 Nov. 1998 Page(s):411 - 414
 Digital Object Identifier 10.1109/APCCAS.1998.743797
[AbstractPlus](#) | Full Text: [PDF](#)(256 KB) IEEE CNF
- ☐ **28. Entropy-constrained gradient-match vector quantization for image codin**
 Shin-Chou Juan; Chen-Yi Lee;
 Acoustics, Speech, and Signal Processing, 1998. ICASSP '98. Proceedings of
 International Conference on
 Volume 5, 12-15 May 1998 Page(s):2665 - 2668 vol.5
 Digital Object Identifier 10.1109/ICASSP.1998.678071
[AbstractPlus](#) | Full Text: [PDF](#)(472 KB) IEEE CNF
- ☐ **29. Experimental results for single period auctions**
 Bernard, J.; Either, R.; Mount, T.; Schulze, W.; Zimmerman, R.; Gan, D.; Murill
 Thomas, R.; Schuler, R.;
 System Sciences, 1998., Proceedings of the Thirty-First Hawaii International C
 Volume 3, 6-9 Jan. 1998 Page(s):15 - 23 vol.3
 Digital Object Identifier 10.1109/HICSS.1998.656007
[AbstractPlus](#) | Full Text: [PDF](#)(480 KB) IEEE CNF
- ☐ **30. Verification of faces in cluttered photographs**
 Govindaraju, V.; Rajapakse, M.;
 Systems, Man, and Cybernetics, 1997. 'Computational Cybernetics and Simul
 International Conference on
 Volume 3, 12-15 Oct. 1997 Page(s):2028 - 2033 vol.3
 Digital Object Identifier 10.1109/ICSMC.1997.635158

[AbstractPlus](#) | Full Text: [PDF\(812 KB\)](#) IEEE CNF

- ☐ **31. A rule-based method for object segmentation in video sequences**
Aydm Alatan, A.; Tuncel, E.; Onural, L.;
Image Processing, 1997. Proceedings., International Conference on
Volume 2, 26-29 Oct. 1997 Page(s):522 - 525 vol.2
Digital Object Identifier 10.1109/ICIP.1997.638823
[AbstractPlus](#) | Full Text: [PDF\(424 KB\)](#) IEEE CNF

- ☐ **32. A methodological approach for improvement of vacuum-insulated HV bu**
Lupo, G.; Petrarca, C.; Egiziano, L.; Spagnuolo, G.; Tucci, V.;
Discharges and Electrical Insulation in Vacuum, 1996. Proceedings. ISDEIV.,
International Symposium on
Volume 1, 21-26 July 1996 Page(s):552 - 556 vol.1
Digital Object Identifier 10.1109/DEIV.1996.545422
[AbstractPlus](#) | Full Text: [PDF\(404 KB\)](#) IEEE CNF

- ☐ **33. Admission power optimization in a window controlled virtual route**
Papir, Z.;
Electrotechnical Conference, 1989. Proceedings. 'Integrating Research, Indust
in Energy and Communication Engineering', MELECON '89., Mediterranean
11-13 April 1989 Page(s):633 - 638
Digital Object Identifier 10.1109/MELCON.1989.50125
[AbstractPlus](#) | Full Text: [PDF\(328 KB\)](#) IEEE CNF

- ☐ **34. Performance evaluation of a self-tuning fuzzy controller**
Daugherty, W.C.; Rathakrishnan, B.; Yen, J.;
Fuzzy Systems, 1992., IEEE International Conference on
8-12 March 1992 Page(s):389 - 397
Digital Object Identifier 10.1109/FUZZY.1992.258646
[AbstractPlus](#) | Full Text: [PDF\(388 KB\)](#) IEEE CNF

- ☐ **35. 3-D Interconnect capacitance calculation for multi-conductor and its appl**
ROM circuit design
Chung, S.S.; Huang, G.-D.;
ASIC Conference and Exhibit, 1992., Proceedings of Fifth Annual IEEE Intern
21-25 Sept. 1992 Page(s):475 - 478
Digital Object Identifier 10.1109/ASIC.1992.270244
[AbstractPlus](#) | Full Text: [PDF\(256 KB\)](#) IEEE CNF

- ☐ **36. Arden-architecture development environment**
Lai, F.; Tsaur, F.; Shang, R.-J.;
TENCON '92. Technology Enabling Tomorrow : Computers, Communications :
towards the 21st Century. 1992 IEEE Region 10 International Conference.
11-13 Nov. 1992 Page(s):181 - 185 vol.1
Digital Object Identifier 10.1109/TENCON.1992.271959
[AbstractPlus](#) | Full Text: [PDF\(352 KB\)](#) IEEE CNF

- ☐ **37. Fuzzy ARTMAP: an adaptive resonance architecture for incremental learn**
maps
Carpenter, G.A.; Grossberg, S.; Markuzon, N.; Reynolds, J.H.; Rosen, D.B.;
Neural Networks, 1992. IJCNN., International Joint Conference on
Volume 3, 7-11 June 1992 Page(s):309 - 314 vol.3
Digital Object Identifier 10.1109/IJCNN.1992.227156
[AbstractPlus](#) | Full Text: [PDF\(440 KB\)](#) IEEE CNF

- ☐ **38. ChemTrains: a language for creating behaving pictures**
Bell, B.; Lewis, C.;

Visual Languages, 1993., Proceedings 1993 IEEE Symposium on
24-27 Aug. 1993 Page(s):188 - 195
Digital Object Identifier 10.1109/VL.1993.269595
[AbstractPlus](#) | Full Text: [PDF](#)(596 KB) IEEE CNF

- ☐ **39. Technology issues of library porting in multi-process environment**
Chang, K.Y.; Rao, R.; Kundaji, V.; Ji-Hyung Chung; Hun-Sub Park; Ki-Soo Hw Oh; Lin, H.; Jensen, D.;
ASIC Conference and Exhibit, 1993. Proceedings., Sixth Annual IEEE Internat
27 Sept.-1 Oct. 1993 Page(s):320 - 325
Digital Object Identifier 10.1109/ASIC.1993.410730
[AbstractPlus](#) | Full Text: [PDF](#)(356 KB) IEEE CNF
- ☐ **40. Fuzzy logic for depth control of unmanned undersea vehicles**
DeBitetto, P.A.;
Autonomous Underwater Vehicle Technology, 1994. AUV '94., Proceedings of
Symposium on
19-20 July 1994 Page(s):233 - 241
Digital Object Identifier 10.1109/AUV.1994.518630
[AbstractPlus](#) | Full Text: [PDF](#)(744 KB) IEEE CNF
- ☐ **41. Continuous time nonlinear adaptive control based on linearization using**
Ishikawa, T.; Ohmori, H.; Sano, A.;
Control, 1994. Control '94. Volume 1., International Conference on
21-24 Mar 1994 Page(s):114 - 119 vol.1
[AbstractPlus](#) | Full Text: [PDF](#)(288 KB) IEE CNF
- ☐ **42. An architecture for time-limited model based diagnosis**
Aldea, A.; Chantler, M.J.;
Intelligent Fault Diagnosis - Part 2: Model-Based Techniques, IEE Colloquium
26 Feb 1992 Page(s):7/1 - 7/4
[AbstractPlus](#) | Full Text: [PDF](#)(196 KB) IEE CNF
- ☐ **43. Energy management onboard the Space Station-a rule-based approach**
Bouzguenda, M.; Rahman, S.;
Aerospace and Electronic Systems, IEEE Transactions on
Volume 27, Issue 2, March 1991 Page(s):302 - 310
Digital Object Identifier 10.1109/7.78305
[AbstractPlus](#) | Full Text: [PDF](#)(704 KB) IEEE JNL
- ☐ **44. Short term load forecasting using fuzzy neural networks**
Bakirtzis, A.G.; Theocharis, J.B.; Kiartzis, S.J.; Satsios, K.J.;
Power Systems, IEEE Transactions on
Volume 10, Issue 3, Aug. 1995 Page(s):1518 - 1524
Digital Object Identifier 10.1109/59.466494
[AbstractPlus](#) | Full Text: [PDF](#)(492 KB) IEEE JNL
- ☐ **45. A fuzzy adaptive multiuser detector in CDMA communication systems**
Jiho Jang; Kilsik Ha; BoSeok Seo; Sangyun Lee; Lee, C.W.;
Communications, 1998. ICC 98. Conference Record.1998 IEEE International (C
Volume 3, 7-11 June 1998 Page(s):1784 - 1788 vol.3
Digital Object Identifier 10.1109/ICC.1998.683136
[AbstractPlus](#) | Full Text: [PDF](#)(324 KB) IEEE CNF
- ☐ **46. Blind equalization using cost function matched to the signal constellation**
Barbarossa, S.; Scaglione, A.;
Signals, Systems & Computers, 1997. Conference Record of the Thirty-First A
Conference on

Volume 1, 2-5 Nov. 1997 Page(s):550 - 554 vol.1
Digital Object Identifier 10.1109/ACSSC.1997.680438
[AbstractPlus](#) | Full Text: [PDF](#)(412 KB) IEEE CNF

- ☐ **47. A massively parallel reverse modeling approach for semiconductor device**
Wu, S.; Vai, M.;
High Speed Semiconductor Devices and Circuits, 1997. Proceedings., 1997 IE
Conference on Advanced Concepts in
4-6 Aug. 1997 Page(s):201 - 209
Digital Object Identifier 10.1109/CORNEL.1997.649359
[AbstractPlus](#) | Full Text: [PDF](#)(496 KB) IEEE CNF
- ☐ **48. Image coding using FSVQ with dynamic states according to the edges in**
Young Tae Kim; Hyung Hwa Ko;
Acoustics, Speech, and Signal Processing, 1995. ICASSP-95., 1995 Internatio
on
Volume 4, 9-12 May 1995 Page(s):2583 - 2586 vol.4
Digital Object Identifier 10.1109/ICASSP.1995.480077
[AbstractPlus](#) | Full Text: [PDF](#)(500 KB) IEEE CNF
- ☐ **49. Cerebellar control of endpoint position-a simulation model**
Sinkjaer, T.; Wu, C.H.; Barto, A.G.; Houk, J.C.;
Neural Networks, 1990., 1990 IJCNN International Joint Conference on
17-21 June 1990 Page(s):705 - 710 vol.2
Digital Object Identifier 10.1109/IJCNN.1990.137783
[AbstractPlus](#) | Full Text: [PDF](#)(460 KB) IEEE CNF
- ☐ **50. A 3-D finite element cardiac model and its application to body surface La**
Yin, J.Z.; He, B.; Cohen, R.J.;
Computers in Cardiology 1992. Proceedings.
11-14 Oct. 1992 Page(s):247 - 250
Digital Object Identifier 10.1109/CIC.1992.269400
[AbstractPlus](#) | Full Text: [PDF](#)(308 KB) IEEE CNF

[View Selected Items](#)

View: [1-](#)

[Help](#) [Contact Us](#) [Privacy & ;](#)

© Copyright 2005 IEEE -

indexed by
 Inspec



Welcome United States Patent and Trademark Office

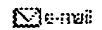
Search Results

BROWSE

SEARCH

IEEE XPLORE GUIDE

Results for "(((simulation<in>metadata) <and> (rule<in>metadata))<and> (match<i>i..."



Your search matched 52 of 1282825 documents.

A maximum of 100 results are displayed, 25 to a page, sorted by Relevance in Descending order.

» Search Options

[View Session History](#)[New Search](#)

Modify Search

(((simulation<in>metadata) <and> (rule<in>metadata))<and> (match<in>metada

☐ Check to search only within this results setDisplay Format: ☒ Citation ☐ Citation & Abstract

» Key

IEEE JNL IEEE Journal or Magazine

IEE JNL IEE Journal or Magazine

IEEE CNF IEEE Conference Proceeding

IEE CNF IEE Conference Proceeding

IEEE STD IEEE Standard

Select Article Information

View: 1-

- ☐ 1. **Efficient multi-attribute pattern matching using the extended Aho-Corasic**
Ando, K.; Okada, M.; Shishibori, M.; Jun-Ichi Aoe;
Systems, Man, and Cybernetics, 1997. 'Computational Cybernetics and Simula
International Conference on
Volume 4, 12-15 Oct. 1997 Page(s):3936 - 3941 vol.4
Digital Object Identifier 10.1109/ICSMC.1997.633286
[AbstractPlus](#) | Full Text: [PDF](#)(464 KB) IEEE CNF
- ☐ 2. **Effect of link flexibility of an adaptive tracking controller for a robot mani**
Hwang, S.-T.; Eltimsahy, A.;
Industrial Electronics, Control and Instrumentation, 1991. Proceedings. IECON
International Conference on
28 Oct.-1 Nov. 1991 Page(s):1289 - 1294 vol.2
Digital Object Identifier 10.1109/IECON.1991.239082
[AbstractPlus](#) | Full Text: [PDF](#)(436 KB) IEEE CNF
- ☐ 3. **Formal verification of digital circuits using hybrid simulation**
Srinivas, N.C.E.; Agrawal, V.D.;
Circuits and Devices Magazine, IEEE
Volume 4, Issue 1, Jan. 1988 Page(s):19 - 27
Digital Object Identifier 10.1109/101.927
[AbstractPlus](#) | Full Text: [PDF](#)(2048 KB) IEEE JNL
- ☐ 4. **A pipelined associated memory implemented in VLSI**
Clark, L.T.; Grondin, R.O.;
Solid-State Circuits, IEEE Journal of
Volume 24, Issue 1, Feb. 1989 Page(s):28 - 34
Digital Object Identifier 10.1109/4.16298
[AbstractPlus](#) | Full Text: [PDF](#)(676 KB) IEEE JNL
- ☐ 5. **An associative architecture for genetic algorithm-based machine learning**
Twardowski, K.;
Computer
Volume 27, Issue 11, Nov. 1994 Page(s):27 - 38
Digital Object Identifier 10.1109/2.330041
[AbstractPlus](#) | Full Text: [PDF](#)(1036 KB) IEEE JNL

- ☐ **6. A reliability model for real-time rule-based expert systems**
Ing-Ray Chen; Tawei Tsao;
Reliability, IEEE Transactions on
Volume 44, Issue 1, March 1995 Page(s):54 - 62
Digital Object Identifier 10.1109/24.376522
[AbstractPlus](#) | Full Text: [PDF\(780 KB\)](#) IEEE JNL

- ☐ **7. Rules for describing multi-attribute information and its efficient pattern m**
Ando, K.; Koyama, M.; Shishibori, M.; Aoe, J.;
Intelligent Processing Systems, 1997. ICIPS '97. 1997 IEEE International Conf
Volume 2, 28-31 Oct. 1997 Page(s):953 - 957 vol.2
Digital Object Identifier 10.1109/ICIPS.1997.669112
[AbstractPlus](#) | Full Text: [PDF\(599 KB\)](#) IEEE CNF

- ☐ **8. A method to match human sulci in 3D-space**
Luo, S.; Evans, A.C.;
Engineering in Medicine and Biology Society, 1995. IEEE 17th Annual Confere
Volume 1, 20-23 Sept. 1995 Page(s):401 - 402 vol.1
Digital Object Identifier 10.1109/IEMBS.1995.575170
[AbstractPlus](#) | Full Text: [PDF\(264 KB\)](#) IEEE CNF

- ☐ **9. Rule-based system for media setup optimization**
Shimp, J.E.; Clarson, V.H.;
Southeastcon '89. Proceedings. 'Energy and Information Technologies in the S
9-12 April 1989 Page(s):273 - 276 vol.1
Digital Object Identifier 10.1109/SECON.1989.132373
[AbstractPlus](#) | Full Text: [PDF\(300 KB\)](#) IEEE CNF

- ☐ **10. Self-organizing multuser detection**
Hottinen, A.;
Spread Spectrum Techniques and Applications, 1994. IEEE ISSSTA '94., IEEE
International Symposium on
4-6 July 1994 Page(s):152 - 156 vol.1
Digital Object Identifier 10.1109/ISSSTA.1994.379605
[AbstractPlus](#) | Full Text: [PDF\(280 KB\)](#) IEEE CNF

- ☐ **11. SYMCELL-a symbolic standard cell system**
Ramachandran, K.; Cordell, R.R.; Daly, D.F.; Deutsch, D.N.; Kwan, A.F.;
Solid-State Circuits, IEEE Journal of
Volume 26, Issue 3, Mar 1991 Page(s):449 - 452
Digital Object Identifier 10.1109/4.75035
[AbstractPlus](#) | Full Text: [PDF\(416 KB\)](#) IEEE JNL

- ☐ **12. Coded M-DPSK with built-in time diversity for fading channels**
Lee-Fang Wei;
Information Theory, IEEE Transactions on
Volume 39, Issue 6, Nov. 1993 Page(s):1820 - 1839
Digital Object Identifier 10.1109/18.265492
[AbstractPlus](#) | Full Text: [PDF\(1524 KB\)](#) IEEE JNL

- ☐ **13. Scaling-parameter-dependent model for subthreshold swing S in double-MOSFET's**
Tosaka, Y.; Suzuki, K.; Sugii, T.;
Electron Device Letters, IEEE
Volume 15, Issue 11, Nov. 1994 Page(s):466 - 468
Digital Object Identifier 10.1109/55.334669
[AbstractPlus](#) | Full Text: [PDF\(140 KB\)](#) IEEE JNL

- ☐ **14. Fuzzy controller for inverter fed induction machines**
Mir, S.A.; Zinger, D.S.; Elbuluk, M.E.;
Industry Applications, IEEE Transactions on
Volume 30, Issue 1, Jan.-Feb. 1994 Page(s):78 - 84
Digital Object Identifier 10.1109/28.273624
[AbstractPlus](#) | Full Text: [PDF](#)(488 KB) IEEE JNL

- ☐ **15. Notes on the simulation of evolution**
Atmar, W.;
Neural Networks, IEEE Transactions on
Volume 5, Issue 1, Jan. 1994 Page(s):130 - 147
Digital Object Identifier 10.1109/72.265967
[AbstractPlus](#) | Full Text: [PDF](#)(1920 KB) IEEE JNL

- ☐ **16. Reinforcement structure/parameter learning for neural-network-based fuzzy systems**
Chin-Teng Lin; Lee, C.S.G.;
Fuzzy Systems, IEEE Transactions on
Volume 2, Issue 1, Feb. 1994 Page(s):46 - 63
Digital Object Identifier 10.1109/91.273126
[AbstractPlus](#) | Full Text: [PDF](#)(1648 KB) IEEE JNL

- ☐ **17. Fuzzy logic for depth control of Unmanned Undersea Vehicles**
DeBitetto, P.A.;
Oceanic Engineering, IEEE Journal of
Volume 20, Issue 3, July 1995 Page(s):242 - 248
Digital Object Identifier 10.1109/48.393079
[AbstractPlus](#) | Full Text: [PDF](#)(644 KB) IEEE JNL

- ☐ **18. Boundary matching detection for recovering erroneously received VQ in channels**
Zeng, W.J.; Huang, Y.F.;
Circuits and Systems for Video Technology, IEEE Transactions on
Volume 6, Issue 1, Feb. 1996 Page(s):108 - 113
Digital Object Identifier 10.1109/76.486425
[AbstractPlus](#) | [References](#) | Full Text: [PDF](#)(768 KB) IEEE JNL

- ☐ **19. Model-based fault diagnosis using fuzzy matching**
Dexter, A.L.; Benouarets, M.;
Systems, Man and Cybernetics, Part A, IEEE Transactions on
Volume 27, Issue 5, Sept. 1997 Page(s):673 - 682
Digital Object Identifier 10.1109/3468.618266
[AbstractPlus](#) | [References](#) | Full Text: [PDF](#)(252 KB) IEEE JNL

- ☐ **20. Implosion dynamics of a radiative composite Z-pinch**
Benattar, R.; Ney, P.; Nikitin, A.; Zakharov, S.V.; Otochin, A.A.; Starostin, A.N.
Roerich, V.K.; Nikiforov, A.F.; Novikov, V.G.; Solomyannaya, A.D.; Gasilov, V.
A.Yu.;
Plasma Science, IEEE Transactions on
Volume 26, Issue 4, Aug. 1998 Page(s):1210 - 1223
Digital Object Identifier 10.1109/27.725153
[AbstractPlus](#) | [References](#) | Full Text: [PDF](#)(272 KB) IEEE JNL

- ☐ **21. A novel approach for multistage inference fuzzy control**
Zong-Mu Yeh; Hung-Pin Chen;
Systems, Man and Cybernetics, Part B, IEEE Transactions on
Volume 28, Issue 6, Dec. 1998 Page(s):935 - 946
Digital Object Identifier 10.1109/3477.735406

[AbstractPlus](#) | [References](#) | Full Text: [PDF\(528 KB\)](#) IEEE JNL

- ☐ **22. Electromagnetic transient simulation of power systems using root-match**
Watson, N.R.; Irwin, G.D.;
Generation, Transmission and Distribution, IEE Proceedings-
Volume 145, Issue 5, Sept. 1998 Page(s):481 - 486
[AbstractPlus](#) | Full Text: [PDF\(500 KB\)](#) IEE JNL
- ☐ **23. Neural network-based F0 text-to-speech synthesiser for Mandarin**
Hwang, S.-H.; Chen, S.-H.;
Vision, Image and Signal Processing, IEE Proceedings-
Volume 141, Issue 6, Dec. 1994 Page(s):384 - 390
[AbstractPlus](#) | Full Text: [PDF\(492 KB\)](#) IEE JNL
- ☐ **24. Case study of a knowledge-based system which plans molecular genetic**
Noordewier, M.O.; Travis, L.E.;
Artificial Intelligence Applications, 1990., Sixth Conference on
5-9 May 1990 Page(s):257 - 263 vol.1
Digital Object Identifier 10.1109/CAIA.1990.89198
[AbstractPlus](#) | Full Text: [PDF\(464 KB\)](#) IEEE CNF
- ☐ **25. Speech understanding system using knowledge engineering techniques**
Yato, F.; Asami, T.; Higuchi, N.;
Acoustics, Speech, and Signal Processing, IEEE International Conference on
Volume 11, Apr 1986 Page(s):1133 - 1136
[AbstractPlus](#) | Full Text: [PDF\(120 KB\)](#) IEEE CNF

[View Selected Items](#)

View: 1-

indexed by
 Inspect

[Help](#) [Contact Us](#) [Privacy & ;](#)

© Copyright 2005 IEEE -


[Home](#) | [Login](#) | [Logout](#) | [Access Information](#) | [Alerts](#) |

Welcome United States Patent and Trademark Office

Search Results

[BROWSE](#)[SEARCH](#)[IEEE XPLORE GUIDE](#)

Results for "((simulation<in>metadata) <and> (rule<in>metadata))<and> (match<in>..."



Your search matched 98 of 1282825 documents.

A maximum of 73 results are displayed, 25 to a page, sorted by Relevance in Descending order.

» Search Options

[View Session History](#)[New Search](#)

Modify Search

((simulation<in>metadata) <and> (rule<in>metadata))<and> (match<in>metadata)

☐ Check to search only within this results setDisplay Format: ☒ Citation ☐ Citation & Abstract

» Key

IEEE JNL IEEE Journal or Magazine

IEE JNL IEE Journal or Magazine

IEEE CNF IEEE Conference Proceeding

IEE CNF IEE Conference Proceeding

IEEE STD IEEE Standard

Select Article Information

View: 1-

- ☐ 1. **Efficient multi-attribute pattern matching using the extended Aho-Corasic**
Ando, K.; Okada, M.; Shishibori, M.; Jun-Ichi Aoe;
Systems, Man, and Cybernetics, 1997. 'Computational Cybernetics and Simul:
International Conference on
Volume 4, 12-15 Oct. 1997 Page(s):3936 - 3941 vol.4
Digital Object Identifier 10.1109/ICSMC.1997.633286
[AbstractPlus](#) | Full Text: [PDF](#)(464 KB) IEEE CNF
- ☐ 2. **Effect of link flexibility of an adaptive tracking controller for a robot mani**
Hwang, S.-T.; Eltimsahy, A.;
Industrial Electronics, Control and Instrumentation, 1991. Proceedings. IECON
International Conference on
28 Oct.-1 Nov. 1991 Page(s):1289 - 1294 vol.2
Digital Object Identifier 10.1109/IECON.1991.239082
[AbstractPlus](#) | Full Text: [PDF](#)(436 KB) IEEE CNF
- ☐ 3. **Formal verification of digital circuits using hybrid simulation**
Srinivas, N.C.E.; Agrawal, V.D.;
Circuits and Devices Magazine, IEEE
Volume 4, Issue 1, Jan. 1988 Page(s):19 - 27
Digital Object Identifier 10.1109/101.927
[AbstractPlus](#) | Full Text: [PDF](#)(2048 KB) IEEE JNL
- ☐ 4. **A pipelined associated memory implemented in VLSI**
Clark, L.T.; Grondin, R.O.;
Solid-State Circuits, IEEE Journal of
Volume 24, Issue 1, Feb. 1989 Page(s):28 - 34
Digital Object Identifier 10.1109/4.16298
[AbstractPlus](#) | Full Text: [PDF](#)(676 KB) IEEE JNL
- ☐ 5. **An associative architecture for genetic algorithm-based machine learning**
Twardowski, K.;
Computer
Volume 27, Issue 11, Nov. 1994 Page(s):27 - 38
Digital Object Identifier 10.1109/2.330041
[AbstractPlus](#) | Full Text: [PDF](#)(1036 KB) IEEE JNL

- ☐ **6. A reliability model for real-time rule-based expert systems**
Ing-Ray Chen; Tawei Tsao;
Reliability, IEEE Transactions on
Volume 44, Issue 1, March 1995 Page(s):54 - 62
Digital Object Identifier 10.1109/24.376522
[AbstractPlus](#) | Full Text: [PDF\(780 KB\)](#) IEEE JNL

- ☐ **7. Rules for describing multi-attribute information and its efficient pattern m**
Ando, K.; Koyama, M.; Shishibori, M.; Aoe, J.;
Intelligent Processing Systems, 1997. ICIPS '97. 1997 IEEE International Conf
Volume 2, 28-31 Oct. 1997 Page(s):953 - 957 vol.2
Digital Object Identifier 10.1109/ICIPS.1997.669112
[AbstractPlus](#) | Full Text: [PDF\(599 KB\)](#) IEEE CNF

- ☐ **8. A method to match human sulci in 3D-space**
Luo, S.; Evans, A.C.;
Engineering in Medicine and Biology Society, 1995. IEEE 17th Annual Confere
Volume 1, 20-23 Sept. 1995 Page(s):401 - 402 vol.1
Digital Object Identifier 10.1109/IEMBS.1995.575170
[AbstractPlus](#) | Full Text: [PDF\(264 KB\)](#) IEEE CNF

- ☐ **9. Rule-based system for media setup optimization**
Shimp, J.E.; Clarson, V.H.;
Southeastcon '89. Proceedings. 'Energy and Information Technologies in the S
9-12 April 1989 Page(s):273 - 276 vol.1
Digital Object Identifier 10.1109/SECON.1989.132373
[AbstractPlus](#) | Full Text: [PDF\(300 KB\)](#) IEEE CNF

- ☐ **10. Self-organizing multiuser detection**
Hottinen, A.;
Spread Spectrum Techniques and Applications, 1994. IEEE ISSSTA '94., IEEE
International Symposium on
4-6 July 1994 Page(s):152 - 156 vol.1
Digital Object Identifier 10.1109/ISSSTA.1994.379605
[AbstractPlus](#) | Full Text: [PDF\(280 KB\)](#) IEEE CNF

- ☐ **11. SYMCELL-a symbolic standard cell system**
Ramachandran, K.; Cordell, R.R.; Daly, D.F.; Deutsch, D.N.; Kwan, A.F.;
Solid-State Circuits, IEEE Journal of
Volume 26, Issue 3, Mar 1991 Page(s):449 - 452
Digital Object Identifier 10.1109/4.75035
[AbstractPlus](#) | Full Text: [PDF\(416 KB\)](#) IEEE JNL

- ☐ **12. Coded M-DPSK with built-in time diversity for fading channels**
Lee-Fang Wei;
Information Theory, IEEE Transactions on
Volume 39, Issue 6, Nov. 1993 Page(s):1820 - 1839
Digital Object Identifier 10.1109/18.265492
[AbstractPlus](#) | Full Text: [PDF\(1524 KB\)](#) IEEE JNL

- ☐ **13. Scaling-parameter-dependent model for subthreshold swing S in double-MOSFET's**
Tosaka, Y.; Suzuki, K.; Sugii, T.;
Electron Device Letters, IEEE
Volume 15, Issue 11, Nov. 1994 Page(s):466 - 468
Digital Object Identifier 10.1109/55.334669
[AbstractPlus](#) | Full Text: [PDF\(140 KB\)](#) IEEE JNL

- ☐ **14. Fuzzy controller for inverter fed induction machines**
Mir, S.A.; Zinger, D.S.; Elbuluk, M.E.;
Industry Applications, IEEE Transactions on
Volume 30, Issue 1, Jan.-Feb. 1994 Page(s):78 - 84
Digital Object Identifier 10.1109/28.273624
[AbstractPlus](#) | Full Text: [PDF](#)(488 KB) IEEE JNL

- ☐ **15. Notes on the simulation of evolution**
Atmar, W.;
Neural Networks, IEEE Transactions on
Volume 5, Issue 1, Jan. 1994 Page(s):130 - 147
Digital Object Identifier 10.1109/72.265967
[AbstractPlus](#) | Full Text: [PDF](#)(1920 KB) IEEE JNL

- ☐ **16. Reinforcement structure/parameter learning for neural-network-based fuzzy systems**
Chin-Teng Lin; Lee, C.S.G.;
Fuzzy Systems, IEEE Transactions on
Volume 2, Issue 1, Feb. 1994 Page(s):46 - 63
Digital Object Identifier 10.1109/91.273126
[AbstractPlus](#) | Full Text: [PDF](#)(1648 KB) IEEE JNL

- ☐ **17. Fuzzy logic for depth control of Unmanned Undersea Vehicles**
DeBitetto, P.A.;
Oceanic Engineering, IEEE Journal of
Volume 20, Issue 3, July 1995 Page(s):242 - 248
Digital Object Identifier 10.1109/48.393079
[AbstractPlus](#) | Full Text: [PDF](#)(644 KB) IEEE JNL

- ☐ **18. Boundary matching detection for recovering erroneously received VQ in channels**
Zeng, W.J.; Huang, Y.F.;
Circuits and Systems for Video Technology, IEEE Transactions on
Volume 6, Issue 1, Feb. 1996 Page(s):108 - 113
Digital Object Identifier 10.1109/76.486425
[AbstractPlus](#) | [References](#) | Full Text: [PDF](#)(768 KB) IEEE JNL

- ☐ **19. Model-based fault diagnosis using fuzzy matching**
Dexter, A.L.; Benouarets, M.;
Systems, Man and Cybernetics, Part A, IEEE Transactions on
Volume 27, Issue 5, Sept. 1997 Page(s):673 - 682
Digital Object Identifier 10.1109/3468.618266
[AbstractPlus](#) | [References](#) | Full Text: [PDF](#)(252 KB) IEEE JNL

- ☐ **20. Implosion dynamics of a radiative composite Z-pinch**
Benattar, R.; Ney, P.; Nikitin, A.; Zakharov, S.V.; Otochin, A.A.; Starostin, A.N.
Roerich, V.K.; Nikiforov, A.F.; Novikov, V.G.; Solomyannaya, A.D.; Gasilov, V.
A.Yu.;
Plasma Science, IEEE Transactions on
Volume 26, Issue 4, Aug. 1998 Page(s):1210 - 1223
Digital Object Identifier 10.1109/27.725153
[AbstractPlus](#) | [References](#) | Full Text: [PDF](#)(272 KB) IEEE JNL

- ☐ **21. A novel approach for multistage inference fuzzy control**
Zong-Mu Yeh; Hung-Pin Chen;
Systems, Man and Cybernetics, Part B, IEEE Transactions on
Volume 28, Issue 6, Dec. 1998 Page(s):935 - 946
Digital Object Identifier 10.1109/3477.735406

[AbstractPlus](#) | [References](#) | Full Text: [PDF\(528 KB\)](#) IEEE JNL

☐ **22. Differentially coherent decorrelating detector for CDMA single-path time-fading channels**

Huaping Liu; Siveski, Z.;
Communications, IEEE Transactions on
Volume 47, Issue 4, April 1999 Page(s):590 - 597
Digital Object Identifier 10.1109/26.764932

[AbstractPlus](#) | [References](#) | Full Text: [PDF\(188 KB\)](#) IEEE JNL

☐ **23. Analytical modelling of HVDC-HVAC systems**

Jovcic, D.; Pahalawaththa, N.; Zavahir, M.;
Power Delivery, IEEE Transactions on
Volume 14, Issue 2, April 1999 Page(s):506 - 511
Digital Object Identifier 10.1109/61.754095

[AbstractPlus](#) | Full Text: [PDF\(416 KB\)](#) IEEE JNL

☐ **24. A new RTD-FET logic family**

Mathews, R.H.; Sage, J.P.; Sollner, T.C.L.G.; Calawa, S.D.; Chang-Lee Chen;
Maki, P.A.; Molvar, K.M.;
Proceedings of the IEEE
Volume 87, Issue 4, April 1999 Page(s):596 - 605
Digital Object Identifier 10.1109/5.752517

[AbstractPlus](#) | [References](#) | Full Text: [PDF\(264 KB\)](#) IEEE JNL

☐ **25. Unstable Morse code recognition with adaptive variable-ratio threshold p physically disabled persons**

Ming-Che Hsieh; Ching-Hsing Luo; Chi-Wu Mao;
Rehabilitation Engineering, IEEE Transactions on [see also IEEE Trans. on Ne Rehabilitation]
Volume 8, Issue 3, Sept. 2000 Page(s):405 - 413
Digital Object Identifier 10.1109/86.867882

[AbstractPlus](#) | [References](#) | Full Text: [PDF\(216 KB\)](#) IEEE JNL

[View Selected Items](#)

View: 1-

indexed by
 Inspec

[Help](#) [Contact Us](#) [Privacy & :](#)

© Copyright 2005 IEEE –


[Home](#) | [Login](#) | [Logout](#) | [Access Information](#) | [Alerts](#) |

Welcome United States Patent and Trademark Office

Search Results

BROWSE

SEARCH

IEEE XPLORE GUIDE

Results for "((simulation<in>metadata) <and> (aspect<in>metadata))<and> (match<..."

email

Your search matched 73 of 1282825 documents.

A maximum of 73 results are displayed, 25 to a page, sorted by Relevance in Descending order.

» Search Options

[View Session History](#)
[New Search](#)

Modify Search

☐ Check to search only within this results set
Display Format: ☒ Citation ☐ Citation & Abstract

» Key

IEEE JNL IEEE Journal or Magazine

IEE JNL IEE Journal or Magazine

IEEE CNF IEEE Conference Proceeding

IEE CNF IEE Conference Proceeding

IEEE STD IEEE Standard

Select Article Information

View: 1-

- ☐ **51. Antijamming aspect of linear FM and phase coded pulse compressions b**
Fu, J.S.; Youan Ke;
Radar, 1996. Proceedings., CIE International Conference of
8-10 Oct. 1996 Page(s):605 - 608
Digital Object Identifier 10.1109/ICR.1996.574548
[AbstractPlus](#) | Full Text: [PDF\(344 KB\)](#) IEEE CNF
- ☐ **52. Design methodology of a cable terminator to reduce reflected voltage on**
Skibinski, G.;
Industry Applications Conference, 1996. Thirty-First IAS Annual Meeting, IAS ' Record of the 1996 IEEE
Volume 1, 6-10 Oct. 1996 Page(s):153 - 161 vol.1
Digital Object Identifier 10.1109/IAS.1996.557009
[AbstractPlus](#) | Full Text: [PDF\(880 KB\)](#) IEEE CNF
- ☐ **53. Accurate doping profile determination using TED/QM models extensible 1**
micron nMOSFETs
Voorde, P.V.; Griffin, P.B.; Yu, Z.; Oh, S.-Y.; Dutton, R.W.;
Electron Devices Meeting, 1996., International
8-11 Dec. 1996 Page(s):811 - 814
Digital Object Identifier 10.1109/EDM.1996.554103
[AbstractPlus](#) | Full Text: [PDF\(344 KB\)](#) IEEE CNF
- ☐ **54. Mechatronic blockset for Simulink-concept and implementation**
Ravn, O.; Szymkat, M.; Uhl, T.; Betemps, M.; Pjetursson, A.; Rod, J.;
Computer-Aided Control System Design, 1996., Proceedings of the 1996 IEEE
Symposium on
15-18 Sept. 1996 Page(s):530 - 535
Digital Object Identifier 10.1109/CACSD.1996.555348
[AbstractPlus](#) | Full Text: [PDF\(644 KB\)](#) IEEE CNF
- ☐ **55. Modelling and simulation of diesel electrical aggregate voltage controller**
sink
Erceg, G.; Tesnjak, S.; Erceg, R.;
Industrial Technology, 1996. (ICIT '96), Proceedings of The IEEE International
2-6 Dec. 1996 Page(s):875 - 879
Digital Object Identifier 10.1109/ICIT.1996.601725
[AbstractPlus](#) | Full Text: [PDF\(404 KB\)](#) IEEE CNF

- ☐ **56. 1.5-D ultrasound transducer array characterization**
Barthe, P.G.; Slayton, M.H.;
Engineering in Medicine and Biology Society, 1996. Bridging Disciplines for Bioengineering
Proceedings of the 18th Annual International Conference of the IEEE
Volume 2, 31 Oct.-3 Nov. 1996 Page(s):895 - 897 vol.2
Digital Object Identifier 10.1109/IEMBS.1996.652029
[AbstractPlus](#) | Full Text: [PDF\(220 KB\)](#) IEEE CNF

☐ **57. Implementing the hierarchical PRAM on the 2D mesh: analyses and experiments**
Chochia, G.; Cole, M.; Heywood, T.;
Parallel and Distributed Processing, 1995. Proceedings. Seventh IEEE Symposium on
25-28 Oct. 1995 Page(s):587 - 594
Digital Object Identifier 10.1109/SPDP.1995.530736
[AbstractPlus](#) | Full Text: [PDF\(708 KB\)](#) IEEE CNF

☐ **58. Design of monolithic 1-3 piezocomposite ultrasonic arrays using finite element analysis**
Bennet, J.; Hayward, G.;
Ultrasonics Symposium, 1995. Proceedings., 1995 IEEE
Volume 2, 7-10 Nov. 1995 Page(s):925 - 928 vol.2
Digital Object Identifier 10.1109/ULTSYM.1995.495716
[AbstractPlus](#) | Full Text: [PDF\(324 KB\)](#) IEEE CNF

☐ **59. A new neural network approach to spatiotemporal pattern recognition**
Filin, N.N.; Sukhov, A.G.; Efimov, V.N.; Arojan, E.V.;
Neuroinformatics and Neurocomputers, 1995., Second International Symposium on
20-23 Sept. 1995 Page(s):393 - 397
Digital Object Identifier 10.1109/ISNINC.1995.480887
[AbstractPlus](#) | Full Text: [PDF\(320 KB\)](#) IEEE CNF

☐ **60. A two-dimensional shift invariant image classification neural network with
the stability/plasticity dilemma**
Pulito, B.L.; Damarla, T.R.; Nariani, S.;
Neural Networks, 1990., 1990 IJCNN International Joint Conference on
17-21 June 1990 Page(s):825 - 833 vol.2
Digital Object Identifier 10.1109/IJCNN.1990.137798
[AbstractPlus](#) | Full Text: [PDF\(560 KB\)](#) IEEE CNF

☐ **61. A dynamical neural network model of sensorimotor transformations in the
limb**
Lockery, S.R.; Fang, Y.; Sejnowski, T.J.;
Neural Networks, 1990., 1990 IJCNN International Joint Conference on
17-21 June 1990 Page(s):183 - 188 vol.1
Digital Object Identifier 10.1109/IJCNN.1990.137566
[AbstractPlus](#) | Full Text: [PDF\(448 KB\)](#) IEEE CNF

☐ **62. Coarse-fine residual gravity cancellation system with magnetic levitation**
Salcudean, S.E.; Davis, H.; Chen, C.T.; Goertz, D.E.; Tryggvason, B.V.;
Robotics and Automation, 1992. Proceedings., 1992 IEEE International Conference on
12-14 May 1992 Page(s):1641 - 1647 vol.2
Digital Object Identifier 10.1109/ROBOT.1992.220142
[AbstractPlus](#) | Full Text: [PDF\(648 KB\)](#) IEEE CNF

☐ **63. Electrical and thermal modeling of a gated field emission triode**
Su, T.; Lee, C.L.; Huang, J.C.-M.;
Electron Devices Meeting, 1993. Technical Digest., International
5-8 Dec. 1993 Page(s):765 - 768
Digital Object Identifier 10.1109/IEDM.1993.347201
[AbstractPlus](#) | Full Text: [PDF\(232 KB\)](#) IEEE CNF

- ☐ **64. Cache designs with partial address matching**
Lishing Liu;
Microarchitecture, 1994. MICRO-27. Proceedings of the 27th Annual International Conference on Computer Architecture, 1994. Page(s):128 - 136
Digital Object Identifier 10.1109/MICRO.1994.717450
[AbstractPlus](#) | Full Text: [PDF\(792 KB\)](#) IEEE CNF

- ☐ **65. Matching curved 3D object models to 2D images**
Jin-Long Chen; Stockman, G.C.;
CAD-Based Vision Workshop, 1994., Proceedings of the 1994 Second International Conference on Computer-Aided Design and Computer Graphics, 1994. Page(s):210 - 218
Digital Object Identifier 10.1109/CADVIS.1994.284499
[AbstractPlus](#) | Full Text: [PDF\(640 KB\)](#) IEEE CNF

- ☐ **66. Simulation of S-UMTS system**
Sumanasena, M.A.K.; Evans, B.G.; Tafazolli, R.;
Simulation and Modelling of Satellite Systems, 2002. IEE Seminar and Exhibition on Satellite Systems, 2002. Page(s):4/1 - 4/5
Digital Object Identifier 10.1109/SEMOSAT.2002.1000074
[AbstractPlus](#) | Full Text: [PDF\(442 KB\)](#) IEE CNF

- ☐ **67. Variations of optical M-waveguides for direct phase matching in AlGaAs**
Oster, B.; Fouckhardt, H.;
Photonics Technology Letters, IEEE
Volume 13, Issue 7, July 2001 Page(s):672 - 674
Digital Object Identifier 10.1109/68.930410
[AbstractPlus](#) | [References](#) | Full Text: [PDF\(84 KB\)](#) IEEE JNL

- ☐ **68. Load modulation at two locations for damping of electro-mechanical oscillations in a multimachine system**
Samuelsson, O.;
Power Engineering Society Summer Meeting, 2000. IEEE
Volume 3, 16-20 July 2000 Page(s):1912 - 1917 vol. 3
Digital Object Identifier 10.1109/PESS.2000.868826
[AbstractPlus](#) | Full Text: [PDF\(516 KB\)](#) IEEE CNF

- ☐ **69. Physics and engineering aspects of the ICRF heating and current drive in the JET**
Hong, B.G.; Ju, M.H.; Bae, Y.D.; Kwak, J.G.; Han, J.M.; Mau, T.K.; Swain, D.V.
Ryan, P.M.;
Fusion Engineering, 1997. 17th IEEE/NPSS Symposium
Volume 1, 6-10 Oct. 1997 Page(s):469 - 472 vol.1
Digital Object Identifier 10.1109/FUSION.1997.687082
[AbstractPlus](#) | Full Text: [PDF\(300 KB\)](#) IEEE CNF

- ☐ **70. {111} and {311} rod-like defects in silicon ion implanted silicon**
Chou, C.T.; Cockayne, D.J.H.; Zou, J.; Kringhoj, P.; Jagadish, C.;
Optoelectronic and Microelectronic Materials And Devices Proceedings, 1996
8-11 Dec. 1996 Page(s):305 - 308
Digital Object Identifier 10.1109/COMMAD.1996.610131
[AbstractPlus](#) | Full Text: [PDF\(468 KB\)](#) IEEE CNF

- ☐ **71. Grid generator tool for MMACE**
Smithe, D.; Ludeking, L.; Warren, G.; Mondelli, A.; Kostas, C.;
Plasma Science, 1995. IEEE Conference Record - Abstracts., 1995 IEEE International Conference on Plasma Science, 1995. Page(s):10/1 - 10/2
Digital Object Identifier 10.1109/PLASMA.1995.4000000
[AbstractPlus](#) | Full Text: [PDF\(100 KB\)](#) IEEE CNF

5-8 June 1995 Page(s):242

Digital Object Identifier 10.1109/PLASMA.1995.533231

AbstractPlus | Full Text: **PDF**(88 KB) **IEEE CNF**

- ☐ **72. Workshop on Directions in Automated CAD-Based Vision. (Cat. No.91TH1)**
Automated CAD-Based Vision, 1991., Workshop on Directions in
2-3 June 1991
Digital Object Identifier 10.1109/CADVIS.1991.148777
[AbstractPlus](#) | Full Text: [PDF](#)(20 KB) [IEEE CNF](#)
- ☐ **73. Model based recognition of specular objects using sensor models**
Sato, K.; Ikeuchi, K.; Kanade, T.;
Automated CAD-Based Vision, 1991., Workshop on Directions in
2-3 June 1991 Page(s):2 - 10
Digital Object Identifier 10.1109/CADVIS.1991.148750
[AbstractPlus](#) | Full Text: [PDF](#)(868 KB) [IEEE CNF](#)

View Selected Items

View: 1-

indexed by
InspeC[®]

[Help](#) [Contact Us](#) [Privacy & :](#)

© Copyright 2005 IEEE –



Welcome United States Patent and Trademark Office

Search Results

BROWSE

SEARCH

IEEE XPLORE GUIDE

Results for "((simulation<in>metadata) <and> (aspect<in>metadata))<and> (match<..."

Your search matched 73 of 1282825 documents.



A maximum of 73 results are displayed, 25 to a page, sorted by Relevance in Descending order.

» Search Options

[View Session History](#)[New Search](#)

Modify Search

((simulation<in>metadata) <and> (aspect<in>metadata))<and> (match<in>meta

☐ Check to search only within this results setDisplay Format: ☒ Citation ☐ Citation & Abstract

» Key

IEEE JNL IEEE Journal or Magazine

IEE JNL IEE Journal or Magazine

IEEE CNF IEEE Conference Proceeding

IEE CNF IEE Conference Proceeding

IEEE STD IEEE Standard

Select Article Information

View: 1-

- ☐ **26. Input modeling**
Leemis, L.;
Simulation Conference, 2003. Proceedings of the 2003 Winter
Volume 1, 7-10 Dec. 2003 Page(s):14 - 24 Vol.1
[AbstractPlus](#) | Full Text: [PDF](#)(638 KB) IEEE CNF
- ☐ **27. Low profile printed antenna with a pair of step-loading for dual-frequency**
Ismail, M.K.H.; Esa, M.;
Applied Electromagnetics, 2003. APACE 2003. Asia-Pacific Conference on
12-14 Aug. 2003 Page(s):54 - 57
[AbstractPlus](#) | Full Text: [PDF](#)(261 KB) IEEE CNF
- ☐ **28. A CDMA system wideband feedforward linearizer design based on an an**
Coskun, A.H.; Demir, S.;
Radio and Wireless Conference, 2003. RAWCON '03. Proceedings
10-13 Aug. 2003 Page(s):191 - 194
Digital Object Identifier 10.1109/RAWCON.2003.1227925
[AbstractPlus](#) | Full Text: [PDF](#)(342 KB) IEEE CNF
- ☐ **29. Well-tempered combination of ultra-high voltage IGBT and diode rated 6.**
Suekawa, E.; Inoue, M.; Mochizuki, K.; Kawakami, M.; Minato, T.; Satoh, K.;
Power Semiconductor Devices and ICs, 2003. Proceedings. ISPSD '03. 2003 I
International Symposium on
14-17 April 2003 Page(s):160 - 163
Digital Object Identifier 10.1109/ISPSD.2003.1225254
[AbstractPlus](#) | Full Text: [PDF](#)(322 KB) IEEE CNF
- ☐ **30. Synchrony and perception in robotic imitation across embodiments**
Alissandrakis, A.; Nehaniv, C.L.; Dautenhahn, K.;
Computational Intelligence in Robotics and Automation, 2003. Proceedings. 20
International Symposium on
Volume 2, 16-20 July 2003 Page(s):923 - 930 vol.2
[AbstractPlus](#) | Full Text: [PDF](#)(638 KB) IEEE CNF
- ☐ **31. Higher order adaptive arithmetic coding using the prediction by partial m**
Soyjaudah, K.M.S.; Jahmeerbacus, I.; Oolun, M.K.; Bhurtun, C.;
Africon Conference in Africa, 2002. IEEE AFRICON. 6th

Volume 1, 2-4 Oct. 2002 Page(s):177 - 180 vol.1

[AbstractPlus](#) | Full Text: [PDF\(343 KB\)](#) IEEE CNF

- ☐ **32. Efficient periodic scheduling by trees**
Bar-Noy, A.; Dreizin, V.; Patt-Shamir, B.;
INFOCOM 2002. Twenty-First Annual Joint Conference of the IEEE Computer Communications Societies. Proceedings. IEEE
Volume 2, 23-27 June 2002 Page(s):791 - 800 vol.2
Digital Object Identifier 10.1109/INFCOM.2002.1019325
[AbstractPlus](#) | Full Text: [PDF\(326 KB\)](#) IEEE CNF

- ☐ **33. Mobile communications based on an emitter/receiver dynamics model**
Sousa, F.M.G.; Leitao, J.M.N.;
Vehicular Technology Conference, 2001. VTC 2001 Spring. IEEE VTS 53rd
Volume 4, 6-9 May 2001 Page(s):2998 - 3002 vol.4
Digital Object Identifier 10.1109/VETECS.2001.944153
[AbstractPlus](#) | Full Text: [PDF\(304 KB\)](#) IEEE CNF

- ☐ **34. Electromagnetic simulations and properties of the fundamental power cc SNS superconducting cavities**
Kang, Y.; Kim, S.; Doleans, M.; Campisi, I.E.; Stirbet, M.; Kneisel, P.; Ciovati, I.; Oijala, P.;
Particle Accelerator Conference, 2001. PAC 2001. Proceedings of the 2001
Volume 2, 18-22 June 2001 Page(s):1122 - 1124 vol.2
Digital Object Identifier 10.1109/PAC.2001.986600
[AbstractPlus](#) | Full Text: [PDF\(324 KB\)](#) IEEE CNF

- ☐ **35. Input modeling techniques for discrete-event simulations**
Leemis, L.;
Simulation Conference, 2001. Proceedings of the Winter
Volume 1, 9-12 Dec. 2001 Page(s):62 - 73 vol.1
Digital Object Identifier 10.1109/WSC.2001.977247
[AbstractPlus](#) | Full Text: [PDF\(675 KB\)](#) IEEE CNF

- ☐ **36. Use of fuzzy clustering for determining mass functions Dempster-Shafer**
Bentabet, L.; Yue Min Zhu; Dupuis, O.; Kaftandjian, V.; Babot, D.; Rombaut, M.
Signal Processing Proceedings, 2000. WCCC-ICSP 2000. 5th International Cc
Volume 3, 21-25 Aug. 2000 Page(s):1462 - 1470 vol.3
Digital Object Identifier 10.1109/ICOSP.2000.893377
[AbstractPlus](#) | Full Text: [PDF\(564 KB\)](#) IEEE CNF

- ☐ **37. Input modeling**
Leemis, L.;
Simulation Conference Proceedings, 2000. Winter
Volume 1, 10-13 Dec. 2000 Page(s):17 - 25 vol.1
Digital Object Identifier 10.1109/WSC.2000.899691
[AbstractPlus](#) | Full Text: [PDF\(564 KB\)](#) IEEE CNF

- ☐ **38. Competitive analysis of on-line algorithms for on-demand data broadcast**
Weizhen Mao;
Parallel Architectures, Algorithms and Networks, 2000. I-SPAN 2000. Proceed
Symposium on
7-9 Dec. 2000 Page(s):292 - 296
Digital Object Identifier 10.1109/ISPAN.2000.900298
[AbstractPlus](#) | Full Text: [PDF\(412 KB\)](#) IEEE CNF

- ☐ **39. The electromagnetic simulation software package MAFIA 4**
Clemens, M.; Drobny, S.; Kruger, H.; Pinder, P.; Podebrad, O.; Schillinger, B.;

Weiland, T.; Wilke, M.; Bartsch, M.; Becker, U.; Zhang, M.;
Computational Electromagnetics and Its Applications, 1999. Proceedings. (ICC
International Conference on
1999 Page(s):565 - 568
Digital Object Identifier 10.1109/ICCEA.1999.825246
[AbstractPlus](#) | Full Text: [PDF](#)(432 KB) IEEE CNF

- ☐ **40. Simulation input modeling**
Leemis, L.;
Simulation Conference Proceedings, 1999. Winter
Volume 1, 5-8 Dec. 1999 Page(s):14 - 23 vol.1
Digital Object Identifier 10.1109/WSC.1999.823047
[AbstractPlus](#) | Full Text: [PDF](#)(580 KB) IEEE CNF

- ☐ **41. Error analysis of an optical current transducer operating with a digital sig
system**
Niewczas, P.; Cruden, A.; Michie, W.C.; Madden, W.I.; McDonald, J.R.;
Instrumentation and Measurement Technology Conference, 1999. IMTC/99. P
16th IEEE
Volume 2, 24-26 May 1999 Page(s):1160 - 1165 vol.2
Digital Object Identifier 10.1109/IMTC.1999.777039
[AbstractPlus](#) | Full Text: [PDF](#)(440 KB) IEEE CNF

- ☐ **42. Spec-based repeater insertion and wire sizing for on-chip interconnect**
Menezes, N.; Chung-Ping Chen;
VLSI Design, 1999. Proceedings. Twelfth International Conference On
7-10 Jan. 1999 Page(s):476 - 482
Digital Object Identifier 10.1109/ICVD.1999.745201
[AbstractPlus](#) | Full Text: [PDF](#)(84 KB) IEEE CNF

- ☐ **43. Statistical aspects of tuning simulators to noisy data**
Davis, J.C.; Rao, S.; Vasanth, K.; Saxena, S.; Burch, R.; Mozumder, P.K.;
Statistical Metrology, 1998. 3rd International Workshop on
7 June 1998 Page(s):18 - 21
Digital Object Identifier 10.1109/IWSTM.1998.729757
[AbstractPlus](#) | Full Text: [PDF](#)(344 KB) IEEE CNF

- ☐ **44. Implementation aspects for noncoherent tracking based on a time-discre
loop**
Olson, H.; Tenhunen, H.;
Personal, Indoor and Mobile Radio Communications, 1998. The Ninth IEEE Int
Symposium on
Volume 1, 8-11 Sept. 1998 Page(s):375 - 380 vol.1
Digital Object Identifier 10.1109/PIMRC.1998.733582
[AbstractPlus](#) | Full Text: [PDF](#)(488 KB) IEEE CNF

- ☐ **45. On-line configuration of a time warp parallel discrete event simulator**
Radhakrishnan, R.; Abu-Ghazaleh, N.; Chetlur, M.; Wilsey, P.A.;
Parallel Processing, 1998. Proceedings. 1998 International Conference on
10-14 Aug. 1998 Page(s):28 - 35
Digital Object Identifier 10.1109/ICPP.1998.708460
[AbstractPlus](#) | Full Text: [PDF](#)(100 KB) IEEE CNF

- ☐ **46. Input modeling**
Leemis, L.;
Simulation Conference Proceedings, 1998. Winter
Volume 1, 13-16 Dec. 1998 Page(s):15 - 22 vol.1
Digital Object Identifier 10.1109/WSC.1998.744893

[AbstractPlus](#) | Full Text: [PDF\(544 KB\)](#) [IEEE CNF](#)

- ☐ **47. Experimental results for single period auctions**
Bernard, J.; Either, R.; Mount, T.; Schulze, W.; Zimmerman, R.; Gan, D.; Murill Thomas, R.; Schuler, R.;
System Sciences, 1998., Proceedings of the Thirty-First Hawaii International C
Volume 3, 6-9 Jan. 1998 Page(s):15 - 23 vol.3
Digital Object Identifier 10.1109/HICSS.1998.656007
[AbstractPlus](#) | Full Text: [PDF\(480 KB\)](#) [IEEE CNF](#)
- ☐ **48. High-perveance electron beams for high-power, slow-wave microwave de**
Basten, M.; Booske, J.H.; Scharer, J.E.; Louis, L.J.;
Plasma Science, 1997. IEEE Conference Record - Abstracts., 1997 IEEE Inter
Conference on
19-22 May 1997 Page(s):161 - 162
Digital Object Identifier 10.1109/PLASMA.1997.604473
[AbstractPlus](#) | Full Text: [PDF\(164 KB\)](#) [IEEE CNF](#)
- ☐ **49. New aspects on nonlinear power amplifier modeling in radio communical
simulations**
Honkanen, M.; Haggman, S.-G.;
Personal, Indoor and Mobile Radio Communications, 1997. 'Waves of the Yea
'97., The 8th IEEE International Symposium on
Volume 3, 1-4 Sept. 1997 Page(s):844 - 848 vol.3
Digital Object Identifier 10.1109/PIMRC.1997.627005
[AbstractPlus](#) | Full Text: [PDF\(432 KB\)](#) [IEEE CNF](#)
- ☐ **50. Design aspects and system evaluations of IS-95 based CDMA systems**
Jin Yang; Lee, W.C.Y.; Sung-Hyuk Shin;
Universal Personal Communications Record, 1997. Conference Record., 1997
International Conference on
Volume 2, 12-16 Oct. 1997 Page(s):381 - 385 vol.2
Digital Object Identifier 10.1109/ICUPC.1997.627191
[AbstractPlus](#) | Full Text: [PDF\(576 KB\)](#) [IEEE CNF](#)

[View Selected Items](#)

View: [1-](#)

Indexed by
 Inspec

[Help](#) [Contact Us](#) [Privacy & :](#)

© Copyright 2005 IEEE -


[Home](#) | [Login](#) | [Logout](#) | [Access Information](#) | [Alerts](#) |

Welcome United States Patent and Trademark Office

Search Results

[BROWSE](#)[SEARCH](#)[IEEE XPLORE GUIDE](#)

Results for "((simulation<in>metadata) <and> (aspect<in>metadata))<and> (match<in>meta"

email

Your search matched 73 of 1282825 documents.

A maximum of 100 results are displayed, 25 to a page, sorted by Relevance in Descending order.

» Search Options

[View Session History](#)[New Search](#)

Modify Search

((simulation<in>metadata) <and> (aspect<in>metadata))<and> (match<in>meta

☐ Check to search only within this results setDisplay Format: ☒ Citation ☐ Citation & Abstract

» Key

IEEE JNL IEEE Journal or Magazine

IEE JNL IEE Journal or Magazine

IEEE CNF IEEE Conference Proceeding

IEE CNF IEE Conference Proceeding

IEEE STD IEEE Standard

Select Article Information

View: 1-

- ☐ 1. **Mix-and-match high performance computing**
Klietz, A.E.; Malevsky, A.V.; Chin-Purcell, K.;
Potentials, IEEE
Volume 13, Issue 3, Aug-Sep 1994 Page(s):6 - 10
Digital Object Identifier 10.1109/45.310918
[AbstractPlus](#) | Full Text: [PDF](#)(504 KB) IEEE JNL
- ☐ 2. **New approach to target identification by use of a robust algorithm for opt of wideband radar signal to target**
Ghadimi, N.; Bastani, M.H.;
Radar, Sonar and Navigation, IEE Proceedings -
Volume 149, Issue 1, Feb. 2002 Page(s):16 - 22
Digital Object Identifier 10.1049/ip-rsn:20020070
[AbstractPlus](#) | Full Text: [PDF](#)(587 KB) IEE JNL
- ☐ 3. **Influence of local matching effects on the accuracy of a sequential A/D-co**
Dollberg, A.; Oehm, J.; Wunderlich, R.; Schumacher, K.;
Electronics, Circuits and Systems, 2001. ICECS 2001. The 8th IEEE Internatio
on
Volume 1, 2-5 Sept. 2001 Page(s):389 - 392 vol.1
Digital Object Identifier 10.1109/ICECS.2001.957761
[AbstractPlus](#) | Full Text: [PDF](#)(360 KB) IEEE CNF
- ☐ 4. **CMOS low-power analog circuit design**
Enz, C.C.; Vittoz, E.A.;
Designing Low Power Digital Systems, Emerging Technologies (1996)
1996 Page(s):79 - 133
Digital Object Identifier 10.1109/ETLPDS.1996.508872
[AbstractPlus](#) | Full Text: [PDF](#)(2340 KB) IEEE CNF
- ☐ 5. **Locally optimal detection in multivariate non-Gaussian noise**
Martinez, A.; Swaszek, P.; Thomas, J.;
Information Theory, IEEE Transactions on
Volume 30, Issue 6, Nov 1984 Page(s):815 - 822
[AbstractPlus](#) | Full Text: [PDF](#)(1000 KB) IEEE JNL
- ☐ 6. **A CAD framework for simulation and optimization of high-speed VLSI int**

Griffith, R.; Chiprout, E.; Zhang, Q.; Nakhla, M.;
Circuits and Systems I: Fundamental Theory and Applications, IEEE Transactions on
Circuits and Systems I: Regular Papers, IEEE Transactions on
Volume 39, Issue 11, Nov. 1992 Page(s):893 - 906
Digital Object Identifier 10.1109/81.199888
[AbstractPlus](#) | Full Text: [PDF](#)(1140 KB) IEEE JNL

- ☐ **7. K/Ka-band coplanar waveguide directional couplers using a three-metal-l process**
Gokdemir, T.; Robertson, I.D.; Wang, Q.H.; Rezazadeh, A.A.;
Microwave and Guided Wave Letters, IEEE [see also IEEE Microwave and Wireless Components Letters]
Volume 6, Issue 2, Feb. 1996 Page(s):76
Digital Object Identifier 10.1109/75.481994
[AbstractPlus](#) | [References](#) | Full Text: [PDF](#)(384 KB) IEEE JNL

- ☐ **8. Determining pose of 3D objects with curved surfaces**
Jin-Long Chen; Stockman, G.C.;
Pattern Analysis and Machine Intelligence, IEEE Transactions on
Volume 18, Issue 1, Jan. 1996 Page(s):52 - 57
Digital Object Identifier 10.1109/34.476010
[AbstractPlus](#) | [References](#) | Full Text: [PDF](#)(840 KB) IEEE JNL

- ☐ **9. Error analysis of an optical current transducer operating with a digital signal system**
Niewczas, P.; Cruden, A.; Michie, W.C.; Madden, W.I.; McDonald, J.R.;
Instrumentation and Measurement, IEEE Transactions on
Volume 49, Issue 6, Dec. 2000 Page(s):1254 - 1259
Digital Object Identifier 10.1109/19.893265
[AbstractPlus](#) | [References](#) | Full Text: [PDF](#)(80 KB) IEEE JNL

- ☐ **10. Incremental compilation for parallel logic verification systems**
Tessier, R.; Jana, S.;
Very Large Scale Integration (VLSI) Systems, IEEE Transactions on
Volume 10, Issue 5, Oct. 2002 Page(s):623 - 636
Digital Object Identifier 10.1109/TVLSI.2002.801614
[AbstractPlus](#) | [References](#) | Full Text: [PDF](#)(1180 KB) IEEE JNL

- ☐ **11. Analysis of aging of piezoelectric crystal resonators**
Asiz, A.; Weiping Zhang; Yunping Xi;
Ultrasonics, Ferroelectrics and Frequency Control, IEEE Transactions on
Volume 50, Issue 12, Dec. 2003 Page(s):1647 - 1655
Digital Object Identifier 10.1109/TUFFC.2003.1256304
[AbstractPlus](#) | Full Text: [PDF](#)(710 KB) IEEE JNL

- ☐ **12. Representing wind turbine electrical generating systems in fundamental simulations**
Slootweg, J.G.; Polinder, H.; Kling, W.L.;
Energy Conversion, IEEE Transactions on
Volume 18, Issue 4, Dec. 2003 Page(s):516 - 524
Digital Object Identifier 10.1109/TEC.2003.816593
[AbstractPlus](#) | [References](#) | Full Text: [PDF](#)(463 KB) IEEE JNL

- ☐ **13. Design of an efficient miniaturized UHF planar antenna**
Sarabandi, K.; Azadegan, R.;
Antennas and Propagation, IEEE Transactions on
Volume 51, Issue 6, June 2003 Page(s):1270 - 1276
Digital Object Identifier 10.1109/TAP.2003.812239

[AbstractPlus](#) | [References](#) | Full Text: [PDF\(841 KB\)](#) IEEE JNL

- ☐ **14. Unifying regularization and Bayesian estimation methods for enhanced in remotely sensed Data-part II: Implementation and performance issues**
Shkvarko, Y.V.;
Geoscience and Remote Sensing, IEEE Transactions on
Volume 42, Issue 5, May 2004 Page(s):932 - 940
Digital Object Identifier 10.1109/TGRS.2003.823279
[AbstractPlus](#) | Full Text: [PDF\(600 KB\)](#) IEEE JNL

- ☐ **15. Refined error analysis in second-order /spl Sigma//spl Delta/ modulation inputs**
Gunturk, C.S.; Thao, N.T.;
Information Theory, IEEE Transactions on
Volume 50, Issue 5, May 2004 Page(s):839 - 860
Digital Object Identifier 10.1109/TIT.2004.826635
[AbstractPlus](#) | [References](#) | Full Text: [PDF\(2168 KB\)](#) IEEE JNL

- ☐ **16. Eigenspace-based face recognition: a comparative study of different app**
Ruiz-del-Solar, J.; Navarrete, P.;
Systems, Man and Cybernetics, Part C, IEEE Transactions on
Volume 35, Issue 3, Aug. 2005 Page(s):315 - 325
Digital Object Identifier 10.1109/TSMCC.2005.848201
[AbstractPlus](#) | Full Text: [PDF\(424 KB\)](#) IEEE JNL

- ☐ **17. Technology development for a mm-wave sheet-beam traveling-wave tube**
Carlsten, B.E.; Russell, S.J.; Earley, L.M.; Krawczyk, F.L.; Potter, J.M.; Fergus
Humphries, S., Jr.;
Plasma Science, IEEE Transactions on
Volume 33, Issue 1, Part 1, Feb 2005 Page(s):85 - 93
Digital Object Identifier 10.1109/TPS.2004.841172
[AbstractPlus](#) | Full Text: [PDF\(920 KB\)](#) IEEE JNL

- ☐ **18. Capacity analysis for compact MIMO systems**
Lau, B.K.; Ow, S.M.S.; Kristensson, G.; Molisch, A.F.;
Vehicular Technology Conference, 2005. VTC 2005-Spring. 2005 IEEE 61st
Volume 1, 30 May-1 June 2005 Page(s):165 - 170 Vol. 1
Digital Object Identifier 10.1109/VETECS.2005.1543271
[AbstractPlus](#) | Full Text: [PDF\(4536 KB\)](#) IEEE CNF

- ☐ **19. BARD: Bayesian-assisted resource discovery in sensor networks**
Stann, F.; Heidemann, J.;
INFOCOM 2005. 24th Annual Joint Conference of the IEEE Computer and Com
Societies. Proceedings IEEE
Volume 2, 13-17 March 2005 Page(s):866 - 877 vol. 2
Digital Object Identifier 10.1109/INFCOM.2005.1498317
[AbstractPlus](#) | Full Text: [PDF\(791 KB\)](#) IEEE CNF

- ☐ **20. Building credible input models**
Leemis, L.M.;
Simulation Conference, 2004. Proceedings of the 2004 Winter
Volume 1, 5-8 Dec. 2004 Page(s):
Digital Object Identifier 10.1109/WSC.2004.1371299
[AbstractPlus](#) | Full Text: [PDF\(350 KB\)](#) IEEE CNF

- ☐ **21. Case study of a knowledge-based system which plans molecular genetic**
Noordewier, M.O.; Travis, L.E.;
Artificial Intelligence Applications, 1990., Sixth Conference on

5-9 May 1990 Page(s):257 - 263 vol.1
Digital Object Identifier 10.1109/CAIA.1990.89198
[AbstractPlus](#) | Full Text: [PDF](#)(464 KB) IEEE CNF

- ☐ **22. An automatic RF matching device**
Martin, R.; Young, L.; Friedman, D.; Runke, G.;
WESCON/59 Conference Record
Volume 3, Part 1, Aug 1959 Page(s):126 - 133
[AbstractPlus](#) | Full Text: [PDF](#)(656 KB) IEEE CNF
- ☐ **23. A Hardware Acceleration Unit for MPI Queue Processing**
Underwood, K.D.; Hemmert, K.S.; Rodrigues, A.; Murphy, R.; Brightwell, R.;
Parallel and Distributed Processing Symposium, 2005. Proceedings. 19th IEEE
04-08 April 2005 Page(s):96b - 96b
Digital Object Identifier 10.1109/IPDPS.2005.30
[AbstractPlus](#) | Full Text: [PDF](#)(232 KB) IEEE CNF
- ☐ **24. Usage of link-level performance indicators for HSDPA network-level simulations**
Brouwer, F.; de Bruin, I.; Silva, J.C.; Souto, N.; Cercas, F.; Correia, A.;
Spread Spectrum Techniques and Applications, 2004 IEEE Eighth International
30 Aug.-2 Sept. 2004 Page(s):844 - 848
[AbstractPlus](#) | Full Text: [PDF](#)(491 KB) IEEE CNF
- ☐ **25. Naturally-commutated cycloconverter versus rectifier-inverter pair grid-connected distributed power generation based on high-speed microturbines**
Kazerani, M.;
Industrial Electronics Society, 2003. IECON '03. The 29th Annual Conference
Volume 1, 2-6 Nov. 2003 Page(s):764 - 769 vol.1
Digital Object Identifier 10.1109/IECON.2003.1280079
[AbstractPlus](#) | Full Text: [PDF](#)(458 KB) IEEE CNF

[View Selected Items](#)

View: 1-

[Help](#) [Contact Us](#) [Privacy & ;](#)

© Copyright 2005 IEEE -

indexed by
 Inspec

[Home](#) | [Login](#) | [Logout](#) | [Access Information](#) | [Alerts](#) |

Welcome United States Patent and Trademark Office

Search Results**BROWSE****SEARCH****IEEE XPLORE GUIDE**

Results for "((simulation domain<in>metadata) <and> (simulation task<in>metadata))<an..."



Your search matched 0 documents.

A maximum of 100 results are displayed, 25 to a page, sorted by Relevance in Descending order.

» Search Options

[View Session History](#)[New Search](#)

Modify Search

 ☐ Check to search only within this results setDisplay Format: ☒ Citation ☐ Citation & Abstract

» Key

IEEE JNL IEEE Journal or Magazine

IEE JNL IEE Journal or Magazine

IEEE CNF IEEE Conference Proceeding

IEE CNF IEE Conference Proceeding

IEEE STD IEEE Standard

No results were found.

Please edit your search criteria and try again. Refer to the Help pages if you need assistance with your search.

[Help](#) [Contact Us](#) [Privacy & Policy](#)

© Copyright 2005 IEEE –



[Home](#) | [Login](#) | [Logout](#) | [Access Information](#) | [Alerts](#) |

Welcome United States Patent and Trademark Office

Search Results

[BROWSE](#)[SEARCH](#)[IEEE XPLORE GUIDE](#)

Results for "((simulation domain<in>metadata) <and> (simulation task<in>metadata))<an..."



Your search matched 0 documents.

A maximum of 100 results are displayed, 25 to a page, sorted by Relevance in Descending order.

» Search Options

[View Session History](#)[New Search](#)

Modify Search

 ☐ Check to search only within this results setDisplay Format: ☒ Citation ☐ Citation & Abstract

» Key

IEEE JNL IEEE Journal or Magazine

IEE JNL IEE Journal or Magazine

IEEE CNF IEEE Conference Proceeding

IEE CNF IEE Conference Proceeding

IEEE STD IEEE Standard

No results were found.

Please edit your search criteria and try again. Refer to the Help pages if you need assistance with your search.

[Help](#) [Contact Us](#) [Privacy & Policy](#)

© Copyright 2005 IEEE – All Rights Reserved

[Home](#) | [Login](#) | [Logout](#) | [Access Information](#) | [Alerts](#) |

Welcome United States Patent and Trademark Office

Search Results**BROWSE****SEARCH****IEEE XPLORE GUIDE**

Results for "((simulation domain<in>metadata) <and> (simulation task<in>metadata))<an..."



Your search matched 0 documents.

A maximum of 100 results are displayed, 25 to a page, sorted by Relevance in Descending order.

» Search Options[View Session History](#)[New Search](#)**Modify Search** (☐ Check to search only within this results setDisplay Format: ☒ Citation ☐ Citation & Abstract**» Key****IEEE JNL** IEEE Journal or Magazine**IEE JNL** IEE Journal or Magazine**IEEE CNF** IEEE Conference Proceeding**IEE CNF** IEE Conference Proceeding**IEEE STD** IEEE Standard**No results were found.**

Please edit your search criteria and try again. Refer to the Help pages if you need assistance with your search.

[Help](#) [Contact Us](#) [Privacy & :](#)

© Copyright 2005 IEEE –

Langley Technical Report Server

1.

M. H. Lucy, R. C. Hardy, E. H. Kist, J. J. Watson and S. A. Wise, **Report on Alternative Devices to Pyrotechnics on Spacecraft**, *10th Annual AIAA/USU Conference on Small Satellites*, Logan, Utah, September 16-19, 1996, (2MB).

Format(s): Postscript, or PDF

Keywords: Nonexplosive actuators; Nonpyrotechnic; Pyrotechnic; Mechanical devices

Abstract: Pyrotechnics accomplish many functions on today's spacecraft, possessing minimum volume/weight, providing instantaneous operation on demand, and requiring little input energy. However, functional shock, safety, and overall system cost issues, combined with emergence and availability of new technologies question their continued use of space missions. Upon request from the National Aeronautics and Space Administration's (NASA) Program Management Council (PMC), Langley Research Center (LaRC) conducted a survey to identify and evaluate state-of-the-art nonexplosively actuated (NEA) alternatives to pyrotechnics, identify NEA devices planned for NASA use, and investigate potential interagency cooperative efforts. In this study, over 135 organizations were contacted, including NASA field centers, Department of Defence (DOD) and other government laboratories, universities, and American and European industrial sources resulting in further detailed discussions with over half, and 18 face-to-face briefings. Unlike their single use pyrotechnic predecessors, NEA mechanisms are typically reusable or refurbishable, allowing flight of actual tested units. NEAs surveyed include spool-based devices, thermal knife, Fast Acting Shockless Separation Nut (FASSN), paraffin actuators, and shape memory alloy (SMA) devices (e.g., Frangibolt). The electro-mechanical spool, paraffin actuator and thermal knife are mature, flight proven technologies, while SMA devices have a limited flight history. There is a relationship between shock, input energy requirements, and mechanism functioning rate. Some devices (e.g., Frangibolt and spool based mechanisms) produce significant levels of functional shock. Paraffin, thermal knife, and SMA devices can provide gentle, shock-free release but cannot perform critically timed, simultaneous functions. The FASSN flywheel-nut release device possesses significant potential for reducing functional shock while activating nearly instantaneously. Specific study recommendations include: (1) development of NEA standards, specifically in areas of material characterization, functioning rates, and test methods; (2) a systems level approach to assure successful NEA technology application; and (3) further investigations into user needs, along with industry/government system-level real spacecraft cost-benefit trade studies to determine NEA application foci and performance requirements. Additional survey observations reveal an industry and government desire to establish partnerships to investigate remaining unknowns and formulate NEA standards, specifically those driven by SMAs. Finally, there is increased interest and need to investigate alternative devices for such functions as stage/shroud separation and high pressure valving. This paper summarizes results of the NASA-LaRC survey of pyrotechnic alternatives. State-of-the-art devices with their associated weight and cost savings are presented. Additionally, a comparison of functional shock characteristics of several devices are shown, and potentially related technology developments are highlighted.

2.

Arthur R. Johnson and Alexander Tessler, **Viscous Effects in the Elastodynamics of Thick Beams**, *14th Army Symposium on Solid Mechanics*, Myrtle Beach, South Carolina, October 1996,

pp. 11, (126KB).

Format(s): Postscript, or PDF

Keywords: Viscoelasticity; Finite elements; Dampin

Abstract: A viscoelastic higher-order thick beam finite element formulation is extended to include elastodynamic deformations. The material constitutive law is a special differential form of the Maxwell solid. In the constitutive model, the elastic strains and the conjugate viscous strains are coupled through a system of first-order ordinary differential equations. The total time-dependent stress is the superposition of its elastic and viscous components. The elastodynamic equations of motion are derived from the virtual work principle. Computational examples are carried out for a thick orthotropic cantilevered beam. A quasi-static relaxation problem is employed as a validation test for the elastodynamic algorithm. The elastodynamic code is demonstrated by analyzing the damped vibrations of the beam which is deformed and then released to freely vibrate.

3.

Karen E. Jackson and W. H. Prosser, **Damage Initiation and Ultimate Tensile Strength of Scaled $[0^\circ_{\text{sub}\{n\}}, 90^\circ_{\text{sub}\{n\}}, 0^\circ_{\text{sub}\{n\}}]_{\text{sub}T}$ Graphite-Epoxy Coupons**, *14th U.S. Army Symposium on Solid Mechanics*, Myrtle Beach, South Carolina, October 16-18, 1996, (80KB).

Format(s): Postscript, or PDF

Keywords: Composites; First ply failure; Acoustic emission

Abstract: Previous research on scaling effects in composite materials has demonstrated that the stress levels at first ply failure and ultimate failure of composite laminates are dependent on the size of the laminate. In particular, the thickness dimension has been shown to be the most influential parameter in strength scaling of composite coupons loaded in tension. Geometrically and constitutively scaled laminates exhibit decreasing strength with increasing specimen size, and the magnitude of the strength-size effect is a function of both material properties and laminate stacking sequence. Some of the commonly used failure criteria for composite materials such as maximum stress, maximum strain, and tensor polynomial (e.g., Tsai-Wu) cannot account for the strength-size effect. In this paper, three concepts are developed and evaluated for incorporating size dependency into failure criteria for composite materials. An experimental program of limited scope was performed to determine the first ply failure stress in scaled cross-ply laminates loaded in tension. Test specimens were fabricated of AS-4/3502 graphite-epoxy composite material with laminate stacking sequences of $[0^\circ_{\text{sub}\{n\}}/90^\circ_{\text{sub}\{n\}}/0^\circ_{\text{sub}\{n\}}]_T$ where $n=1-6$. Two experimental techniques were used to determine first ply failure, defined as a transverse matrix crack in the 90° ply: (1) step loading with dye penetrant x-ray of the specimen at each load interval, and (2) acoustic emission.

4.

J. J. Singh, **Microstructural Characterization of Polymers With Positrons**, *14th International*

Conference on the Applications of Accelerators in Research and Industry, Denton, Texas, November 6-9, 1996, (347KB).

Format(s): Postscript, or PDF

Keywords: Polymers; Positron lifetime spectroscopy; Free volume; Dielectric constant; Electrostatic interactions

Abstract: Positrons provide a versatile probe for monitoring microstructural features of molecular solids. In this paper, we report on positron lifetime measurements in two different types of polymers. The first group comprises polyacrylates processed on earth and in space. The second group includes fully-compatible and totally-incompatible Semi-Interpenetrating polymer networks of thermosetting and thermoplastic polyimides. On the basis of lifetime measurements, it is concluded that free volumes are a direct reflection of physical/electromagnetic properties of the host polymers.

5.

B. D. Joshi, R. Unal, N. H. White and W. D. Morris, **A Framework for the Optimization of Discrete-Event Simulation Models**, *17th American Society for Engineering Management National Conference*, Dallas, Texas, October 10-12, 1996, pp. 6, (42KB).

Format(s): Postscript, or PDF

Keywords: Optimization; Genetic algorithm; Discrete-event; Simulation; Stochastic

Abstract: With the growing use of computer modeling and simulation, in all aspects of engineering, the scope of traditional optimization has to be extended to include simulation models. Some unique aspects have to be addressed while optimizing via stochastic simulation models. The optimization procedure has to explicitly account for the randomness inherent in the stochastic measures predicted by the model. This paper outlines a general-purpose framework for optimization of terminating discrete-event simulation models. The methodology combines a chance constraint approach for problem formulation, together with standard statistical estimation and analyses techniques. The applicability of the optimization framework is illustrated by minimizing the operation and support resources of a launch vehicle, through a simulation model.

6.

Thomas J. Yager, **NASA Boeing 737 Aircraft Test Results From 1996 Joint Winter Runway Friction Measurement Program**, *First International Meeting on Aircraft Performance on Contaminated Runways (IMAPCR '96)*, Montreal, Quebec, October 22-23, 1996, pp. 9, (677KB).

Format(s): Postscript, or PDF

Keywords: Ground handling; Breaking friction; Winter runway

Abstract: A description of the joint test program objectives and scope is given together with the performance capability of the NASA Langley B-737 instrumented aircraft. The B-737 test run

matrix conducted during the first 8 months of this 5-year program is discussed with a description of the different runway conditions evaluated. Some preliminary test results are discussed concerning the Electronic Recording Decelerometer (ERD) readings and a comparison of B-737 aircraft braking performance for different winter runway conditions. Detailed aircraft parameter time history records, analysis of ground vehicle friction measurements and harmonization with aircraft braking performance, assessment of induced aircraft contaminant drag, and evaluation of the effects of other factors on aircraft/ground vehicle friction performance will be documented in a NASA Technical Report which is being prepared for publication next year.

7.

Thomas J. Yager, **The Joint Winter Runway Friction Measurement Program---NASA Perspective**, *First International Meeting on Aircraft Performance on Contaminated Runways (IMAPCR '96)*, Montreal, Quebec, October 22-23, 1996, (2MB).

Format(s): Postscript, or PDF

Keywords: Aircraft braking performance; Ground vehicle friction measurements; Winter runway

Abstract: Some background information is given together with the scope and objectives of the 5-year, Joint National Aeronautics and Space Administration (NASA)/Transport Canada (TC)/Federal Aviation Administration (FAA) Winter Runway Friction Measurement Program. The range of the test equipment, the selected test sites and a tentative test program schedule are described. NASA considers the success of this program critical in terms of insuring adequate ground handling performance capability in adverse weather conditions for future aircraft being designed and developed as well as improving the safety of current aircraft ground operations.

8.

S. A. Gorton, J. F. Meyers and J. D. Berry, **Laser Velocimetry and Doppler Global Velocimetry Measurements of Velocity Near the Empennage of a Small-Scale Helicopter Model**, *20th Army Science Conference*, Norfolk, Virginia, June 24-27, 1996, pp. 5, (658KB).

Format(s): Postscript, or PDF

Keywords: Rotor; Helicopter; Laser velocimeter; Doppler global velocimetry; Empennage;

Abstract: A test program was conducted in the NASA Langley 14- by 22-Foot Subsonic Tunnel to measure the flow near the empennage of a small-scale powered helicopter model with an operating tail fan. Three-component velocity profiles were measured with Laser Velocimetry (LV) one chord forward of the horizontal tail for four advance ratios to evaluate the effect of the rotor wake impingement on the horizontal tail angle of attack. These velocity data indicate the horizontal tail can experience unsteady downwash angle variations of over 30 degrees due to the rotor wake influence. The horizontal tail is most affected by the rotor wake above advance ratios of 0.10. Velocity measurements of the flow on the inlet side of the fan were made for a low-speed flight condition using both conventional LV techniques and a promising, non-intrusive, global, three-component velocity measurement technique called Doppler Global Velocimetry (DGV). The

velocity data show an accelerated flow near the fan duct, and vorticity calculations track the passage of main rotor wake vortices through the measurement plane. DGV shows promise as an evolving tool for rotor flowfield diagnostics.

9.

Clarence C. Poe, Jr., **Mechanics Methodology for Textile Preform Composite Materials**, *28th International SAMPE Technical Conference*, Seattle, WA, Nov. 1996, pp. 17, (229KB) Appeared in Proceedings of the 28th International SAMPE Technical Conference, pp. 324-338. The Postscript file is not the standard letter size and needs to be viewed under Media as U.S. Legal.

Format(s): Postscript, or PDF

Keywords: Composites; Textiles; Mechanical properties; Database; Analysis

Abstract: NASA and its contractors have completed a program to develop a basic mechanics underpinning for textile composites. Three major deliverables were produced by the program: (1.) a set of test methods for measuring material properties and design allowables, (2.) mechanics models to predict the effects of the fiber preform architecture and constituent properties on engineering moduli, strength, damage resistance, and fatigue life, (3.) an electronic data base of coupon type test data. This report describes these three deliverables.

10.

Kenneth S. Brentner, Jared S. Cox, Christopher L. Rumsey and Bassam A Younis, **Computation of Sound Generated by Flow Over a Circular Cylinder: An Acoustic Analogy Approach**, *Second Computational Aeroacoustics Workshop on Benchmark Problems*, Tallahassee, FL, November 4-5, 1996, pp. 7, (217KB).

Format(s): Postscript, or PDF

Keywords: Acoustic analogy; Aeolean tones; Circular cylinder; Vortex shedding; Noise prediction

Abstract: The sound generated by viscous flow past a circular cylinder is predicted via the Lighthill acoustic analogy approach. The two dimensional flow field is predicted using two unsteady Reynolds-averaged Navier-Stokes solvers. Flow field computations are made for laminar flow at three Reynolds numbers ($Re=1000$, $Re=10,000$, and $Re=90,000$) and two different turbulent models at $Re=90,000$. The unsteady surface pressures are utilized by an acoustics code that implements Farassat's formulation 1A to predict the acoustic field. The acoustic code is a 3-D code -- 2-D results are found by using a long cylinder length. The 2-D predictions overpredict the acoustic amplitude; however, if correlation lengths in the range of 3 to 10 cylinder diameters are used, the predicted acoustic amplitude agrees well with experiment.

11.

Paul C. Schutte and Anna C. Trujillo, **Flight Crew Task Management in Non-Normal**

Situations , *40th Annual Meeting of the Human Factors and Ergonomics Society*, Philadelphia, Pennsylvania, September 2-6, 1996, pp. 6, (101KB).

Format(s): Postscript, or PDF

Keywords: Aircraft-failure; Human-error; Task-management; Fault-management; Fuel-leak

Abstract: Task management (TM) is always performed on the flight deck, although not always explicitly, consistently, or rigorously. Nowhere is TM as important as it is in dealing with non-normal situations. The objective of this study was to analyze pilot TM behavior for non-normal situations. Specifically, the study observed pilots' performance in a full workload environment in order to discern their TM strategies. This study identified four different TM prioritization and allocation strategies: 'Aviate-Navigate-Communicate-Manage Systems;' 'Perceived Severity;' 'Procedure Based;' and 'Event/Interrupt Driven.' Subjects used these strategies to manage their personal workload and to schedule monitoring and assessment of the situation. The 'Perceived Severity' strategy for personal workload management combined with the 'Aviate-Navigate-Communicate- Manage Systems' strategy for monitoring and assessing appeared to be the most effective (fewest errors and fastest response times) in responding to the novel system failure used in this study.

12.

S. A. Gorton, J. F. Meyers and J. D. Berry, **Velocity Measurements Near the Empennage of a Small-Scale Helicopter Model** , *American Helicopter Society Forum 52*, Washington, DC, June 4-6, 1996, pp. 15, (2MB).

Format(s): Postscript, or PDF

Keywords: Rotor; Helicopter; Laser velocimeter; Doppler global velocimetry; Empennage; Tail fan

Abstract: A test program was conducted in the NASA Langley 14- by 22-Foot Subsonic Tunnel to measure the flow near the empennage of a small-scale powered helicopter model with an operating tail fan. Three-component velocity profiles were measured with Laser Velocimetry (LV) one chord forward of the horizontal tail for four advance ratios to evaluate the effect of the rotor wake impingement on the horizontal tail angle of attack. These velocity data indicate the horizontal tail can experience unsteady downwash angle variations of over 30 degrees due to the rotor wake influence. The horizontal tail is most affected by the rotor wake above advance ratios of 0.10. Velocity measurements of the flow on the inlet side of the fan were made for a low-speed flight condition using both conventional LV techniques and a promising, non-intrusive, global, three-component velocity measurement technique called Doppler Global Velocimetry(DGV). The velocity data show an accelerated flow near the fan duct, and vorticity calculations track the passage of main rotor wake vortices through the measurement plane. DGV shows promise as an evolving tool for rotor flowfield diagnostics.

13.

James F. Meyers, **Evolution of Doppler Global Velocimetry Data Processing** , *Eighth*

International Symposium on Applications of Laser Techniques to Fluid Mechanics, Lisbon, Portugal, July 8-11, 1996, (6MB).

Format(s): Postscript, or PDF

Keywords: Laser; Laser velocimetry; Velocity measurements; Flow measurements

Abstract: The development of data processing techniques and algorithms for Doppler Global Velocimetry is presented. The discussion begins with the fundamental calculation of the velocity dependent transfer function of Iodine vapor, and proceeds through laboratory and wind tunnel investigations to develop insight into the physics of the technique. The knowledge gained through this process provided the basis for the development of algorithms to correct for optical distortions, electronic noise, and camera misalignment.

14.

Zia-ur Rahman, Daniel J. Jobson and Glenn A. Woodell, **A Multiscale Retinex for Color Rendition and Dynamic Range Compression**, *Applications of Digital Image Processing XIX*, Denver, CO, August, 1996, pp. 9, Also in SPIE 2847.

Keywords: Nonlinear color image enhancement; Retinex

Abstract: The human vision system performs the tasks of dynamic range compression and color constancy almost effortlessly. The same tasks pose a very challenging problem for imaging systems whose dynamic range is restricted by either the dynamic response of film, in case of analog cameras, or by the analog-to-digital converters, in the case of digital cameras. The images thus formed are unable to encompass the wide dynamic range present in most natural scenes (often > 500:1). Whereas the human visual system is quite tolerant to spectral changes in lighting conditions, these strongly affect both the film response for analog cameras and the filter responses for digital cameras, leading to incorrect color formulation in the acquired image. Our multiscale retinex, based in part on Edwin Land's work on color constancy, provides a fast, simple, and automatic technique for simultaneous dynamic range compression and accurate color rendition. The retinex algorithm is non-linear, and global---output at a point is also a function of its surround---in extent. A comparison with conventional dynamic range compression techniques such as the application of point non-linearities, e.g. $\log(x,y)$, and global histogram equalization and/or modification shows that the multiscale retinex simultaneously provides the best dynamic range compression and color rendition. The applications of such an algorithm are many; from medical imaging to remote sensing; and from commercial photography to color transmission.

15.

D. A. Hinton, **An Aircraft Vortex Spacing System (AVOSS) for Dynamical Wake Vortex Spacing Criteria**, *78th Fluid Dynamics Panel Symposium*, Trondheim, Norway, May 20-23, 1996, (69KB).

Format(s): Postscript, or PDF

Keywords: Aircraft wake vortex; Air traffic control; Airport operations; Airport capacity;

Meteorology; Computational fluid dynamics; Doppler lidar; Doppler radar; Aircraft separation; AVOSS

Abstract: A concept is presented for the development and implementation of a prototype Aircraft vortex Spacing System (AVOSS). The purpose of the AVOSS is to use current and short-term predictions of the atmospheric state in approach and departure corridors to provide, to ATC facilities, dynamical weather dependent separation criteria with adequate stability and lead time for use in establishing arrival scheduling. The AVOSS will accomplish this task through a combination of wake vortex transport and decay predictions, weather state knowledge, defined aircraft operational procedures and corridors, and wake vortex safety sensors. Work is currently underway to address the critical disciplines and knowledge needs so as to implement and demonstrate a prototype AVOSS in the 1999/2000 time frame.

16.

Kenneth S. Brentner, Anastasios S. Lyrintzis and Evangelos K. Koutsavdis, **A Comparison of Computational Aeroacoustic Prediction Methods for Transonic Rotor Noise**, *American Helicopter Society 52nd Annual Forum*, Washington, D.C., June, 1996, pp. 12, (343KB).

Format(s): Postscript, or PDF

Keywords: Quadrupole noise; Rotor noise prediction; Acoustic analogy; Kirchhoff formulation

Abstract: This paper compares two methods for predicting transonic rotor noise for helicopters in hover and forward flight. Both methods rely on a computational fluid dynamics (CFD) solution as input to predict the acoustic near and far fields. For this work, the same full-potential rotor code has been used to compute the CFD solution for both acoustic methods. The first method employs the acoustic analogy as embodied in the Ffowcs Williams-Hawkings (FW-H) equation, including the quadrupole term. The second method uses a rotating Kirchhoff formulation. Computed results from both methods are compared with one other and with experimental data for both hover and advancing rotor cases. The results are quite good for all cases tested. The sensitivity of both methods to CFD grid resolution and to the choice of the integration surface/volume is investigated. The computational requirements of both methods are comparable; in both cases these requirements are much less than the requirements for the CFD solution.

17.

Dennis M. Bushnell, **Frontiers of the 'Responsibly Imaginable' in Aeronautics**, *Aero India '96 Proceedings*, Bangalore, India, December 3-6, 1996, pp. 12, (457KB).

Format(s): Postscript, or PDF

Keywords: Aeronautics; Frontiers; Responsibly imaginable

Abstract: Paper discusses alternatives to currently deployed systems which could provide revolutionary improvements in metrics applicable to civilian aeronautics. Specific missions addressed include subsonic transports, supersonic transports and personal aircraft. These alternative systems and concepts are enabled by recent and envisaged advancements in

electronics, communications, computing and "Designer Fluid Mechanics" in conjunction with a design approach employing extensive synergistic interactions between propulsion, aerodynamics and structures.

18.

Ronald D. Joslin, **Simulation of Three-Dimensional Symmetric and Asymmetric Instabilities in Attachment-Line Boundary Layers**, *AIAA Journal*, vol. 34, no. 11, November 1996, pp. 2432-2434, (131KB).

Format(s): Postscript, or PDF

Keywords: DNS; Boundary-layer transition; Attachment-line flow

Abstract: Direct Numerical Simulation (DNS) is used to validate a 2D-eigenvalue method which predicts symmetric and asymmetric disturbances in attachment-line boundary-layer flow. The DNS results are shown to match the calculated results for the first dominant symmetric and asymmetric mode.

19.

Willie R. Watson, Michael G. Jones, Sharon E. Tanner and Tony L. Parrott, **Validation of a Numerical Method for Extracting Liner Impedance**, *AIAA Journal*, vol. Volume 34, no. 3, March, 1996, pp. 548-554, (133KB).

Format(s): Postscript, or PDF

Keywords: Normal incidence impedance; Nonprogressive acoustic fields, Variable impedance

Abstract: We report the initial results of a test series to evaluate a method for extracting the normal-incidence impedance of a locally reacting liner located in a grazing incidence environment. This initial evaluation tests the method's ability to converge to the known impedance of a solid steel plate, and to the impedance of an absorbing test specimen whose impedance was measured in a normal incidence impedance tube. The method converges to the measured normal-incidence impedance values and thus is an adequate tool for extracting the impedance of specimens in a grazing-incidence, multimodal, nonprogressive acoustic wave environment for a broad range of source frequencies.

20.

R. L. Cravey, M. D. Deshpande, C. J. Reddy and P. I. Tiemsin, **Evaluation of Complex Permittivities of Multilayer Dielectric Substrates at Microwave Frequencies Using Waveguide Measurements**, *1996 Antenna Measurement Techniques Association Symposium*, Seattle, Washington, September 30--October 4, 1996, pp. 6, (74KB).

Format(s): Postscript, or PDF

Keywords: Permittivity; Waveguide; Multilayer; Substrates; Finite Element Method

Abstract: The techniques that are presently available for the measurement of complex permittivities of dielectric substrates are only applicable to single layer substrates. This paper presents a new technique which uses the Finite Element Method (FEM) to estimate the complex permittivities of individual layers from the measurement of the S-parameters of a rectangular waveguide holding a multilayer dielectric substrate sample. In this method, a network analyzer is used to measure reflection and transmission coefficients of a rectangular waveguide loaded with a layered sample. Using FEM, the reflection and transmission coefficients are determined as a function of the complex permittivities of the multilayer substrate. Measured and calculated values of the reflection and transmission coefficients are then matched using the Newton-Raphson Method to estimate the complex permittivities of the layers of the sample.

21.

W. Keats Wilkie, W. Keith Belvin and K. C. Park, **Aeroelastic Analysis of Helicopter Rotor Blades Incorporating Anisotropic Piezoelectric Twist Actuation**, *1996 Fall American Society of Mechanical Engineers Congress and Exhibition*, Atlanta, GA, November 17-22, 1996, pp. 11, (343KB) In Proceedings of the ASME Aerospace Division, ASME 1996, AD-Vol.52, pp.423-433..

Format(s): Postscript, or PDF

Keywords: Helicopters; Piezoelectric actuation; Aeroelasticity; Adaptive structures

Abstract: A simple aeroelastic analysis of a helicopter rotor blade incorporating embedded piezoelectric fiber composite, interdigitated electrode blade twist actuators is described. The analysis consists of a linear torsion and flapwise bending model coupled with a nonlinear ONERA based unsteady aerodynamics model. A modified Galerkin procedure is performed upon the rotor blade partial differential equations of motion to develop a system of ordinary differential equations suitable for dynamics simulation using numerical integration. The twist actuation responses for three conceptual full-scale blade designs with realistic constraints on blade mass are numerically evaluated using the analysis. Numerical results indicate that useful amplitudes of nonresonant elastic twist, on the order of one to two degrees, are achievable under one-g hovering flight conditions for interdigitated electrode poling configurations. Twist actuation for the interdigitated electrode blades is also compared with the twist actuation of a conventionally poled piezoelectric fiber composite blade. Elastic twist produced using the interdigitated electrode actuators was found to be four to five times larger than that obtained with the conventionally poled actuators.

22.

C. C. Johnson, D. J. Reichle, Jr., N. P. Barnes, G. J. Quarles, J. W. Early and N. J. Cockroft, **High Energy Diode Side-Pumped Cr:LiSAF Laser**, *Advanced Solid State Lasers Topical Meeting*, San Francisco, California, January 31--February 3, 1996, (607KB).

Format(s): Postscript, or PDF

Keywords: Rare earth and transition metal solid-state lasers; Lidar; Diode laser arrays; Laser material processing

Abstract: A diode side-pumped Cr:LiSAF laser has been demonstrated with a 33 mJ normal mode output energy, and an optical to optical efficiency of 17 percent. Improved optical quality laser material has been grown with several Cr concentrations. Optimum Cr concentration has been calculated and experimentally confirmed.

23.

Michael L. Nelson and David E. Corder, **The Workstation Clustering Environment at NASA Langley Research Center**, *3rd Annual Computational Aerosciences (CAS) Workshop*, Mountain View, CA, August 13-15, 1996, pp. 6, (96KB).

Format(s): Postscript, or PDF

Keywords: Workstation clustering; Distributed Computing Environment; DCE; Distributed File Service, DFS

Abstract: This paper introduces the status of and lessons learned from the workstation clustering projects at NASA Langley Research Center: the Borg, a tightly coupled, homogeneous cluster and the Hive, a loosely coupled, heterogeneous cluster. Specifically, the role of the Open Software Foundation's Distributed Computing Environment and Distributed File Service (DCE/DFS) is discussed with emphasis on cluster functionality gained and lost through DCE/DFS. Finally, future directions for DCE/DFS for Langley Research Center and the rest of NASA are proposed.

24.

William H. Prosser, **Applications of Advanced, Waveform Based AE Techniques for Testing Composite Materials**, *SPIE Conference on Nondestructive Evaluation Techniques for Aging Infrastructure and Manufacturing: Materials and Composites*, Scottsdale, Arizona, December 3-5, 1996, pp. 8, (84KB).

Format(s): Postscript, or PDF

Keywords: Acoustic emission; Composite materials; Nondestructive evaluation; Plate waves; Attenuation; Modal analysis

Abstract: Advanced, waveform based acoustic emission (AE) techniques have been previously used to evaluate damage progression in laboratory tests of composite coupons. In these tests, broad band, high fidelity acoustic sensors were used to detect signals which were then digitized and stored for analysis. Analysis techniques were based on plate mode wave propagation characteristics. This approach, more recently referred to as Modal AE, provides an enhanced capability to discriminate and eliminate noise signals from those generated by damage mechanisms. This technique also allows much more precise source location than conventional, threshold crossing arrival time determination techniques. To apply Modal AE concepts to the interpretation of AE on larger composite structures, the effects of wave propagation over larger distances and through structural complexities must be well characterized and understood. In this

research, measurements were made of the attenuation of the extensional and flexural plate mode components of broad band simulated AE signals in large composite panels. As these materials have applications in a cryogenic environment, the effects of cryogenic insulation on the attenuation of plate mode AE signals were also documented.

25.

Xian-He Sun and Stuti Moitra, **Performance Comparison of a Set of Periodic and Non-Periodic Tridiagonal Solvers on SP2 and Paragon Parallel Computers**, *Concurrency: Practice and Experience*, vol. 9, no. 8, 1997, pp. 781-801, (196KB).

Format(s): Postscript, or PDF

Keywords: Parallel; Tridiagonal solvers; Periodic; Non-Periodic

Abstract: Various tridiagonal solvers have been proposed in recent years for different parallel platforms. In this paper, the performance of three tridiagonal solvers, namely, the parallel partition LU algorithm, the parallel diagonal dominant algorithm, and the reduced diagonal dominant algorithm, is studied. These algorithms are designed for distributed-memory machines and are tested on an Intel Paragon and an IBM SP2 machines. Measured results are reported in terms of execution time and speedup. Analytical study are conducted for different communication topologies and for different tridiagonal systems. The measured results match the analytical results closely. In addition to address implementation issues, performance considerations such as problem sizes and models of speedup are also discussed.

26.

Eugene A. Morelli, **Piloted Parameter Identification Flight Test Maneuvers for Closed Loop Modeling of the F-18 High Alpha Research Vehicle (HARV)**, CR-198268, May 1996, pp. 31, (215KB).

Keywords: Flight test maneuvers; Parameter identification; Optimal input design; Closed loop modeling; Pilot implementation; F-18 HARV

Abstract: Flight test maneuvers are specified for the F-18 High Alpha Research Vehicle (HARV). The maneuvers were designed for closed loop parameter identification purposes, specifically for longitudinal and lateral linear model parameter estimation at 5, 20, 30, 45, and 60 degrees angle of attack, using the NASA 1A control law. Each maneuvers is to be realized by the pilot applying square wave inputs to specific pilot station controls. Maneuver descriptions and complete specifications of the time/amplitude points defining each input are included, along with plots of the input time histories.

27.

Eugene A. Morelli, **Parameter Identification Flight Test Maneuvers for Closed Loop Modeling of the F-18 High Alpha Research Vehicle (HARV)**, CR-198269, May 1996, pp. 35, (256KB).

Keywords: Flight test maneuvers; Parameter identification; Optimal input design; Closed loop modeling; Thrust vectoring; F-18 HARV

Abstract: Flight test maneuvers are specified for the F-18 High Alpha Research Vehicle (HARV). The maneuvers were design for closed loop parameter identification purposed, specifically for longitudinal and lateral linear model parameter estimation at 5, 20, 30, 45, and 60 degrees angle of attack, using the Actuated Nose Strakes for Enhanced Rolling (ANSER) control law in Thrust Vectoring (TV) mode. Each maneuver is to be realized by applying square wave inputs to specific pilot station controls using the On-Board Excitation System (OBES). Maneuver descriptions and complete specifications of the time/amplitude points defining each input are included, along with plots of the input time histories.

28.

Eugene A. Morelli, **Flight Test Maneuvers for Closed Loop Lateral-Directional Modeling of the F-18 High Alpha Research Vehicle (HARV) Using Forebody Strakes**, CR-198270, May 1996, pp. 23, (182KB).

Keywords: Flight test maneuvers; Parameter identification; Optimal input design; Closed loop modeling; Forebody strakes; F-18 HARV

Abstract: Flight test maneuvers are specified for the F-18 High Alpha Research Vehicle (HARV). The maneuvers were designed for closed loop parameter identification purposes, specifically for lateral linear model parameter estimation at 30, 45, and 60 degrees angle of attack, using the Actuated Nose Strakes for Enhanced Rolling (ANSER) control law in Strake (s) model and Strake/Thrust Vectoring (STV) mode. Each maneuver is to be realized by applying square wave inputs to specific pilot station controls using the On-Board Excitation System (OBES). Maneuver descriptions and complete specification of the time/amplitude points defining each input are included, along with plots of the input time histories.

29.

Bart A. Singer, **Large-Eddy Simulation of Turbulent Wall-Pressure Fluctuations**, NASA CR-198276, February 1996, pp. 33, (596KB).

Format(s): Postscript, or PDF

Keywords: Large-Eddy simulation; Aircraft noise; LES; Wall-Pressure fluctuations

Abstract: Large-eddy simulations of a turbulent boundary layer with Reynolds number based on displacement thickness equal to 3500 were performed with two grid resolutions. The computations were continued for sufficient time to obtain frequency spectra with resolved frequencies that correspond to the most important structural frequencies on an aircraft fuselage. The turbulent stresses were adequately resolved with both resolutions. Detailed quantitative analysis of a variety of statistical quantities associated with the wall-pressure fluctuations revealed similar behavior for both simulations. The primary differences were associated with the lack of resolution of the high-frequency data in the coarse-grid calculation and the increased jitter (due to the lack of multiple realizations for averaging purposes) in the fine-grid calculation. A new curve

fit was introduced to represent the spanwise coherence of the cross-spectral density.

30.

S. Gupta, **Constrained Solutions of a System of Matrix Equations**, NASA CR-198288, February 1996, pp. 13, (63KB).

Format(s): Postscript, or PDF

Keywords: Eigensystem assignment; Constant gain dissipative controller; Minimax programming

Abstract: This report presents a technique for constrained solution of a system of matrix equations which arises in the problem of pole placement with static dissipative output feedback. Previously developed necessary conditions for the existence of a solution are shown to be sufficient as well. A minimax approach is presented to determine a feasible coefficient vector that satisfies these conditions. A procedure to construct the desired solution matrix, based on minimax programming techniques is detailed. Numerical examples are presented to illustrate the application of this approach.

31.

J. Rushby, **A Formally Verified Algorithm for Clock Synchronization Under a Hybrid Fault Model**, NASA CR-198289, March 1996, pp. 41, (75KB).

Format(s): Postscript, or PDF

Keywords: Clock synchronization; Formal methods; Byzantine fault tolerance; Hybrid fault models; Formal methods; Formal verification

Abstract: A small modification to the interactive convergence clock synchronization algorithm allows it to tolerate a larger number of simple faults than the standard algorithm, without reducing its ability to tolerate arbitrary or "Byzantine" faults. Because the extended case-analysis required by the new fault model complicates the already intricate argument for correctness of the algorithm, it has been subjected to mechanically-checked formal verification. The fault model examined is similar to the "hybrid" one previously used for the problem of distributed consensus: In addition to arbitrary faults, we also admit symmetric (i.e., consistent) and manifest (i.e., detectable) faults. With n processors, the modified algorithm can withstand a arbitrary s symmetric, and m manifest faults simultaneously, provided $n > 3a + 2s + m$. A further extension to the fault model includes link faults with bound $n > 3a + 2s + m + l$ where l is the maximum, over all pairs of processors, of the number of processors that have faulty links to one or other of the pair. The mechanically-checked formal verification of the modified algorithm was achieved by extending one for the classical Interactive Convergence algorithm, and was accomplished relatively easily. A mechanically-checked formal specification and verification is a reusable intellectual resource whose initial cost is amply repaid by the support it provides for inexpensive and reliable investigation of modified assumptions and algorithms such as those reported here.

32.

B. A. Singer, **Turbulent Wall-Pressure Fluctuations: New Model for Off-Axis Cross-Spectral Density**, NASA CR-198297, March 1996, pp. 11, (185KB) Corrected Copy (December 1996).

Format(s): Postscript, or PDF

Keywords: Wall-pressure; Pressure model; Corcos model; Cross-spectral density

Abstract: Models for the distribution of the wall-pressure under a turbulent boundary layer often estimate the coherence of the cross-spectral density in terms of a product of two coherence functions. One such function describes the coherence as a function of separation distance in the mean-flow direction, the other function describes the coherence in the cross-stream direction. Analysis of data from a large-eddy simulation of a turbulent boundary layer reveals that this approximation dramatically underpredicts the coherence for separation directions that are neither aligned with nor perpendicular to the mean-flow direction. These models fail even when the coherence functions in the directions parallel and perpendicular to the mean flow are known exactly. A new approach for combining the parallel and perpendicular coherence functions is presented. The new approach results in vastly improved approximations for the coherence.

33.

M. B. Lance, **CLMNANAL: A C++ Program for Application of the Coleman Stability Analysis to Rotorcraft**, NASA CR-201592, August 1996, pp. 71, (101KB).

Format(s): Postscript, or PDF

Keywords: Ground resonance; Rotorcraft; Multiple-bladed rotor systems

Abstract: This program is an adaptation of the theory of Robert P. Coleman and Arnold M. Feingold as presented in NACA Report 1351, 1958. This theory provided a method for the analysis of multiple-bladed rotor systems to determine the system susceptibility to ground resonance. Their treatment also provided a simple means for determining the required product of rotor and chassis damping factors to suppress the resonance. This C++ program is based on a FORTRAN 77 version of a similar code.

34.

D. S. Prichard, **ROTONET Primer**, NASA CR-201593, October 1996, pp. 87, (210KB).

Format(s): Postscript, or PDF

Keywords: Aircraft noise; Noise prediction; Rotorcraft; Helicopter

Abstract: This document provides a brief overview of use of the ROTONET rotorcraft system noise prediction capability within the Aircraft Noise Program (ANOPP). Reviews are given on rotorcraft noise, the state-of-the-art of system noise prediction, and methods for using the various ROTONET prediction modules.

35.

G. F. Switzer and C. L. Britt, **Performance of the NASA Airborne Radar With the Windshear Database for Forward-Looking Systems**, NASA CR-201607, September 1996, pp. 85, (643KB).

Format(s): Postscript, or PDF

Keywords: Weather radar; Airborne; Doppler radar; Windshear Microburst; Aircraft safety; FAA certification

Abstract: This document contains a description of the simulation approach used to test the performance of the NASA airborne windshear radar. Explanation of the actual radar hardware and processing algorithms provides an understanding of the parameters used in the simulation program. This report also contains a brief overview of the NASA airborne windshear radar experimental flight test results. A description of the radar simulation program shows the capabilities of the program and the techniques used for certification evaluation. Simulation of the NASA radar is comprised of three steps. First, the choice of the ground clutter data must be made. The ground clutter is the return from objects in or nearby an airport facility. The choice of the ground clutter also dictates the aircraft flight path since ground clutter is gathered while in flight. The second step is the choice of the radar parameters and the running of the simulation program which properly combines the ground clutter data with simulated windshear weather data. The simulated windshear weather data is comprised of a number of TASS (Terminal Area Simulation System) model results. The final step is the comparison of the radar simulation results to the known windshear data base. The final evaluation of the radar simulation is based on the ability to detect hazardous windshear with the aircraft at a safe distance while at the same time not displaying false alerts.

36.

Brian R. Hollis, **Experimental and Computational Aerothermodynamics of a Mars Entry Vehicle**, NASA CR-201633, December 1996, pp. 638, (26MB).

Format(s): Postscript, or PDF

Keywords: Entry vehicle; Wake flow; Computational fluid dynamics; Wind tunnel; Expansion tube; Grid adaptation; Aerothermodynamics; Mars

Abstract: An aerothermodynamic database has been generated through both experimental testing and computational fluid dynamics simulations for a 70 deg sphere-cone configuration based on the NASA Mars-Pathfinder entry vehicle. The aerothermodynamics of several related parametric configurations were also investigated. Experimental heat-transfer data were obtained at hypersonic test conditions in both a perfect-gas air wind tunnel and in a hypervelocity, high-enthalpy expansion tube in which both air and carbon dioxide were employed at test gases. In these facilities, measurements were made with thin-film temperature-resistance gages on both the entry vehicle models and on the support stings of the models. Computational results for freestream conditions equivalent to those of the test facilities were generated using an axisymmetric/2D laminar Navier-Stokes solver with both perfect-gas and nonequilibrium thermochemical models.

Forebody computational and experimental heating distributions agreed to within the experimental uncertainty for both the perfect-gas and high-enthalpy test conditions. In the wake, quantitative differences between experimental and computational heating distributions for the perfect-gas conditions indicated transition of the free shear layer near the reattachment point on the sting. For the high-enthalpy cases, agreement to within, or slightly greater than, the experimental uncertainty was achieved in the wake except within the recirculation region, where further grid resolution appeared to be required. Comparisons between the perfect-gas and high-enthalpy results indicated that the wake remained laminar at the high-enthalpy test conditions, for which the Reynolds number was significantly lower than that of the perfect-gas conditions.

37.

Sandra V. Koppen, **A Description of the Software Element of the NASA EME Flight Tests**, NASA CR-201635, December 1996, pp. 10, (126KB).

Format(s): Postscript, or PDF

Keywords: Electromagnetic environment (EME); NASA Boeing 757; Data acquisition; Data reduction; Radio Frequency (RF); EME modeling; Flight test; ARINC 429; GPS; General Purpose Interface Bus (GPIB)

Abstract: In support of NASA's Fly-By-Light/Power-By-Wire (FBL/PBW) program, a series of flight tests were conducted by NASA Langley Research Center in February, 1995. The NASA Boeing 757 was flown past known RF transmitters to measure both external and internal radiated fields. The aircraft was instrumented with strategically located sensors for acquiring data on shielding effectiveness and internal coupling. The data are intended to support computational and statistical modeling codes used to predict internal field levels of an electromagnetic environment (EME) on aircraft. The software was an integral part of the flight tests, as well as the data reduction process. The software, which provided flight test instrument control, data acquisition, and a user interface, executes on a Hewlett Packard (HP) 300 series workstation and uses HP VEEtest development software and the C programming language. Software tools were developed for data processing and analysis, and to provide a database organized by frequency bands, test runs, and sensors. This paper describes the data acquisition system on board the aircraft and concentrates on the software portion. Hardware and software interfaces are illustrated and discussed. Particular attention is given to data acquisition and data format. The data reduction process is discussed in detail to provide insight into the characteristics, quality, and limitations of the data. An analysis of obstacles encountered during the data reduction process is presented.

38.

W. E. Milholen, II and N. Chokani, **Computational Analysis of Semi-Span Model Test Techniques**, CR-4709, March 1996, pp. 225, (25MB).

Format(s): Postscript, or PDF

Keywords: Semi-span model; Navier-Stokes solutions; Stand-off height; Metric stand-off; Local blowing jets; Upstream blowing slot; Sidewall suction; National Transonic Facility

Abstract: A computational investigation was conducted to support the development of a semi-span model test capability in the NASA LaRC's National Transonic Facility. This capability is required for the testing of high-lift systems at flight Reynolds numbers. A three-dimensional Navier-Stokes solver was used to compute the low-speed flow over both a full-span configuration and a semi-span configuration. The computational results were found to be in good agreement with the experimental data. The computational results indicate that the stand-off height has a strong influence on the flow over a semi-span model. The semi-span model adequately replicates the aerodynamic characteristics of the full-span configuration when a small stand-off height, approximately twice the tunnel empty sidewall boundary layer displacement thickness, is used. Several active sidewall boundary layer control techniques were examined including: upstream blowing, local jet blowing, and sidewall suction. Both upstream tangential blowing, and sidewall suction were found to minimize the separation of the sidewall boundary layer ahead of the semi-span model. The required mass flow rates are found to be practicable for testing in the NTF. For the configuration examined, the active sidewall boundary layer control techniques were found to be necessary only near the maximum lift conditions.

39.

Sandeep Gupta, **Robust Stabilization of Uncertain Systems Based on Energy Dissipation Concepts**, NASA CR-4713, March 1996, pp. 94, (323KB).

Format(s): Postscript, or PDF

Keywords: State space characterization of dissipative LTI systems; Stability of interconnected dissipative systems; Linear Matrix Inequalities (LMI's) for robust stability

Abstract: Robust stability conditions obtained through generalization of the notion of energy dissipation in physical systems are discussed in this report. Linear time-invariant (LTI) systems which dissipate energy corresponding to quadratic power functions are characterized in the time-domain and the frequency-domain, in terms of linear matrix inequalities (LMIs) and algebraic Riccati equations (AREs). A novel characterization of strictly dissipative LTI systems is introduced in this report. Sufficient conditions in terms of dissipativity and strict dissipativity are presented for (1) stability of the feedback interconnection of dissipative LTI systems, (2) stability of dissipative LTI systems with memoryless feedback nonlinearities, and (3) quadratic stability of uncertain linear systems. It is demonstrated that the framework of dissipative LTI systems investigated in this report unifies and extends small gain, passivity, and sector conditions for stability. Techniques for selecting power functions for characterization of uncertain plants and robust controller synthesis based on these stability results are introduced. A spring-mass-damper example is used to illustrate the application of these methods for robust controller synthesis.

40.

J. Crow, **Finite-State Analysis of Space Shuttle Contingency Guidance Requirements**, NASA CR-4741, May 1996, pp. 43, (158KB).

Format(s): Postscript, or PDF

Keywords: Formal methods; Shuttle flight software; Requirements analysis

Abstract: This report describes a finite-state analysis of the mode-sequencing requirements for the contingency Three-Engines-Out Guidance function of the Space Shuttle flight control system.

41.

J. Delbrey, **Database of Mechanical Properties for Textile Composites**, NASA CR-4747, August 1996, pp. 34, (359KB) Also contains a TAR File containing ASCII, tab delimited files which can be imported into any spreadsheet program and an MVISION Database Program.

Format(s): Postscript, or PDF

Keywords: Database; Mechanical properties; Textile composites

Abstract: This report describes the approach followed to develop a database for mechanical properties of textile composites. The data in this database is assembled from NASA Advanced Composites Technology (ACT) programs and from data in the public domain. This database meets the data documentation requirements of MIL-HDBK-17, Section 8.1.2, which describes in detail the type and amount of information needed to completely document composite material properties. The database focuses on mechanical properties of textile composite. Properties are available for a range of parameters such as direction, fiber architecture, materials, environmental condition, and failure mode. The composite materials in the database contain innovative textile architectures such as the braided, woven, and knitted materials evaluated under the NASA ACT programs. In summary, the database contains results for approximately 3500 coupon level tests, for ten different fiber/resin combinations, and seven different textile architectures. It also includes a limited amount of prepreg tape composites data from ACT programs where side-by-side comparisons were made.

42.

K. E. Tatum, **Computation of Thermally Perfect Properties of Oblique Shock Waves**, NASA CR-4749, August 1996, pp. 45, (1MB).

Format(s): Postscript, or PDF

Keywords: Thermally perfect gas; Calorically imperfect gas; Thermally perfect gas computer code; Compressible flow relations; Oblique shock waves; Imperfect gas effects

Abstract: A set of compressible flow relations describing flow properties across oblique shock waves, derived for a thermally perfect, calorically imperfect gas, is applied within the existing thermally perfect gas (TPG) computer code. The relations are based upon a value of c_p expressed as a polynomial function of temperature. The updated code produces tables of compressible flow properties of oblique shock waves, as well as the original properties of normal shock waves and basic isentropic flow, in a format similar to the tables for normal shock waves found in NACA Rep. 1135. The code results are validated in both the calorically perfect and the calorically imperfect, thermally perfect temperature regimes through comparisons with the theoretical methods of NACA Rep. 1135, and with a state-of-the-art computational fluid dynamics code. The advantages of the TPG code for oblique shock wave calculations, as well as for the properties of isentropic flow and normal shock waves, are its ease of use, and its applicability to any type of gas

(monatomic, diatomic, triatomic, polyatomic, or any specified mixture thereof).

43.

J. E. Masters and M. A. Portanova, **Standard Test Methods for Textile Composites**, NASA CR-4751, September 1996, pp. 82, (311KB).

Format(s): Postscript, or PDF

Keywords: Textile composites; Standard test methods; Size effects

Abstract: Standard testing methods for composite laminates reinforced with continuous networks of braided, woven, or stitched fibers have been evaluated. The microstructure of these "textile" composite materials differs significantly from that of tape laminates. Consequently, specimen dimensions and loading methods developed for tape type composites may not be applicable to textile composites. To this end, a series of evaluations were made comparing testing practices currently used in the composite industry. Information was gathered from a variety of sources and analyzed to establish a series of recommended test methods for textile composites. The current practices established for laminated composite materials by ASTM and the in-plane and out-of-plane properties. Specifically, test methods are suggested for unnotched tension and compression, open and filled hole tension, open hole compression, bolt bearing, and interlaminar tension. A detailed description of the material architectures evaluated is also provided, as is a recommended instrumentation practice.

44.

B. L. Di Vito and L. W. Roberts, **Using Formal Methods to Assist in the Requirements Analysis of the Space Shuttle GPS Change Request**, NASA CR-4752, August 1996, pp. 93, (1MB).

Format(s): Postscript, or PDF

Keywords: Formal methods; Requirements analysis; Space shuttle; Flight software; Global positioning system (GPS)

Abstract: We describe a recent NASA-sponsored pilot project intended to gauge the effectiveness of using formal methods in Space Shuttle software requirements analysis. Several Change Requests (CRs) were selected as promising targets to demonstrate the utility of formal methods in this application domain. A CR to add new navigation capabilities to the Shuttle, based on Global Positioning System (GPS) technology, is the focus of this report. Carried out in parallel with the shuttle program's conventional requirements analysis process was a limited form of analysis based on formalized requirements. Portions of the GPS CR were modeled using the language of SRI's Prototype Verification System (PVS). During the formal methods-based analysis, numerous requirements issues were discovered and submitted as official issues through the normal requirements inspection process. Shuttle analysts felt that many of these issues were uncovered earlier than would have occurred with conventional methods. We present a summary of these encouraging results and conclusions we have drawn from the pilot project.

45.

B. R. Hollis, **Real-Gas Flow Properties for NASA Langley Research Center Aerothermodynamic Facilities Complex Wind Tunnels**, NASA CR-4755, September 1996, pp. 62, (375KB).

Format(s): Postscript, or PDF

Keywords: Wind tunnels; Thermodynamic properties; Real gas

Abstract: A computational algorithm has been developed which can be employed to determine the flow properties of an arbitrary real (virial) gas in a wind tunnel. A multiple-coefficient virial gas equation of state and the assumption of isentropic flow are used to model the gas and to compute flow properties throughout the wind tunnel. This algorithm has been used to calculate flow properties for the wind tunnels of the Aerothermodynamics Facilities complex at the NASA Langley Research Center, in which air, CF/subscript 4, He, and N/subscript 2 are employed as test gases. The algorithm is detailed in this paper and sample results are presented for each of the Aerothermodynamic Facilities complex wind tunnels.

46.

G. F. Switzer, **Validation Tests of TASS for Application to 3-D Vortex Simulations**, NASA CR-4756, October 1996, pp. 43, (1MB).

Format(s): Postscript, or PDF

Keywords: Beltrami flow; CFD validation; Aircraft wake vortices; Numerical methods; Computational meteorology

Abstract: Direct analytical solutions can be useful in validating the core formulation of numerical systems. In this document an exact analytical solution to the nonlinear Navier-Stokes equation is compared to the numerical results from the three-dimensional Terminal Area Simulation System (TASS). This exact solution, of which the derivation is included, is for Beltrami type flow. Direct comparison of TASS to the analytical Beltrami solution is then used in evaluating the accuracy of TASS.

47.

C. J. Reddy and M. D. Deshpande, **Application of AWE for RCS Frequency Response Calculations Using Method of Moment**, NASA CR-4758, October 1996, pp. 29, (159KB).

Format(s): Postscript, or PDF

Keywords: Asymptotic Waveform Evaluation (AWE); Method of Moments (MoM); Radar Cross Section (RCS); Frequency response

Abstract: An implementation of the Asymptotic Waveform Evaluation (AWE) technique is

presented for obtaining the frequency response of the Radar Cross Section (RCS) of arbitrarily shaped, three-dimensional perfect electric conductor (PEC) bodies. An Electric Field Integral Equation (EFIE) is solved using the Method of Moments (MoM) to compute the RCS. The electric current, thus obtained, is expanded in a Taylor series around the frequency of interest. The coefficients of the Taylor series (called "moments") are obtained using the frequency derivatives of the EFIE. Using the moments, the electric current on the PEC body is obtained over a frequency band. Using the electric current at different frequencies, RCS of the PEC body is obtained over a wide frequency band. Numerical results for a square plate, a cube, and a sphere are presented over a bandwidth. A good agreement between AWE and the exact solution over the bandwidth is observed.

48.

M. W. Hooker, **Preparation and Properties of High-T_c Bi-Pb-Sr-Ca-Cu-O Thick Film Superconductors on YSZ Substrates**, NASA CR-4761, December 1996, pp. 14, (575KB).

Format(s): Postscript, or PDF

Keywords: Superconductors; Bi-Pb-Sr-Ca-Cu-O; Thick films

Abstract: An evaluation of four firing profiles was performed to determine the optimum processing conditions for producing high-T_c Bi-PB-SR-Ca-Cu-O thick films on yttria-stabilized zirconia substrates. Using these four profiles, the effects of sintering temperatures of 830-850 degrees C and soak times of 0.5 to 12 hours were examined. In this study T_c, zero values of 100K were obtained using a firing profile in which the films were sintered for 1.5 to 2 hours at 840 to 845 degrees C and then quenched to room temperature. X-ray diffraction analyses of these specimens confirmed the presence of the high-T_c phase. Films which were similarly fired and furnace-cooled from the peak processing temperature exhibited a two-step superconductive transition to zero resistance, with T_c, zero values ranging from 85 to 92K. The other firing profiles evaluated in this investigation yielded specimens which either exhibited critical transition temperatures below 90K or did not exhibit a superconductive transition above 77K.

49.

S. C. Johnson, D. K. Chin, R. B. Rovinsky, P. F. Kostiuk, D. A. Lee, R. V. Hemm and E. R. Wingrove, III, **Reduction of Weather-Related Terminal Area Delays in the Free-Flight Era**, *IEEE/AIAA Digital Avionics Systems Conference and Technical Display*, Atlanta, Georgia, October 27-31, 1996, (910KB).

Format(s): Postscript, or PDF

Keywords: Airspace operations; Air traffic management; Cost/benefit analysis

Abstract: While much of the emphasis of the free-flight movement has been concentrated on reducing enroute delays, airport capacity is a major bottleneck in the current airspace system, particularly during bad weather. According to the Air Transport Association (ATA) Air Carrier Delay Reports, ground delays (gate-hold, taxi-in, and taxi-out) comprise 75 percent of total delays. It is likely that the projected steady growth in traffic will only exacerbate these losses.

Preliminary analyses show that implementation of the terminal area technologies and procedures under development in NASA's Terminal Area Productivity program can potentially save the airlines at least \$350M annually in weather-related delays by the year 2005 at Boston Logan and Detroit airports alone. This paper briefly describes the Terminal Area Productivity program, outlines the cost/benefit analyses that are being conducted in support of the program, and presents some preliminary analysis results.

50.

Ronald D. Joslin, **Simulation of Nonlinear Instabilities in an Attachment-Line Boundary Layer**, *Fluid Dynamics Research*, vol. 18, no. 2, October 1996, pp. 81-97, (243KB).

Format(s): Postscript, or PDF

Keywords: Nonlinear disturbances; DNS; Attachment-line transition

Abstract: The linear and nonlinear stability of disturbances that propagate along the attachment line of a three-dimensional boundary layer are considered. The spatially evolving disturbances in the boundary layer are computed by direct numerical simulation (DNS) of the unsteady, incompressible Navier-Stokes equations. Disturbances are introduced either by forcing at the inflow or by applying suction and blowing at the wall. Quasi-parallel linear stability theory and a nonparallel theory yield notably different stability characteristics for disturbances near the critical Reynolds number; the DNS results confirm the latter theory. Previously, a weakly nonlinear theory and computations revealed a high wave-number region of subcritical disturbance growth. More recent computations have failed to achieve this subcritical growth. The present computational results indicate the presence of subcritically growing disturbances; the results support the weakly nonlinear theory. Furthermore, an explanation is provided for the previous theoretical and computational discrepancy. In addition, the present results demonstrate that steady suction can be used to stabilize disturbances that otherwise grow subcritically along the attachment line.

51.

Ronald D. Joslin, Max D. Gunzburger, Roy A. Nicolaides, Gordon Erlebacher and M. Yousuff Hussaini, **A Methodology for the Automated Optimal Control of Flows including Transitional Flows**, *1996 ASME Fluids Engineering Division Conference*, San Diego, California, July 7-11, 1996, pp. 287-294, (214KB).

Format(s): Postscript, or PDF

Keywords: Optimal control theory; DNS; Boundary-layer transition; Adjoint system; Active flow control

Abstract: This paper describes a self-contained, automated methodology for active flow control which couples the time-dependent Navier-Stokes system with the adjoint Navier-Stokes system and optimality conditions from which optimal states, i.e., unsteady flow fields and controls (e.g., actuators), may be determined. The problem of boundary-layer instability suppression through wave cancellation is used as the initial validation case to test the methodology. Here, the objective

of control is to match the wall-normal stress along a portion of the boundary to a given vector; instability suppression is achieved by choosing the given vector to be that of a steady base flow. Control is effected through the injection or suction of fluid through a single orifice on the boundary. The results demonstrate that instability suppression can be achieved without any a priori knowledge of the disturbance. The present methodology may potentially be applied to separation control, relaminarization, and turbulence control applications using one or more sensors and actuators.

52.

J. L. Rogers, C. M. McCulley and C. L. Bloebaum, **Integrating a Genetic Algorithm Into a Knowledge-Based System for Ordering Complex Design Processes**, *Fourth International Conference on Artificial Intelligence in Design '96*, Stanford, California, June 24-27, 1996, (139KB).

Format(s): Postscript, or PDF

Keywords: Design; Scheduling; Genetic algorithm; Sensitivities; Knowledge-based system; Coupling strengths; Decomposition

Abstract: The design cycle associated with large engineering systems requires an initial decomposition of the complex system into design processes which are coupled through the transference of output data. Some of these design processes may be grouped into iterative subcycles. In analyzing or optimizing such a coupled system, it is essential to be able to determine the best ordering of the processes within these subcycles to reduce design cycle time and cost. Many decomposition approaches assume the capability is available to determine what design processes and couplings exist and what order of execution will be imposed during the design cycle. Unfortunately, this is often a complex problem and beyond the capabilities of a human design manager. A new feature, a genetic algorithm, has been added to DeMAID (Design Manager's Aid for Intelligent Decomposition) to allow the design manager to rapidly examine many different combinations of ordering processes in an iterative subcycle and to optimize the ordering based on cost, time, and iteration requirements. Two sample test cases are presented to show the effects of optimizing the ordering with a genetic algorithm.

53.

P. D. Arbuckle, M. S. Lewis, and D. A. Hinton, **Airborne Systems Technology Application to the Windshear Threat**, *20th Congress of the International Council of the Aeronautical Sciences*, Sorrento, Italy, ICAS Paper No. 96-5.7.1, September 8-13, 1996, pp. 1640-1650, (205KB).

Format(s): Postscript, or PDF

Keywords: Airborne windshear detection; Predictive windshear systems

Abstract: The general approach and products of the NASA/FAA Airborne Windshear Program conducted by NASA Langley Research Center are summarized, with references provided for the major technical contributions. During this period, NASA conducted 2 years of flight testing to characterize forward-looking sensor performance. The NASA/FAA Airborne Windshear Program

was divided into three main elements: Hazard Characterization, Sensor Technology, and Flight Management Systems. Simulation models developed under the Hazard Characterization element are correlated with flight test data. Flight test results comparing the performance and characteristics of the various Sensor Technologies (microwave radar, lidar, and infrared) are presented. Most of the activities in the Flight Management Systems element were conducted in simulation. Simulation results from a study evaluating windshear crew procedures and displays for forward-looking sensor-equipped airplanes are discussed. NASA Langley researchers participated heavily in the FAA process of generating certification guidelines for predictive windshear detection systems. NASA participants felt that more valuable technology products were generated by the program because of this interaction. NASA involvement in the process and the resulting impact on products and technology transfer are discussed in this paper.

54.

Paul S. Miner and James F. Leathrum, Jr., **Verification of IEEE Compliant Subtractive Division Algorithms**, *International Conference on Formal Methods in Computer-Aided Design*, Palo Alto, California, November 6-8, 1996, (70KB).

Format(s): Postscript, or PDF

Abstract: A parameterized definition of subtractive floating point division algorithms is presented and verified using PVS. The general algorithm is proven to satisfy a formal definition of an IEEE standard for floating point arithmetic. The utility of the general specification is illustrated using a number of different instances of the general algorithm.

55.

Zia-ur Rahman, Daniel J. Jobson and Glenn A. Woodell, **Multi-Scale Retinex for Color Image Enhancement**, *IEEE 1996 International Conference on Image Processing*, Lausanne, Switzerland, September, 1996, pp. 1003-1006.

Keywords: Image enhancement; Color enhancement; Dynamic range compression

Abstract: The retinex is a human perception-based image processing algorithm which provides color constancy and dynamic range compression. We have previously reported on a single-scale retinex (SSR) and shown that it can either achieve color/lightness rendition or dynamic range compression, but not both simultaneously. We now present a multi-scale retinex (MSR) which overcomes this limitation for most scenes. Both color rendition and dynamic range compression are successfully accomplished except for some "pathological" scenes that have very strong spectral characteristics in a single band.

56.

C. W. Mastin, **Arc Length Based Grid Distribution for Surface and Volume Grids**, *Fifth International Conference on Numerical Grid Generation in Computational Field Simulations*, Starkville, Mississippi, April 1-5, 1996, In Proceedings (192KB).

Format(s): Postscript, or PDF

Keywords: Arc length; Grid generation

Abstract: Techniques are presented for distributing grid points on parametric surfaces and in volumes according to a specified distribution of arc length. Interpolation techniques are introduced which permit a given distribution of grid points on the edges of a three-dimensional grid block to be propagated through the surface and volume grids. Examples demonstrate how these methods can be used to improve the quality of grids generated by transfinite interpolation.

57.

C. Michael Holloway and Ricky W. Butler, **Impediments to Industrial Use of Formal Methods**, *IEEE Computer*, vol. 29, no. 4, April 1996, pp. 25-26.

Keywords: Formal methods; Technology transfer; Mathematics

Abstract: In this piece we argue that the three primary impediments to the wide-scale industrial use of formal methods are (1) inadequate tools, (2) inadequate examples, and (3) a "build it and they will come" expectation. We also suggest ways to overcome each of these impediments.

58.

C. J. Reddy, M. D. Deshpande, C. R. Cockrell and F. B. Beck, **Radiation Characteristics of Cavity Backed Aperture Antennas in Finite Ground Plane Using the Hybrid FEM/MoM Technique and Geometrical Theory of Diffraction**, *IEEE Transactions on Antennas and Propagation*, vol. 10, October 1996, pp. 7, (430KB).

Format(s): Postscript, or PDF

Abstract: A technique using hybrid Finite Element Method (FEM)/Method of Moments(MoM), and Geometrical Theory of Diffraction (GTD) is presented to analyze the radiation characteristics of cavity fed aperture antennas in a finite ground plane. The cavity which excites the aperture is assumed to be fed by a cylindrical transmission line. the electromagnetic (EM) fields inside the cavity are obtained using FEM. The EM fields and their normal derivatives required for FEM solution are obtained using (1) the modal expansion in the feed region and (2) the MoM for the radiating aperture region (assuming an infinite ground plane). The finiteness of the ground plane is taken into account using GTD. The input admittance of open ended circular, rectangular, and coaxial line radiating into free space through an infinite ground plane are computed and compared with earlier published results. Radiation characteristics of a coaxial cavity fed circular aperture in a finite rectangular ground plane are verified with experimental results.

59.

S. Mayor, W. L. Smith, Jr., L. Nguyen, T. A. Alberta, P. Minnis, C. H. Whitlock and G. L. Schuster, **Asymmetry in the Diurnal Variation of Surface Albedo**, *International Geoscience and Remote Sensing Symposium*, Lincoln, Nebraska, May 27-31, 1996, (29KB).

Format(s): Postscript, or PDF

Keywords: Albedo; Radiation budget; Surface albedo; ARM; Dew; Remote sensing

Abstract: Remote sensing of surface properties and estimation of clear-sky and surface albedo generally assumes that the albedo depends only on the solar zenith angle. The effects of dew, frost, and precipitation as well as evaporation and wind can lead to some systematic diurnal variability resulting in an asymmetric diurnal cycle of albedo. This paper examines the symmetry of both surface-observed albedos and top-of-the-atmosphere (TOA) albedos derived from satellite data. Broadband and visible surface albedos were measured at the Department of Energy Atmospheric Radiation Measurement (ARM) Program Southern Great Plains Central Facility, at some fields near the ARM site, and over a coniferous forest in eastern Virginia. Surface and wind conditions are available for most cases. GOES-8 satellite radiance data are converted to broadband albedo using bidirectional reflectance functions and an empirical narrowband-to-broadband relationship. The initial results indicate that surface moisture has a significant effect and can change the albedo in the afternoon by 20 percent relative to its morning counterpart. Such effects may need to be incorporated in mesoscale and even large-scale models of atmospheric processes.

60.

A. S. Moore, K. E. Brown, W. M. Hall, J. C. Barnes, W. C. Edwards, L. B. Petway, A. D. Little, W. S. Luck, I. W. Jones, C. W. Antill, E. V. Browell and S. Ismail, **Development of the Lidar Atmospheric Sensing Experiment (LASE) - An Advanced Airborne DIAL Instrument**, *18th International Laser Radar Conference (ILRC)*, Berlin, Germany, July 22-26, 1996, (93KB).

Format(s): Postscript, or PDF

Keywords: Lidar; DIAL; Laser; Ti:Sapphire; Water vapor; Atmospheric sensor

Abstract: The Lidar Atmospheric Sensing Experiment (LASE) Instrument is the first fully-engineered, autonomous differential Absorption Lidar (DIAL) System for the measurement of water vapor in the troposphere (aerosol and cloud measurements are included). LASE uses a double-pulsed Ti:Sapphire laser for the transmitter with a 30 ns pulse length and 150 mJ/pulse. The laser beam is "seeded" to operate on a selected water vapor absorption line in the 815-nm region using a laser diode and an onboard absorption reference cell. A 40 cm diameter telescope collects the backscattered signals and directs them onto two detectors. LASE collects DIAL data at 5 Hz while onboard a NASA/Ames ER-2 aircraft flying at altitudes from 16-21 km. LASE was designed to operate autonomously within the environment and physical constraints of the ER-2 aircraft and to make water vapor profile measurements across the troposphere to better than 10 percent accuracy. LASE has flown 19 times during the development of the instrument and the validation of the science data. This paper describes the design, operation, and reliability of the LASE Instrument.

61.

R. E. Campbell, E. V. Browell, S. Ismail, A. E. Dudenzak, A. I. Carswell and A. Ulitsky, **Feasibility Study for a Spaceborne Ozone/Aerosol Lidar System**, *18th International Laser Radar Conference (ILRC)*, Berlin, Germany, July 22-26, 1996, (72KB).

Format(s): Postscript, or PDF

Keywords: Ozone; Remote sensing; Differential absorption lidar; Spacecraft; Clouds; Aerosols; Lasers

Abstract: Because ozone provides a shield against harmful ultraviolet radiation, determines the temperature profile in the stratosphere, plays important roles in tropospheric chemistry and climate, and is a health risk near the surface, changes in natural ozone layers at different altitudes and their global impact are being intensively researched. Global ozone coverage is currently provided by passive optical and microwave satellite sensors that cannot deliver high spatial resolution measurements and have particular limitations in the troposphere. Vertical profiling Differential Absorption Lidars (DIAL) have shown excellent range-resolved capabilities, but these systems have been large, inefficient, and have required continuous technical attention for long term operations. Recently, successful, autonomous DIAL measurements have been performed from a high-altitude aircraft (LASE - Lidar Atmospheric Sensing Experiment), and a space-qualified aerosol lidar system (LITE - Laser In-space Technology Experiment) has performed well on Shuttle. Based on the above successes, NASA and the Canadian Space Agency are jointly studying the feasibility of developing ORACLE (Ozone Research with Advanced Cooperative Lidar Experiments), and autonomously operated, compact DIAL instrument to be placed in orbit using a Pegasus class launch vehicle.

62.

Nancy Holloway, **Fabricating Adhesiveless Polyimide Multilayer Flex Circuits**, *IPC National Conference on Flex Circuits*, Bedford, Massachusetts, April 22-23, 1996, (6MB).

Format(s): Postscript, or PDF

Keywords: Adhesiveless; Circuits; Electronic; Flexible; Multilayer; Polyimide; Self-bonding; Spray coating

Abstract: Future electronic systems for aeronautical, space, and consumer applications will have to be smaller, lighter, require more efficient circuitry and survive harsher environments. As these electronic systems become increasingly more complex, the requirements are driven towards denser circuitry and higher layer count (multilayer) circuits. To meet these needs, designers will have to increasingly rely on lightweight multilayer flexible circuits and cables made from higher performance materials. Flex circuits have been produced on numerous materials, from aramid paper to very thin flexible fiberglass. Currently, most flex circuits are produced on either polyester or polyimide film. Polyester, being economically feasible to produce and having favorable dielectric properties, makes it a widely used material in the flex circuit industry. The main disadvantage to using polyester is its inability to withstand high temperatures; therefore making soldering a difficult process. Polyimide, a premium thermoplastic, can be exposed to elevated temperatures, numerous chemicals, and be repeatedly soldered without degradation. The main disadvantage to using polyimide film is the greater cost compared to polyester. Polyimide film, because of its high performance characteristics, is almost always used to produce military and aerospace flex circuits.

63.

Michael L. Nelson and Ming-Hokng Maa, **Optimizing the NASA Technical Report Server**, *Internet Research: Electronic Network Applications and Policy*, vol. 6, no. 1, August 1996, pp. 64-70.

Keywords: World Wide Web; NASA Technical Report Server (NTIS); Information distribution, Electronic publishing; Digital Libraries, Information dissemination; Scientific and Technical Information (STI); Parallel information retrieval

Abstract: The NASA Technical Report Server (NTRS), a World Wide Web report distribution NASA technical publications service, is modified for performance enhancement, greater protocol support, and human interface optimization. Results include: Parallel database queries, significantly decreasing user access times by an average factor of 2.3; access from clients behind firewalls and/or proxies which truncate excessively long Uniform Resource Locators (URLs); access to non- Wide Area Information Server (WAIS) databases and compatibility with the Z39-50.3 protocol; and a streamlined user interface.

64.

H. A. Aldridge and J-N. Juang, **System Wide Joint Position Sensor Fault Tolerance in Robot Systems Using Cartesian Accelerometers**, *SPIE's International Symposium on Intelligent Systems and Advanced Manufacturing*, Boston, Massachusetts, November 18-22, 1996, pp. 9, (965KB).

Format(s): Postscript, or PDF

Keywords: Robot control; Fault tolerance; Position sensor; Accelerometer

Abstract: Joint position sensors are necessary for most robot control systems. A single position sensor failure in a normal robot system can greatly degrade performance. This paper presents a method to obtain position information from Cartesian accelerometers without integration. Depending on the number and location of the accelerometers, the proposed system can tolerate the loss of multiple position sensors. A solution technique suitable for real-time implementation is presented. Simulations were conducted using 5 triaxial accelerometers to recover from the loss of up to 4 joint position sensors on a 7 degree of freedom robot moving in general three dimensional space. The simulations show good estimation performance using non-ideal accelerometer measurements.

65.

William H. Prosser, **Advanced AE Techniques in Composite Material Research**, *Journal of Acoustic Emission*, vol. 14, no. 3-4, 1996, pp. 1-11, (147KB).

Format(s): Postscript, or PDF

Keywords: Acoustic emission; Composite materials; Nondestructive evaluation

Abstract: Advanced, waveform based acoustic emission (AE) techniques have been successfully

used to evaluate damage mechanisms in laboratory testing of composite coupons. An example is presented in which the initiation of transverse matrix cracking was monitored. In these tests, broad band, high fidelity acoustic sensors were used to detect signals which were then digitized and stored for analysis. Analysis techniques were based on plate mode wave propagation characteristics. This approach, more recently referred to as Modal AE, provides an enhanced capability to discriminate and eliminate noise signals from those generated by damage mechanisms. This technique also allows much more precise source location than conventional, threshold crossing arrival time determination techniques. To apply Modal AE concepts to the interpretation of AE on larger composite specimens or structures, the effects of modal wave propagation over larger distances and through structural complexities must be well characterized and understood. To demonstrate these effects, measurements of the far field, peak amplitude attenuation of the extensional and flexural plate mode components of broad band simulated AE signals in large composite panels are discussed. These measurements demonstrated that the flexural mode attenuation is dominated by dispersion effects. Thus, it is significantly affected by the thickness of the composite plate. Furthermore, the flexural mode attenuation can be significantly larger than that of the extensional mode even though its peak amplitude consists of much lower frequency components.

66.

M. R. Gorman and W. H. Prosser, **Application of Normal Mode Expansion to AE Waves in Finite Plates**, *Transaction of the ASME: Journal of Applied Mechanics*, vol. 63, no. 2, June, 1996, pp. 555-557, (74KB).

Format(s): Postscript, or PDF

Keywords: Acoustic emission; Plate modes; Flexural mode

Abstract: Breckenridge et al. (1975), Hsu (1985) and Pao (1978) adapted approaches from seismology to calculate the response at the surface of an infinite half-space and an infinite plate. These approaches have found use in calibrating acoustic emission (AE) transducers. However, it is difficult to extend this theoretical approach to AE testing of practical structures. Weaver and Pao (1982) considered a normal mode solution to the Lamb equations. Hutchinson (1983) pointed out the potential relevance of Mindlin's plate theory (1951) to AE. Pao (1982) reviewed Medickos (1961) classical plate theory for a point source, but rejected it as useful for AE and no one seems to have investigated its relevance to AE any further. Herein, a normal mode solution to the classical plate bending equation was investigated for its applicability to AE. The same source-time function chosen by Weaver and Pao is considered. However, arbitrary source and receiver positions are chosen relative to the boundaries of the plate. This is another advantage of the plate theory treatment in addition to its simplicity. The source does not have to be at the center of the plate as in the axisymmetric treatment. The plate is allowed to remain finite and reflections are predicted. The importance of this theory to AE is that it can handle finite plates, realistic boundary conditions, and can be extended to composite materials.

67.

W. K. Anderson, Russ D. Rausch and Daryl L. Bonhaus, **Implicit/Multigrid Algorithms for Incompressible Turbulent Flows on Unstructured Grids**, *Journal of Computational Physics*,

vol. 128, no. 2, October 15, 1996, pp. 391-408, (4MB).

Format(s): Postscript, or PDF

Keywords: Unstructured; Navier Stokes; Incompressible

Abstract: An implicit code for computing inviscid and viscous incompressible flows on unstructured grids is described. The foundation of the code is a backward Euler time discretization for which the linear system is approximately solved at each time step with either a point implicit method or a preconditioned Generalized Minimal Residual (GMRES) technique. For the GMRES calculations, several techniques are investigated for forming the matrix-vector product. Convergence acceleration is achieved through a multigrid scheme that uses non-nested coarse grids that are generated using a technique described in the present paper. Convergence characteristics are investigated and results are compared with an exact solution for the inviscid flow over a four-element airfoil. Viscous results, which are compared with experimental data, include the turbulent flow over a NACA 4412 airfoil, a three-element airfoil for which Mach number effects are investigated, and three-dimensional flow over a wing with a partial-span flap.

68.

Ronald D. Joslin, Gordon Erlebacher and M. Y. Hussaini, **Active Control of Instabilities in Laminar Boundary Layers---Overview and Concept Validation**, *Journal of Fluids Engineering*, vol. 118, September 1996, pp. 494-497, (84KB).

Format(s): Postscript, or PDF

Keywords: Optimal control theory; DNS; Active flow control; Wave-cancellation

Abstract: This paper focuses on using active-control methods to maintain laminar flow in a region of the flow in which the natural instabilities, if left unattended, lead to turbulent flow. The authors review previous studies that examine wave cancellation (currently the most prominent method) and solve the unsteady, nonlinear Navier-Stokes equations to evaluate this method of controlling instabilities. It is definitely shown that instabilities are controlled by the linear summation of waves (i.e., wave cancellation). Although a mathematically complete method for controlling arbitrary instabilities has been developed, the review, duplication, and physical explanation of previous studies are important steps for providing an independent verification of those studies, for establishing a framework for the work which will involve automated transition control, and for detailing the phenomena by-which the automated studies can be used to expand knowledge of flow control.

69.

K. B. Lim and W. Gawronski, **Hankel Singular Values of Flexible Structures in Discrete Time**, *Journal of Guidance, Control, and Dynamics*, vol. 19, no. 6, November--December 1996, pp. 1370-1377, (243KB) Also appeared as AIAA Paper 96-3757.

Format(s): Postscript, or PDF

Keywords: Hankel singular values; Flexible structures; Actuator and sensor placement

Abstract: Approximate analytical expressions for controllability and observability grammian matrices and Hankel singular values of discrete LTI flexible structures are derived. The diagonal dominance property of the discrete grammians is shown which results in the invariance of the principal directions. The approximate discrete Hankel singular values converge to the continuous formula with increased sampling rate while the controllability and observability grammians go to zero and infinity respectively. The approximate formula are accurate up to frequencies close to the Nyquist.

70.

Kyong B. Lim, **Robust Control Design Framework for Substructure Models**, *Journal of Guidance, Control, and Dynamics*, vol. 19, no. 1, January-February, 1996, pp. 181-190, (332KB)
Also appeared as AIAA Paper No 94-1699.

Format(s): Postscript, or PDF

Keywords: Robust control; Substructure synthesis; Component mode synthesis; Decentralized control; Large flexible structures

Abstract: A framework for designing control systems directly from substructure models and uncertainties is proposed. The technique is based on combining a set of substructure robust control problems by an interface stiffness matrix which appears as a constant gain feedback. Variations of uncertainties in the interface stiffness are treated as a parametric uncertainty. It is shown that multivariable robust control can be applied to generate centralized or decentralized controllers that guarantee performance with respect to uncertainties in the interface stiffness, reduced component modes and external disturbances. The technique is particularly suited for large, complex, and weakly coupled flexible structures.

71.

D. F. Perey, **A Portable Surface Contamination Monitor Based on the Principle of Optically Stimulated Electron Emission (OSEE)**, *1996 JANNAF Propulsion and Joint Subcommittee Meetings*, Albuquerque, New Mexico, December 9-13, 1996, pp. 8, (56KB).

Format(s): Postscript, or PDF

Keywords: Quantitative; Surface; Contaminant; Measurement; Instrument; Optical; Non-contact

Abstract: Many industrial and aerospace processes involving the joining of materials, require sufficient surface cleanliness to insure proper bonding. Processes as diverse as painting, welding, or the soldering of electronic circuits will be compromised if prior inspection and removal of surface contaminants is inadequate. As process requirements become more stringent and the number of different materials and identified contaminants increases, various instruments and techniques have been developed for improved inspection. One such technique, based on the principle of Optically Stimulated Electron Emission (OSEE), has been explored for a number of years as a tool for surface contamination monitoring. Some of the benefits of OSEE are: it is non-

contacting; requires little operator training; and has very high contamination sensitivity. This paper describes the development of a portable OSEE based surface contamination monitor. The instrument is suitable for both hand-held and robotic inspections with either manual or automated control of instrument operation. In addition, instrument output data is visually displayed to the operator and may be sent to an external computer for archiving or analysis.

72.

John V. Shebalin, **Absolute Equilibrium Entropy**, *Journal of Plasma Physics*, vol. 56, December 1996, pp. 419-426, (50KB).

Format(s): Postscript, or PDF

Keywords: Ideal flows; H-theorems; Entropy

Abstract: The entropy associated with absolute equilibrium ensemble theories of ideal, homogeneous, fluid and magnetofluid turbulence is discussed, and the three-dimensional fluid case is examined in detail.

73.

G. L. Pellett, **Review of $H_{sub}xP_{sub}yO_{sub}z$ ---Catalyzed $H + OH$ Recombination in Scramjet Nozzle Expansions; and Possible Phosphoric Acid Enhancement of Scramjet Flameholding, From Extinction of $H_{sub}3PO_{sub}4 + H_{sub}2$ ---Air Counterflow Diffusion Flames**, 1996 JANNAF Propulsion and Subcommittee Joint Meeting, Albuquerque, New Mexico, December 9-13, 1996, Published in Proceedings, CPIA Pub. 654, Volume 1, December 1996, p. 369-384. (807KB).

Format(s): Postscript, or PDF

Keywords: Scramjet; Nozzle; Expansion; Recombination; H-Atom; Catalyzed; Phosphorus; Phosphoric acid; Combustion; Extinction; Flameholding

Abstract: Recent detailed articles by Twarowski indicate that small quantities of phosphorus oxides and acids in the fuel-rich combustion products of $H_{sub}2$ plus phosphine ($PH_{sub}3$) plus air should significantly catalyze H, OH and O recombination kinetics during high-speed nozzle expansions---to reform $H_{sub}2O$, release heat, and approach equilibrium more rapidly and closely than uncatalyzed kinetics. This paper is an initial feasibility study to determine (a) if addition of phosphoric acid vapor ($H_{sub}3PO_{sub}4$) to a $H_{sub}2$ fuel jet---which is much safer than using $PH_{sub}3$ ---will allow combustion in a high-speed scramjet engine test without adverse effects on localized flameholding, and (b) if phosphorus-containing exhaust emissions are environmentally acceptable. A well-characterized axisymmetric straight-tube opposed jet burner (OJB) tool is used to evaluate $H_{sub}3PO_{sub}4$ addition effects on the air velocity extinction limit (flame strength) of a $H_{sub}2$ versus air counterflow diffusion flame. Addition of nitric oxide (NO), also believed to promote catalytic H-atom recombination, was evaluated for comparison. Two to five mass percent $H_{sub}3PO_{sub}4$ in the $H_{sub}2$ jet increased flame strength 4.2 percent, whereas airside addition decreased it 1 percent. Adding 5 percent NO to the $H_{sub}2$ caused a 2 percent decrease. Products of H-atom attack on $H_{sub}3PO_{sub}4$ produced an intense green chemiluminescence near the

stagnation point. The resultant exothermic production of phosphorus oxides and acids, with accelerated H-atom recombination, released sufficient heat near the stagnation point to increase flame strength. In conclusion, the addition of H_3PO_4 vapor (or more reactive P sources) to hydrogen in scramjet engine tests may positively affect flameholding stability in the combustor and thrust production during supersonic expansion---a possible dual benefit with system design/performance implications. Finally, a preliminary assessment of possible environmental effects indicates that scramjet exhaust emissions should consist of phosphoric acid aerosol, with gradual conversion to phosphate aerosol. This is compared to various natural abundances and sources.

74.

J. O. Simpson, Z. Ounaies and C. C. Fay, **Polarization and Piezoelectric Properties of a Nitrile Substituted Polyimide**, *Materials Research Society 1996 Fall Meeting*, Boston, Massachusetts, December 2-6, 1996, (720KB).

Format(s): Postscript, or PDF

Abstract: This research focuses on the synthesis and characterization of a piezoelectric (Beta-CN)-APB/ODPA polyimide. the remanent polarization and piezoelectric d_{31} and g_{33} coefficients are reported to assess the effect of synthesis variations. Each of the materials exhibits a level of piezoelectricity which increases with temperature. the remanent polarization is retained at temperatures close to the glass transition temperature of the polyimide.

75.

Z. Ounaies, J. A. Young, J. O. Simpson and B. L. Farmer, **Dielectric Properties of Piezoelectric Polyimides**, *Materials Research Society 1996 Fall Meeting*, Boston, Massachusetts, December 2-6, 1996, pp. 6, (659KB).

Format(s): Postscript, or PDF

Keywords: Polyimides; Remanent polarization; Molecular modeling; Piezoelectricity

Abstract: Molecular modeling and dielectric measurements are used to identify mechanisms governing piezoelectric behavior in polyimides such as dipole orientation during poling and degree of piezoelectricity achievable. Molecular modeling on polyimides containing pendant, polar nitrile (CN) groups has been completed to determine their remanent polarization. Experimental investigation of dielectric properties evaluated as a function of temperature and frequency has substantiated numerical predictions. With this information, we are able to suggest changes in the molecular structures which will improve the piezoelectric response.

76.

Yvette Y. Tang, Richard J. Silcox and Jay H. Robinson, **Modeling of Sound Transmission Through Shell Structures With Turbulent Boundary Layer Excitation**, *1996 National Conference on Noise Control Engineering (NOISE-CON 96)*, Bellevue, Washington, September

29--October 2, 1996, pp. 6, (188KB).

Format(s): Postscript, or PDF

Keywords: Sound transmission; Turbulent boundary layer; Cylindrical shell; Modal compositions

Abstract: This paper is to develop an analytical model of sound transmission through a simple unstiffened cylindrical aluminum shell excited by a TBL pressure field based on the Corcos formulation for the cross-spectral density (CSD) of the pressure fluctuations. The coupled shell and interior and exterior acoustic equations are solved for the structural displacement and the interior acoustic response using a Galerkin approach to obtain analytical solutions. Specifically, this study compares the real part of the normalized CSD of the TBL excitation field, the structural displacement and the interior acoustic field. Further the modal compositions of the structural and cavity response are examined and some inference of the dominant mechanism of noise transmission is made. Result indicates that the CSD of the shell response are generally correlated at low frequency and the envelope of the correlation function decays with an increase of the spatial separation. The decay occurs much more rapidly at higher frequencies. However, the correlation function of the CSD of the cavity response does not decay with an increase of the spatial separation and frequency. With wavenumber filtering, highly excited cavity modes are reduced in number compared with the shell modes. Most of the cavity mode response is forced by the shell modes. However, some low order cavity resonant modes are excited.

77.

J. W. Wilson, F. A. Cucinotta, J. L. Shinn, L. C. Simonsen and F. F. Badavi, **Overview of HZETRN and BRNTRN Space Radiation Shielding Codes**, *Photonics for Space Environments IV*, Denver, Colorado, August 4-9, 1996, (1MB).

Format(s): Postscript, or PDF

Keywords: Cosmic rays; Ionizing radiation; Shielding

Abstract: The NASA Radiation Health Program has supported basic research over the last decade in radiation physics to develop ionizing radiation transport codes and corresponding data bases for the protection of astronauts from galactic and solar cosmic rays on future deep space missions. The codes describe the interactions of the incident radiations with shield materials where their content is modified by the atomic and nuclear reactions through which high energy heavy ions are fragmented into less massive reaction products and reaction products are produced as radiations as direct knockout of shield constituents or produced as de-excitation products in the reactions. This defines the radiation fields to which specific devices are subjected onboard a spacecraft. Similar reactions occur in the device itself which is the initiating event for the device response. An overview of the computational procedures and data base with some applications to photonic and data processing devices will be given.

78.

James H. Starnes, Jr., Cheryl A. Rose and Charles C. Rankin, **Effects of Combined Loads on the Nonlinear Response and Residual Strength of Damaged Stiffened Shells**, *FAA/NASA*

Symposium on Continued Airworthiness of Aircraft Structures, Atlanta, Georgia, August 28-30, 1996, (1.5MB).

Format(s): Postscript, or PDF

Keywords: Stiffened shells; Nonlinear response; Long cracks; Residual strength; Combined loads

Abstract: The results of an analytical study of the nonlinear response of stiffened fuselage shells with long cracks are presented. The shells are modeled with a hierarchical modeling strategy and analyzed with a nonlinear shell analysis code that maintains the shell in a nonlinear equilibrium state while the crack is grown. The analysis accurately accounts for global and local structural response phenomena. Results are presented for various combinations of internal pressure and mechanical loads, and the effects of crack orientation on the shell response are described. The effects of combined loading conditions and the effects of varying structural parameters on the stress-intensity factors associated with a crack are presented.

79.

R. L. O'Neal, A. S. Levine and C. C. Kiser, Photographic Survey of the LDEF Mission , NASA SP-531, September 1996, pp. 446 .

Keywords: Spacecraft materials; Spacestation materials; Space structure

Abstract: This publication documents a selected number of preflight, in-flight, and postflight photographs of the LDEF and experiments. Changes in condition of the experiments caused by space exposure are discussed.

80.

K. Elliott Cramer and William P. Winfree, Thermal Characterization of Defects in Aircraft Structures Via Spatially Controlled Heat Application , *Thermosense XVIII*, Orlando, Florida, April 8-12, 1996, (254KB).

Format(s): Postscript, or PDF

Keywords: Thermography; Infrared imaging; Corrosion; Aging aircraft; Nondestructive inspection

Abstract: Recent advances in thermal imaging technology have spawned a number of new thermal NDE techniques that provide quantitative information about flaws in aircraft structures. Thermography has a number of advantages as an inspection technique. It is a totally noncontacting, nondestructive, imaging technology capable of inspecting a large area in a matter of a few seconds. The development of fast, inexpensive image processors have aided in the attractiveness of thermography as an NDE technique. These image processors have increased the signal to noise ratio of thermography and facilitated significant advances in post-processing. The resulting digital images enable archival records for comparison with later inspections thus providing a means of monitoring the evolution of damage in a particular structure. The National Aeronautics and Space Administration's Langley Research Center has developed a thermal NDE

technique designed to image a number of potential flaws in aircraft structures. The technique involves injecting a small, spatially controlled heat flux into the outer surface of an aircraft. Images of fatigue cracking, bond integrity and material loss due to corrosion are generated from measurements of the induced surface temperature variations. This paper will present a discussion of the development of the thermal imaging system as well as the techniques used to analyze the resulting thermal images. Spatial tailoring of the heat coupled with the analysis techniques represent a significant improvement in the detectability of flaws over conventional thermal imaging. Results of laboratory experiments of fabricated crack, disbond and material loss samples will be presented to demonstrate the capabilities of the technique. An integral part of the development of this technology is the use of analytic and computational modeling. The experimental results will be compared with these models to demonstrate the utility of such an approach.

81.

L. G. Horta, J-N. Juang and C-W. Chen, **Frequency Domain Identification Toolbox** , NASA TM-109039, September 1996, pp. 28, (144KB).

Format(s): Postscript, or PDF

Keywords: Identification; Vibration; State space identification; MATLAB software

Abstract: This report documents software written in MATLAB programming language for performing identification of systems from frequency response functions. MATLAB is a commercial software environment which allows easy manipulation of data matrices and provide other intrinsic matrix functions capabilities. Algorithms programmed in this collection of subroutines have been documented elsewhere but all references are provided in this document. A main feature of this software is the use of matrix fraction descriptions and system realization theory to identify state space models directly from test data. All subroutines have templates for the user to use as guidelines.

82.

T. S. Daniels and T. L. Jordan, **Dynamic Stability Instrumentation System (DSIS) Volume II: Operation Software Manual** , TM-109041, April 1996, pp. 81, (224KB).

Format(s): Postscript, or PDF

Keywords: Dynamic stability instrumentation system; Aerodynamic stability coefficients; PC based data acquisition and reduction; Digital signal processing

Abstract: This document is a software manual describing the operational control of the Dynamic Stability Instrumentation System (DSIS). The system, developed at Langley Research Center in 1992, is used to determine aerodynamic stability coefficients from forced-oscillation wind tunnel tests. Two additional documents describe the DSIS hardware and use of the system. A single program performs all data acquisition, system control, and data display and storage. Source code for this program, written in the C programming language for a personal computer (PC) platform, is described at a functional level. Instructions are also provided to enable users to modify this

software.

83.

Christian M. Fernholz and Jay H. Robinson, **Fully-Coupled Fluid/Structure Vibration Analysis Using MSC/NASTRAN**, NASA TM-110215, January 1996, pp. 84, (3.6MB) .

Format(s): Postscript, or PDF

Keywords: NASTRAN; Cylindrical shells, Fluid/structure modeling; Finite elements; Frequency response; Structural acoustics

Abstract: MSC/NASTRAN's performance in the solution of fully-coupled fluid/structure problems is evaluated. NASTRAN is used to perform normal modes (SOL 103) and forced-response analyses (SOL 108,111) on cylindrical and cubic fluid/structure models. Bulk data file cards unique to the specification of a fluid element are discussed and analytic partially-coupled solutions are derived for each type of problem. These solutions are used to evaluate NASTRAN's solutions for accuracy. Appendices to this work include NASTRAN data presented in fringe plot form, FORTRAN source code listings written in support of this work, and NASTRAN data file usage requirements for each analysis.

84.

M. D. Messina, M. E. Strickland, K. D. Hoffer, S. W. Carzoo, W. T. Bundick, J. C. Yeager and F. L. Beissner, Jr., **Simulation Model of the F/A-18 High Angle-of-Attack Research Vehicle Utilized for the Design of Advanced Control Laws**, TM-110216, May 1996, pp. 161, (868KB).

Format(s): Postscript, or PDF

Keywords: F/A-18 High-Alpha Research Vehicle (HARV); Actuated nose strakes for enhanced rolling (ANSER); Batch simulation; Aero model; Engine model; Sensor models; Thrust-vector system model; Actuator models; Non-linear; Six-degree-of-freedom; Aerodynamic database

Abstract: The f18harv six degree-of-freedom nonlinear batch simulation used to support research in advanced control laws and flight dynamics issues as part of NASA's High Alpha Technology Program is described in this report. This simulation models an F/A-18 airplane modified to incorporate a multi-axis thrust-vectoring system for augmented pitch and yaw control power and actuated forebody strakes for enhanced aerodynamic yaw control power. The modified configuration is known as the High Alpha Research Vehicle (HARV). The f18harv simulation was an outgrowth of the f18bas simulation which modeled the basic F/A-18 with a preliminary version of a thrust-vectoring system designed for the HARV. The preliminary version consisted of two thrust-vectoring vanes per engine nozzle compared with the three vanes per engine actually employed on the F/A-18 HARV. The modeled flight envelope is extensive in that the aerodynamic database covers an angle-of-attack range of -10 degrees to +90 degrees, sideslip range of -20 degrees to +20 degrees, a Mach Number range between 0.0 and 2.0, and an altitude range between 0 and 60000 feet.

85.

H. D. Fuhrmann and E. C. Stewart, **An Evaluation of the Measurement Requirements for an In-Situ Wake Vortex Detection System**, TM-110218, May 1996, pp. 21, (969KB) The PDF file of this paper is missing figures 1, 3, and 4. Please see [question 16](#) of the Frequently Asked Questions (FAQ) for information on how to obtain a hardcopy of this document.

Format(s): [Postscript](#), or [PDF](#)

Keywords: Wake vortex; Airborne detection systems; Airborne hazard; Wake vortex detection; Wake vortex avoidance; Measurement requirements; Aircraft separation

Abstract: Results of a numerical simulation are presented to determine the feasibility of estimating the location and strength of a wake vortex from imperfect in-situ measurements. These estimates could be used to provide information to a pilot on how to avoid a hazardous wake vortex encounter. An iterative algorithm based on the method of secants was used to solve the four simultaneous equations describing the two-dimensional flow field around a pair of parallel counter-rotating vortices of equal and constant strength. The flow field information used by the algorithm could be derived from measurements from flow angle sensors mounted on the wing tips of the detecting aircraft and an inertial navigation system. The study determined the propagated errors in the estimated location and strength of the vortex which resulted from random errors added to theoretically perfect measurements. The results are summarized in a series of charts and a table which make it possible to estimate these propagated errors for many practical situations. The situations include several generator-detector-airplane combinations, different distances between the vortex and the detector airplane, as well as different levels of total measurement error.

86.

H. M Reimer and D. D. Vicroy, **A Preliminary Study of a Wake Vortex Encounter Hazard Boundary for a B737-100 Airplane**, NASA TM-110223, April 1996, pp. 14, (697KB).

Format(s): [Postscript](#), or [PDF](#)

Keywords: Wake vortex; Wake vortex encounters; Wake vortex hazard criteria; Wake vortex encounter simulation

Abstract: A preliminary batch simulation study was conducted to define the wake decay required for a Boeing 737-100 airplane to safely encounter a Boeing 727 wake and land. The baseline six-degree-of-freedom B737 simulation was modified to include a wake model and the strip-theory calculation of the vortex-induced forces and moments. The guidance and control inputs for the airplane were provided by an autoland system. The wake was positioned such that the desired flight path traversed the core of the port vortex. Various safe landing criteria were evaluated for defining a safe encounter boundary. A sensitivity study was also conducted to assess the effects of encounter model inaccuracies.

87.

M. A. Scott, Time Varying Compensator Design for Reconfigurable Structures Using Non-Collocated Feedback , NASA TM-110226, October 1996, pp. 166, (928KB).

Format(s): Postscript, or PDF

Keywords: Robotic manipulator; Nonlinear control; Non-collocated feedback; Control of flexible systems; Reconfigurable systems; Time varying compensator

Abstract: Analysis and synthesis tools are developed to improve the dynamic performance of reconfigurable nonminimum phase, nonstrictly positive real-time variant systems. A novel Spline Varying Optimal (SVO) controller is developed for the kinematic nonlinear system. There are several advantages to using the SVO controller, in which the spline function approximates the system model, observer, and controller gain. They are: The spline function approximation is simply connected, thus the SVO controller is more continuous than traditional gain scheduled controllers when implemented on a time varying plant; it is easier for real-time implementations in storage and computational effort; where system identification is required, the spline function requires fewer experiments, namely four experiments; and initial startup estimator transients are eliminated. The SVO compensator was evaluated on a high fidelity simulation of the Shuttle Remote Manipulator System. The SVO controller demonstrated significant improvement over the present arm performance: (1) Damping level was improved by a factor of 3: and (2) Peak joint torque was reduced by a factor of 2 following Shuttle thruster firings.

88.

J. A. Woods-Vedeler and L. G. Horta, On-Orbit Application of H-Infinity to the Middeck Active Controls Experiment: Overview of Results , TM-110239, March 1996, pp. 16, (503KB).

Format(s): Postscript, or PDF

Keywords: Robust control; Vibration control; Spacecraft, H-Infinity; MACE

Abstract: The Middeck Active Control Experiment (MACE) was successfully completed during the flight of STS-67 in March 1995. MACE provided an on-orbit validation of modern robust control theory and system identification techniques through the testing of a flexible, multi-instrument, science platform in the micro-gravity environment of the Space Shuttle's Middeck. As part of this experiment, H-infinity control design was validated in zero gravity (0-G) environment. The control objective was to isolate a payload sensor from a 50Hz bandwidth disturbance occurring on the test article. Controllers were designed with the use of finite element models developed using 1-G measurements and a measurement model obtained by applying system identification techniques to open loop data obtained on orbit. Over 50 single-input and multi-input, multi-output, single and multi-axis H-infinity control designs were evaluated on-orbit. Up to 19 dB reduction in vibration levels and 25 Hz bandwidth of control were achieved.

89.

J. L. Rogers, DeMAID/GA User's Guide---Design Manager's Aid for Intelligent Decomposition With a Genetic Algorithm , TM-110241, April 1996, pp. 53, (375KB) .

Format(s): Postscript, or PDF

Keywords: Design; Scheduling; Genetic Algorithm; Sensitivities; Knowledge-based system; Coupling strengths; Decomposition; Concurrent Engineering

Abstract: Many companies are looking for new tools and techniques to aid a design manager in making decisions that can reduce the time and cost of a design cycle. One tool that is available to aid in this decision making process is the Design Manager's Aid for Intelligent Decomposition (DeMAID). Since the initial release of DeMAID in 1989, numerous enhancements have been added to aid the design manager in saving both cost and time in a design cycle. The key enhancement is a genetic algorithm (GA) and the enhanced version is called DeMAID/GA. The GA orders the sequence of design processes to minimize the cost and time to converge to a solution. These enhancements as well as the existing features of the original version of DeMAID are described. Two sample problems are used to show how these enhancements can be applied to improve the design cycle. This report serves as a user's guide for DeMAID/GA.

90.

R. S. Piascik and J. C. Newman, Jr., **An Extended Compact Tension Specimen for Fatigue Crack Propagation and Fracture**, TM-110243, March 1996, pp. 11, (471KB).

Format(s): Postscript, or PDF

Keywords: Crack; Stress-intensity; Factor; Displacements; Strains; Stress analysis

Abstract: An extended compact tension specimen, EC(T) has been developed for fatigue and fracture testing. Documented herein are stress-intensity factor and compliance expressions for the EC(T) specimen.

91.

T. B. Gatski, **Prediction of Airfoil Characteristics With Higher Order Turbulence Models**, TM-110246, April 1996, pp. 20, (210KB).

Format(s): Postscript, or PDF

Keywords: Turbulence modeling; Airfoil characteristics; Reynolds number scaling

Abstract: This study focuses on the prediction of airfoil characteristics, including lift and drag, over a range of Reynolds numbers. Two different turbulence models, which represent two different types of models, are tested. The first is a standard isotropic eddy-viscosity two-equation model, and the second is an explicit algebraic stress model (EASM). The turbulent flow field over a general-aviation airfoil (GA(W)-2) at three Reynolds numbers is studied. At each Reynolds number, predicted lift and drag values at different angles of attack are compared with experimental results, and predicted variations of stall locations with Reynolds number are compared with experimental data. Finally, the size of the separation zone predicted by each model is analyzed, and correlated with the behavior of the lift coefficient near stall. In summary, the EASM model is able to predict the lift and drag coefficients over a wider range of angles of attack

than the two-equation model for the three Reynolds numbers studied. However, both models are unable to predict the correct lift and drag behavior near the stall angle, and for the lowest Reynolds number case, the two-equation model did not predict separation on the airfoil near stall.

92.

J. L. Rogers, C. M. McCulley and C. L. Bloebaum, **Integrating a Genetic Algorithm Into a Knowledge-Based System for Ordering Complex Design Processes**, TM-110247, April 1996, pp. 13, (140KB).

Format(s): Postscript, or PDF

Keywords: Design; Scheduling; Genetic algorithm; Sensitivities; Knowledge-based system; Coupling strengths, Decomposition

Abstract: The design cycle associated with large engineering systems requires an initial decomposition of the complex system into design processes which are coupled through the transference of output data. Some of these design processes may be grouped into iterative subcycles. In analyzing or optimizing such a coupled system, it is essential to be able to determine the best ordering of the processes within these subcycles to reduce design cycle time and cost. Many decomposition approaches assume the capability is available to determine what design processes and couplings exist and what order of execution will be imposed during the design cycle. Unfortunately, this is often a complex problem and beyond the capabilities of a human design manager. A new feature, a genetic algorithm, has been added to DeMAID (Design Manager's Aid for Intelligent Decomposition) to allow the design manager to rapidly examine many different combinations of ordering processes in an iterative subcycle and to optimize the ordering based on cost, time, and iteration requirements. Two sample test cases are presented to show the effects of optimizing the ordering with a genetic algorithm.

93.

C. M. Fernholz and J. H. Robinson, **The Influence of Lamination Angles on Interior Noise Levels of an Aircraft**, NASA TM-110250, August 1996, pp. 89, (3MB).

Format(s): Postscript, or PDF

Keywords: Optimization; Lamination angle; Composites; Cylindrical shell; Acoustics; NASTRAN; Structural acoustics; Frequency response; Starship; Finite elements; Design sensitivity

Abstract: The feasibility of reducing the interior noise levels of an aircraft passenger cabin through an optimization of the composite lay up of the fuselage is investigated. MSC/NASTRAN, a commercially available finite element code, is used to perform the dynamic analysis and subsequent optimization of the fuselage. The numerical calculation of sensitivity of acoustic pressure to lamination angle is verified using a simple thin, cylindrical shell with point force excitations as noise sources. The thin shell is used because it represents a geometry similar to the fuselage and analytic solutions are available for the cylindrical thin shell equations of motion. Optimization of lamination angle for the reduction of interior noise is performed using a finite

element model of an actual aircraft fuselage. The aircraft modeled for this study is the Beech Starship. Point forces simulate the structure borne noise produced by the engines and are applied to the fuselage at the wing mounting locations. These forces are the noise source for the optimization problem. The acoustic pressure response is reduced at a number of points in the fuselage and over a number of frequencies. The objective function is minimized with the constraint that it be larger than the maximum sound pressure level at the response points in the passenger cabin for all excitation frequencies in the range of interest. Results from the study of the fuselage model indicate that a reduction in interior noise levels is possible over a finite frequency range through an optimal configuration of the lamination angles in the fuselage. Noise reductions of roughly 4 dB were attained. For frequencies outside the optimization range, the acoustic pressure response may increase after optimization. The effects of changing lamination angle on the overall structural integrity of the airframe are not considered in this study.

94.

W. K. Wilkie and K. C. Park, **An Aeroelastic Analysis of Helicopter Rotor Blades Incorporating Piezoelectric Fiber Composite Twist Actuation**, NASA TM-110252, May 1996, pp. 62, (612KB) [ERRATA](#).

Format(s): [Postscript](#), or [PDF](#)

Keywords: Helicopters; Piezoelectric actuation; Aeroelasticity; Adaptive structures

Abstract: A simple aeroelastic analysis of a helicopter rotor blade incorporating embedded piezoelectric fiber composite, interdigitated electrode blade twist actuators is described. The analysis consist of a linear torsion and flapwise bending model coupled with a nonlinear ONERA based unsteady aerodynamics model. A modified Galerkin procedure is performed upon the rotor blade partial differential equations of motion to develop a system of ordinary differential equations suitable for numerical integration. The twist actuation responses for three conceptual full-scale blade designs with realistic constraints on blade mass are numerically evaluated using the analysis. Numerical results indicate that useful amplitudes of nonresonant elastic twist, on the order of one to two degrees, are achievable under one-g hovering flight conditions for interdigitated electrode poling configurations. Twist actuation for the interdigitated electrode blades is also compared with the twist actuation of a conventionally poled piezoelectric fiber composite blade. Elastic twist produced using the interdigitated electrode actuators was found to be four to five times larger than that obtained with the conventionally poled actuators.

95.

S. M. Joshi and A. G. Kelkar, **On Longitudinal Control of High Speed Aircraft in the Presence of Aeroelastic Modes**, NASA TM-110254, May 1996, pp. 25, (439KB).

Format(s): [Postscript](#), or [PDF](#)

Keywords: Flexible aircraft control; Robust control; Aeroelasticity

Abstract: Longitudinal control system design is considered for a linearized dynamic model of a supersonic transport aircraft concept characterized by relaxed static stability and significant

aeroelastic interactions. Two LQG-type controllers are designed using the frequency-domain additive uncertainty formulation to ensure robustness to unmodeled flexible modes. The first controller is based on a 4th-order model containing only the rigid-body modes, while the second controller is based on an 8th-order model that additionally includes the two most prominent flexible modes. The performance obtainable from the 4th-order controller is not adequate, while the 8th-order controller is found to provide better performance. Frequency-domain and time-domain (Lyapunov) methods are subsequently used to assess the robustness of the 8th-order controller to parametric uncertainties in the design model.

96.

R. W. Butler, **An Introduction to Requirements Capture Using PVS: Specification of a Simple Autopilot**, NASA TM-110255, May 1996, pp. 33, (101KB).

Format(s): Postscript, or PDF

Keywords: Formal methods; Software requirements; Verification; Autopilot

Abstract: This paper presents an introduction to capturing software requirements in the PVS formal language. The object of study is a simplified digital autopilot that was motivated in part by the mode control panel of NASA Langley's Boeing 737 research aircraft. The paper first presents the requirements for this autopilot in English and then steps the reader through a translation of these requirements into formal mathematics. Along the way deficiencies in the English specification are noted and repaired. Once completed, the formal PVS requirement is analyzed using the PVS theorem prover and shown to maintain an invariant over its state space.

97.

G. P. Warren and J. M. Seaton, **A Comprehensive and Cost-Effective Computer Infrastructure for K-12 Schools**, TM-110256, April 1996, pp. 37, (461KB).

Format(s): Postscript, or PDF

Keywords: Networking; Education; Caching; Internet

Abstract: Since 1993, NASA Langley Research Center has been developing and implementing a low-cost Internet connection model, including system architecture, training, and support, to provide Internet access for an entire network of computers. This infrastructure allows local area networks which exceed 50 machines per school to independently access the complete functionality of the Internet by connecting to a central site, using state-of-the-art commercial modem technology, through a single standard telephone line. By locating high-cost resources at this central site and sharing these resources and their costs among the school districts throughout a region, a practical, efficient, and affordable infrastructure for providing scaleable Internet connectivity has been developed. As the demand for faster Internet access grows, the model has a simple expansion path that eliminates the need to replace major system components and retrain personnel. Observations of typical Internet usage within an environment, particularly school classrooms, have shown that after an initial period of "surfing," the Internet traffic becomes repetitive. By automatically storing requested Internet information on a high-capacity, networked

disk drive at the local site (network-based disk caching), then updating this information only when it changes, well over 80 percent of the Internet traffic that leaves a location can be eliminated by retrieving the information from the local disk cache.

98.

A. R. Johnson and A. Tessler, **A Viscoelastic Higher-Order Beam Finite Element** , TM-110260, June 1996, pp. 15, Also presented at MAFELAP 1996 (Ninth Conference on the Mathematics of Finite Elements and Applications) held June 25-28, 1996, at Brunel University, Uxbridge, United Kingdom. (368KB).

Format(s): Postscript, or PDF

Keywords: Viscoelasticity; Thick beams; Beam finite elements; Maxwell solid

Abstract: A viscoelastic internal variable constitutive theory is applied to a higher-order elastic beam theory and finite element formulation. The behavior of the viscous material in the beam is approximately modeled as a Maxwell solid. The finite element formulation requires additional sets of nodal variables for each relaxation time constant needed by the Maxwell solid. Recent developments in modeling viscoelastic material behavior with strain variables that are conjugate to the elastic strain measures are combined with advances in modeling through-the-thickness stresses and strains in thick beams. The result is a viscous thick-beam finite element that possesses superior characteristics for transient analysis since its nodal viscous forces are not linearly dependent on the nodal velocities, which is the case when damping matrices are used. Instead, the nodal viscous forces are directly dependent on the material's relaxation spectrum and the history of the nodal variables through a differential form of the constitutive law for a Maxwell solid. The thick beam quasistatic analysis is explored herein as a first step towards developing more complex viscoelastic models for thick plates and shells, and for dynamic analyses. The internal variable constitutive theory is derived directly from the Boltzmann superposition theorem. The mechanical strains and the conjugate internal strains are shown to be related through a system of first-order, ordinary differential equations. The total time-dependent stress is the superposition of its elastic and viscous components. Equations of motion for the solid are derived from the virtual work principle using the total time-dependent stress. Numerical examples for the problems of relaxation, creep, and cyclic creep are carried out for a beam made from an orthotropic Maxwell solid.

99.

W. A. Wood, **Multigrid Approach to Incompressible Viscous Cavity Flows** , NASA TM-110262, May 1996, pp. 12, (644KB).

Format(s): Postscript, or PDF

Keywords: Multigrid; Viscous flow; Driven cavity

Abstract: Two dimensional incompressible viscous driven-cavity flows are computed for Reynolds numbers on the range 100-20,000 using a loosely coupled, implicit, second-order centrally-different scheme. Mesh sequencing and three-level V-cycle multigrid error smoothing

are incorporated into the symmetric Gauss-Seidel time-integration algorithm. Parametrics on the numerical parameters are performed, achieving reductions in solution times by more than 60 percent with the full multigrid approach. Details of the circulation patterns are investigated in cavities of 2-to-1, 1-to-1, and 1-to-2 depth to width ratios.

100.

S. V. Tsynkov, **Artificial Boundary Conditions Based on the Difference Potentials Method** , NASA TM-110265, July 1996, pp. 31, (163KB).

Format(s): Postscript, or PDF

Keywords: Infinite-domain problems; Artificial boundary conditions; Pseudodifferential equations; Difference potentials method; Auxiliary problem; Boundary equations with projections

Abstract: When numerically solving an infinite-domain problem, one typically truncates the domain, which necessitates setting the artificial boundary conditions (ABC's) at the newly formed external boundary. The issue of ABC's appears most significant in many areas of scientific computing, e.g., in numerical problems that originate from acoustics, electrodynamics, solid mechanics, and fluid dynamics. In particular, in computational fluid dynamics the proper treatment of external boundaries has a profound impact on the overall quality and performance on numerical algorithms. Most of the currently used ABC's techniques can basically be classified into two groups. The methods from the first group (global ABC's usually provide high accuracy and robustness of the numerical procedure but often appear fairly cumbersome and expensive. The methods from the second group (local ABC's) are algorithmically simple, numerically cheap, and geometrically universal; however, they usually lack the accuracy of computations. In this paper we first present a survey and provide a comparative assessment of different existing methods for constructing the ABC's. Then, we describe our new ABC's technique and review the corresponding results. This new technique is currently one of the most promising in the field. It yields the ABC's that combine the advantages relevant to the two aforementioned classes of existing methods. Our approach is based on application of the difference potentials method by V.S. Ryaben'kii. The resulting ABC's are obtained in the form of certain (nonlocal) boundary operator equations. The operators involved are similar to the pseudodifferential boundary projections first introduced by A.P. Calderon and then also studied by R. T. Seeley.

101.

B. J. Holmes, **(Re)inventing Government-Industry R&D Collaboration** , NASA TM-110271, August 1996, pp. 35, (82KB).

Format(s): Postscript, or PDF

Keywords: Reinventing government; Strategic public/private alliances; New enterprise charters & government business; New aeronautics technology development

Abstract: This paper describes the lessons learned in developing & operating a large-scale strategic alliance whose organization & coordination is U.S. Government-led using new means for R&D collaboration. Consortia in the U.S. counter a century of 1884 Sherman Anti-Trust Law-

based governmental and legal policy & a longstanding business tradition of unfettered competition. Success in public-private collaboration in America requires compelling vision & motivation by both partners to reinvent our ways of doing business. The foundations for reinventing government and alliance building were laid in 1994 with Vice President Al Gore's mandates for Federal Lab Reviews & other examinations of the roles & missions for the nation's more than 700 government labs. In addition, the 1984 National Cooperative Research Act (NCRA) set in motion the abilities for U.S. companies to collaborate in pre-competitive technology development. The budget realities of the 1990's for NASA & other government agencies demand that government discover the means to accomplish its mission by leveraging resources through streamlining as well as alliances. Federal R&D investments can be significantly leveraged for greater national benefit through strategic alliances with industry & university partners. This paper presents early results from one of NASA's first large-scale public/private joint R&D ventures.

102.

Ricky W. Butler, Paul S. Miner, Mandayam K. Srivas, Dave A. Greve and Steven P. Miller, **A Bitvectors Library for PVS**, NASA TM-110274, August 1996, pp. 18, (72KB).

Format(s): Postscript, or PDF

Keywords: Hardware verification; Bitvectors; Formal methods; Formal verification

Abstract: This paper describes a bitvectors library that has been developed for PVS. The library defines a bitvector as a function from a subrange of the integers into $\{0, 1\}$. The library provides functions that interpret a bitvector as a natural number, as a 2's complement number, as a vector of logical values and as a 2's complement fraction. The library provides a concatenation operator and an extractor. Shift, extend and rotate operations are also defined. Fundamental properties of each of these operations have been proved in PVS.

103.

M. L. Morris, **Evaluation of Alternatives for Trichlorotrifluoroethane (CFC-113) to Clean and Verify Liquid Oxygen Systems**, NASA TM-110275, September 1996, pp. 33, (230KB).

Format(s): Postscript, or PDF

Keywords: Trichlorotrifluoroethane; CFC-113; Solvents; Oxygen cleaning; Verification

Abstract: NASA-Langley Research Center (LaRC) investigated several alternatives to the use of trichlorotrifluoroethane (CFC-113) in oxygen cleaning and verification. Alternatives investigated include several replacement solvents, Non-Destructive Evaluation (NDE) and Total Organic Carbon (TOC) analysis. Among the solvents, 1, 1-dichloro-1 fluoroethane (HCFC 141b) and dichloropentafluoropropane (HCFC 225) are the most suitable alternatives for cleaning and verification. However, use of HCFC 141b is restricted, HCFC 225 introduces toxicity hazards, and the NDE and TOC methods of verification are not suitable for processes at LaRC. Therefore, the interim recommendation is to sparingly use CFC-113 for the very difficult cleaning tasks where safety is critical and to use HCFC 225 to clean components in a controlled laboratory

environment. Meanwhile, evaluation must continue on new solvents and procedures to find one suited to LaRC's oxygen cleaning needs.

104.

V. Mukhopadhyay, **An Interactive Software for Conceptual Wing Flutter Analysis and Parametric Study**, NASA TM-110276, August 1996, pp. 17, (193KB).

Format(s): Postscript, or PDF

Keywords: Computer-aided interactive design; Conceptual flutter analysis; Blended wing body; Flutter instability; Torsional frequency; Regier number; Mathcad

Abstract: An interactive computer program was developed for wing flutter analysis in the conceptual design stage. The objective was to estimate the flutter instability boundary of a flexible cantilever wing, when well-defined structural and aerodynamic data are not available, and then study the effect of change in Mach number, dynamic pressure, torsional frequency, sweep, mass ratio, taper ratio, center of gravity, and pitch inertia, to guide the development of the concept. The software was developed for Macintosh or IBM compatible personal computers, on MathCad application software with integrated documentation, graphics, data base and symbolic mathematics. The analysis method was based on non-dimensional parametric plots of two primary flutter parameters, namely Reiger number and Flutter number, with normalization factors based on torsional stiffness, sweep, mass ratio, taper ratio, aspect ratio, center of gravity location and pitch inertia radius of gyration. The parametric plots were compiled in a Vought Corporation report from a vast data base of past experiments and wind-tunnel tests. The computer program was utilized for flutter analysis of the outer wing of a Blended-Wing-Body concept, proposed by McDonnell Douglas Corp. Using a set of assumed data, preliminary flutter boundary and flutter dynamic pressure variation with altitude, Mach number and torsional stiffness were determined.

105.

D. J. Baker and C. Q. Rousseau, **Design and Evaluation of a Bolted Joint for a Discrete Carbon-Epoxy Rod-Reinforced Hat Section**, NASA TM-110277, September 1996, pp. 20, (6MB).

Format(s): Postscript, or PDF

Keywords: Shear panels; Rod-reinforced structure; Cutouts

Abstract: The use of prefabricated pultruded carbon-epoxy rods has reduced the manufacturing complexity and costs of stiffened composite panels while increasing the damage tolerance of the panels. However, repairability of these highly efficient discrete stiffeners has been a concern. Design, analysis, and test results are presented in this paper for a bolted-joint repair for the pultruded rod concept that is capable of efficiently transferring axial loads in a hat-section stiffener on the upper skin segment of a heavily loaded aircraft wing component. A tension and a compression joint design were evaluated. The tension joint design achieved approximately 1.0 percent strain in the carbon-epoxy rod-reinforced hat-section and failed in a metal fitting at 166 percent of the design ultimate load. The compression joint design failed in the carbon-epoxy rod-

reinforced hat-section test specimen area at approximately 0.7 percent strain and at 110 percent of the design ultimate load. This strain level of 0.7 percent in compression is similar to the failure strain observed in previously reported carbon-epoxy rod-reinforced hat-section column tests.

106.

C. G. Davila, C. Smith and F. Lumban-Tobing, **Analysis of Thick Sandwich Shells With Embedded Ceramic Tiles**, NASA TM-110278, September 1996, pp. 13, (1MB).

Format(s): Postscript

Keywords: Thick composites; Composite armor; Element-layering; Shear correction factor

Abstract: The Composite Armored Vehicle (CAV) is an advanced technology demonstrator of an all-composite ground combat vehicle. The CAV upper hull is made of a tough light-weight S2-glass/epoxy laminate with embedded ceramic tiles that serve as armor. The tiles are bonded to a rubber mat with a carefully selected, highly viscoelastic adhesive. The integration of armor and structure offers an efficient combination of ballistic protection and structural performance. The analysis of this anisotropic construction, with its inherent discontinuous and periodic nature, however, poses several challenges. The present paper describes a shell-based "element-layering" technique that properly accounts for these effects and for the concentrated transverse shear flexibility in the rubber mat. One of the most important advantages of the element-layering technique over advanced higher-order elements is that it is based on conventional elements. This advantage allows the models to be portable to other structural analysis codes, a prerequisite in a program that involves the computational facilities of several manufacturers and government laboratories. The element-layering technique was implemented into an auto-layering program that automatically transforms a conventional shell model into a multi-layered model. The effects of tile layer homogenization, tile placement patterns, and tile gap size on the analysis results are described.

107.

Robert W. Moses and Ed Pendleton, **A Comparison of Pressure Measurements Between a Full-Scale and a 1/6-Scale F/A-18 Twin Tail During Buffet**, NASA TM-110282, August 1996, pp. 13, Also presented and included in the proceedings of the 83rd Structures and Materials Panel Meeting of AGARD held September 2-6, 1996, in Florence, Italy. (2MB).

Format(s): Postscript, or PDF

Keywords: Tail buffet; Pressure measurements; Tail buffeting

Abstract: In 1993, tail buffet tests were performed on a full-scale, production model F/A-18 in the 80- by 120-Foot Wind Tunnel at NASA Ames Research Center. Steady and unsteady pressures were recorded on both sides of the starboard vertical tail for an angle-of-attack range of 20 to 40 degrees and at a sideslip range of -16 to 16 degrees at freestream velocities up to 100 knots (Mach 0.15, Reynolds number 1.23×10^8). The aircraft was equipped with removable leading edge extension (LEX) fences that are used in Flight to reduce tail buffet loads. In 1995, tail buffet tests were performed on a 1/6-scale F-18 A/B model in the Transonic Dynamics Tunnel

(TDT) at NASA Langley Research Center. Steady and unsteady pressures were recorded on both sides of both vertical tails for an angle-of-attack range of 7 to 37 degrees at freestream velocities up to 65 knots (Mach 0.10). Comparisons of steady and unsteady pressures and root bending moments are presented for these wind-tunnel models for selected test cases. Representative pressure and root bending moment power spectra are also discussed, as are selected pressure cross-spectral densities.

108.

F. Farassat, **The Kirchhoff Formulas for Moving Surfaces in Aeroacoustics--The Subsonic and Supersonic Cases**, NASA TM-110285, September 1996, pp. 112, (580KB).

Format(s): Postscript, or PDF

Keywords: Aeroacoustics; Kirchhoff Formulas; Noise prediction; Generalized functions

Abstract: One of the active areas of computational aeroacoustics is the application of the Kirchhoff formulas to the problems of the rotating machinery noise prediction. The original Kirchhoff formula was derived for a stationary surface. In 1988, Farassat and Myers derived a Kirchhoff Formula obtained originally by Morgans using modern mathematics. These authors gave a formula particularly useful for applications in aeroacoustics. This formula is for a surface moving at subsonic speed. Later in 1995 these authors derived the Kirchhoff formula for a supersonically moving surface. This technical memorandum presents the viewgraphs of a day long workshop by the author on the derivation of the Kirchhoff formulas. All necessary background mathematics such as differential geometry and multidimensional generalized function theory are discussed in these viewgraphs. Abstraction is kept at a minimum level here. These viewgraphs are also suitable for understanding the derivation and obtaining the solutions of the Ffowcs Williams-Hawkings equation. In the first part of this memorandum, some introductory remarks are made on generalized functions, the derivation of the Kirchhoff formulas and the development and validation of Kirchhoff codes. Separate lists of references by Lyrantzis, Long, Strawn and their co-workers are given in this memorandum. This publication is aimed at graduate students, physicists and engineers who are in need of the understanding and applications of the Kirchhoff formulas in acoustics and electromagnetics.

109.

J. R. Cruz, C. H. Shah and A. S. Postyn, **Properties of Two Carbon Composite Materials Using LTM25 Epoxy Resin**, NASA TM-110286, November 1996, pp. 25, (345KB).

Format(s): Postscript, or PDF

Keywords: Composites; Carbon/epoxy; Graphite/epoxy; Material evaluation

Abstract: In this report, the properties of two carbon-epoxy prepreg materials are presented. The epoxy resin used in these two materials can yield lower manufacturing costs due to its low initial cure temperature, and the capability of being cured using vacuum pressure only. The two materials selected for this study are MR50/LTM25, and CFS003/LTM25 with Amoco T300 fiber; both prepregs are manufactured by The Advanced Composites Group. MR50/LTM25 is a

unidirectional prepreg tape using Mitsubishi MR50 carbon fiber impregnated with LTM25 epoxy resin. CRS003/LTM25 is a 2 by 2 twill fabric using Amoco T300 fiber and impregnated with LTM25 epoxy resin. Among the properties presented in this report are strength, stiffness, bolt bearing, and damage tolerance. Many of these properties were obtained at three environmental conditions: cold temperature/dry (CTD), room temperature/dry (RTD), and elevated temperature/wet (ETW). A few properties were obtained at room temperature/wet (RTW), and elevated temperature/dry (ETD). The cold and elevated temperatures used for testing were -125 degrees F and 180 degrees F, respectively. In addition, several properties related to processing are presented.

110.

L. J. Foernsler, **Integration of Multiple Non-Normal Checklist Procedures Into a Single Checklist Procedure for Transport Aircraft--A Preliminary Investigation**, NASA TM-110290, October 1996, pp. 38, (957KB).

Format(s): Postscript, or PDF

Keywords: Checklists; Non-normal procedures

Abstract: Checklists are used by the flight crew to properly configure an aircraft for safe flight and to ensure a high level of safety throughout the duration of the flight. In addition, the checklist provides a sequential framework to meet cockpit operational requirements, and it fosters cross-checking of the flight deck configuration among crew members. This study examined the feasibility of integrating multiple checklists for non-normal procedures into a single procedure for a typical transport aircraft. For the purposes of this report, a typical transport aircraft is one that represents a midpoint between early generation aircraft (B-727/737-200 and DC-10) and modern glass cockpit aircraft (B747-400/777 and MD-11). In this report, potential conflicts among non-normal checklist procedure that would take precedence for each of the identified multiple failure flight conditions is also identified. The rationale behind this research is that potential conflicts among checklist items might exist when integrating multiple checklists for non-normal procedures into a single checklist. As a rule, multiple failures occurring in today's highly automated and redundant system transport aircraft are extremely improbable. In addition, as shown in this analysis, conflicts among checklist items in a multiple failure flight condition are exceedingly unlikely. The possibility of a multiple failure flight condition occurring with a conflict among checklist items is so remote that integration of the non-normal checklists into a single checklist appears to be a plausible option.

111.

R. S. Pappa, S. E. Woodard and J-N. Juang, **A Benchmark Problem for Development of Autonomous Structural Modal Identification**, NASA TM-110291, October 1996, pp. 8, (390KB) Also presented at the 15th International Modal Analysis Conference and Exposition, February 3-6, 1997, in Orlando, Florida.

Format(s): Postscript, or PDF

Keywords: Autonomous structural modal identification, Modal testing; Spacecraft vibration,

Space Station, Autonomous Dynamics Determination experiment

Abstract: This paper summarizes modal identification results obtained using an autonomous version of the Eigensystem Realization algorithm on a dynamically complex, laboratory structure. The benchmark problem uses 48 of 768 free-decay responses measured in a complete modal survey test. The true modal parameters of the structure are well known from two previous, independent investigations. Without user involvement, the autonomous data analysis identified 24 to 33 structural modes with good to excellent accuracy in 62 seconds of CPU time (on a DEC alpha 4000 computer). The modal identification technique described in the paper is the baseline algorithm for NASA's Autonomous Dynamics Determination (ADD) experiment scheduled to fly on International Space Station assembly flights in 1997-1999.

112.

C. R. Cockrell and F. B. Beck, **Asymptotic Waveform Evaluation (AWE) Technique for Frequency Domain Electromagnetic Analysis**, NASA TM-110292, November 1996, (892KB).

Format(s): Postscript, or PDF

Keywords: Asymptotic waveform evaluation, Method of moments; Radar cross section

Abstract: The Asymptotic Waveform Evaluation (AWE) technique is applied to a generalized frequency domain electromagnetic problem. Most of the frequency domain techniques in computational electromagnetics result in a matrix equation, which is solved at a single frequency. In the AWE technique, the Taylor series expansion around that frequency is applied to the matrix equation. The coefficients of the Taylor's series are obtained in terms of the frequency derivatives of the matrices evaluated at the expansion frequency. The coefficients hence obtained will be used to predict the frequency response of the system over a frequency range. The detailed derivation of the coefficients (called "moments") is given along with an illustration for electric field integral equation (or Method of Moments) technique. The radar cross section (RCS) frequency response of a square plate is presented using the AWE technique and is compared with the exact solution at various frequencies.

113.

J. A. Kaplan, R. Chen, P. S. Kenney, C. M. Koval and B. K. Hutchinson, **User's Guide for Flight Simulation Data Visualization Workstation**, NASA TM-110294, November 1996, pp. 19, (349KB).

Format(s): Postscript, or PDF

Keywords: Heads-up display; Out of the cockpit view

Abstract: Today's modern flight simulation research produces vast amounts of time sensitive data. The meaning of this data can be difficult to assess while in its raw format. Therefore, a method of breaking the data down and presenting it to the user in a graphical format is necessary. Simulation Graphics (SimGraph) is intended as a data visualization software package that will incorporate simulation data into a variety of animated graphical displays for easy interpretation by

the simulation researcher. This document is intended as an end user's guide.

114.

M. M. Hussaini and J. J. Korte, **Investigation of Low-Reynolds-Number Rocket Nozzle Design Using PNS-Based Optimization**, NASA TM-110295, November 1996, pp. 13, (272KB).

Format(s): Postscript, or PDF

Keywords: PNS; Optimization; Rocket nozzle design; Resistojet

Abstract: An optimization approach to rocket nozzle design, based on computational fluid dynamics (CFD) methodology, is investigated for low-Reynolds-number cases. This study is undertaken to determine the benefits of this approach over those of classical design processes such as Rao's method. A CFD-based optimization procedure, using the parabolized Navier-Stokes (PNS) equations, is used to design conical and contoured axisymmetric nozzles. The advantage of this procedure is that it accounts for viscosity during the design process; other processes make an approximated boundary-layer correction after an inviscid design is created. Results showed significant improvement in the nozzle thrust coefficient over that of the baseline case; however, the unusual nozzle design necessitates further investigation of the accuracy of the PNS equations for modeling expanding flows with thick laminar boundary layers.

115.

M. L. Blosser, **Development of Metallic Thermal Protection Systems for the Reusable Launch Vehicle**, NASA TM-110296, October 1996, pp. 22, (2MB).

Format(s): Postscript, or PDF

Keywords: Thermal protection systems; Reusable launch vehicle; Thermal/structural testing

Abstract: A reusable Thermal Protection System (TPS) that is not only lightweight, but durable, operable and cost effective is one of the technologies required by the Reusable Launch Vehicle (RLV) to achieve the goal of drastically reducing the cost of delivering payload to orbit. Metallic TPS is one of the systems being developed to meet this challenge. Current efforts involve improving the superalloy honeycomb TPS concept, which consists of a foil-gage metallic box encapsulating a low density fibrous insulation, and evaluating it for RLV requirements. The superalloy honeycomb TPS concept is mechanically attached to the vehicle structure. Improvements include more efficient internal insulation, a simpler, lighter weight configuration, and a quick-release fastener system for easier installation and removal. Evaluation includes thermal and structural analysis, fabrication and testing of both coupons and TPS panels under conditions simulating RLV environments. Coupons of metallic honeycomb sandwich, representative of the outer TPS surface, were subjected to low speed impact, hypervelocity impact, and rain erosion testing as well as subsequent arcjet exposure. Arrays of TPS panels have been subjected to radiant heating in a thermal/vacuum facility, aerodynamic heating in an arcjet facility and acoustic loading.

116.

B. K. Taleghani and R. S. Pappa, **Finite-Element Vibration Analysis and Modal Testing of Graphite Epoxy Tubes and Correlations Between the Data**, NASA TM-110298, November 1996, pp. 66, (2MB).

Format(s): Postscript, or PDF

Keywords: Composite materials; Vibration analysis; Modal testing; Finite element model

Abstract: Structural materials in the form of graphite epoxy composites with embedded rubber layers are being used to reduce vibrations in rocket motor tubes. Four filament-wound, graphite epoxy tubes were studied to evaluate the effects of the rubber layer on the modal parameters (natural vibration frequencies, damping, and mode shapes). Tube 1 contained six alternating layers of 30-degree helical wraps and 90-degree hoop wraps. Tube 2 was identical to tube 1 with the addition of an embedded 0.030-inch-thick rubber layer. Tubes 3 and 4 were identical to tubes 1 and 2, respectively, with the addition of a Textron Kelpoxy elastomer. This report compares experimental modal parameters obtained by impact testing with analytical modal parameters obtained by NASTRAN finite-element analysis. Four test modes of tube 1 and five test modes of tube 3 correlate highly with corresponding analytical predictions. Unsatisfactory correlation of test and analysis results occurred for tubes 2 and 4 and these comparisons are not shown. Work is underway to improve the analytical models of these tubes. Test results clearly show that the embedded rubber layers significantly increase structural modal damping as well as decrease natural vibration frequencies.

117.

John B. Davidson and Dominick Andrisani, II, **Lateral-Directional Eigenvector Flying Qualities Guidelines for High Performance Aircraft**, NASA TM-110306, December 1996, pp. 58, (779KB).

Format(s): Postscript, or PDF

Keywords: Eigenspace assignment; Lateral-directional dynamics

Abstract: This report presents the development of lateral-directional flying qualities guidelines with application to eigenspace (eigenstructure) assignment methods. These guidelines will assist designers in choosing eigenvectors to achieve desired closed-loop flying qualities or performing trade-offs between flying qualities and other important design requirements, such as achieving realizable gain magnitudes or desired system robustness. This has been accomplished by developing relationships between the system's eigenvectors and the roll rate and sideslip transfer functions. Using these relationships, along with constraints imposed by system dynamics, key eigenvector elements are identified and guidelines for choosing values of these elements to yield desirable flying qualities have been developed. Two guidelines are developed - one for low roll-to-sideslip ratio and one for moderate-to-high roll-to-sideslip ratio. These flying qualities guidelines are based upon the Military Standard lateral-directional coupling criteria for high performance aircraft - the roll rate oscillation criteria and the sideslip excursion criteria. Example guidelines are generated for a moderate-to-large, an intermediate, and low value of roll-to-sideslip ratio.

118.

J. A. Kaplan, R. Chen, P. S. Kenney, C. M. Koval and B. K. Hutchinson, **Development of a Flight Simulation Data Visualization Workstation**, NASA TM-110308, December 1996, pp. 56, (674KB).

Format(s): [Postscript](#), or [PDF](#)

Keywords: Heads-up display; Out of the cockpit view

Abstract: Today's modern flight simulation research produces vast amounts of time sensitive data. The meaning of this data can be difficult to assess while in its raw format. Therefore, a method of breaking the data down and presenting it to the user in a graphical format is necessary. Simulation Graphics (SimGraph) is intended as a data visualization software package that will incorporate simulation data into a variety of animated graphical displays for easy interpretation by the simulation researcher. Although it was created for the flight simulation facilities at NASA Langley Research Center, SimGraph can be reconfigured to almost any data visualization environment. This paper traces the design, development and implementation of the SimGraph program, and is intended to be a programmer's reference guide.

119.

Julio Chu and James M. Luckring, **Experimental Surface Pressure Data Obtained on 65-Degree Delta Wing Across Reynolds Number and Mach Number Ranges, Volume 1-Sharp Leading Edge**, NASA TM-4645, Vol. 1, February 1996, pp. 28, (4.9MB), Appendix C [[Postscript](#)] or [[PDF](#)] and Appendix D [[Postscript](#)] or [[PDF](#)] NASA-STI 02.

Format(s): [Postscript](#), or [PDF](#)

Keywords: Aerodynamics; Delta wing; Reynolds number; Leading-edge bluntness; Vortex flow; Cryogenic testing

Abstract: An experimental wind tunnel test of a 65-Degree delta wing model with interchangeable leading edges was conducted in the Langley National Transonic Facility (NTF). The objective was to investigate the effects of Reynolds and Mach numbers on slender-wing leading-edge vortex flows with four values of wing leading-edge bluntness. Experimentally obtained pressure data are presented without analysis in tabulated and graphical formats across a Reynolds number range of $6 \times E+06$ to $36 \times E+06$ at a Mach number of 0.85 and across a Mach number range of 0.4 to 0.9 at a Reynolds number of $6 \times E+06$. Normal-force and pitching-moment coefficient plots for these Reynolds number and Mach number ranges are also presented.

120.

Julio Chu and James M. Luckring, **Experimental Surface Pressure Data Obtained on 65-Degree Delta Wing Across Reynolds Number and Mach Number Ranges, Volume 2-Small-Radius Leading Edge**, NASA TM-4645, Vol. 2, February 1996, pp. 31, (5.0MB), Appendix C [[Postscript](#)] or [[PDF](#)], Appendix D [[Postscript](#)] or [[PDF](#)] and Appendix E [[Postscript](#)] or [[PDF](#)].

Format(s): Postscript, or PDF

Keywords: Aerodynamics; Delta wing; Reynolds number; Leading-edge bluntness; Vortex flow; Cryogenic testing

Abstract: An experimental wind tunnel test of a 65-Degree delta wing model with interchangeable leading edges was conducted in the Langley National Transonic Facility (NTF). The objective was to investigate the effects of Reynolds and Mach numbers on slender-wing leading-edge vortex flows with four values of wing leading-edge bluntness. Experimentally obtained pressure data are presented without analysis in tabulated and graphical formats across a Reynolds number range of $6 \times E+06$ to $84 \times E+06$ at a Mach number of 0.85 and across a Mach number range of 0.4 to 0.9 at Reynolds numbers of $6 \times E+06$ and $60 \times E+06$. Normal-force and pitching-moment coefficient plots for these Reynolds number and Mach number ranges are also presented.

121.

Julio Chu and James M. Luckring, **Experimental Surface Pressure Data Obtained on 65-Degree Delta Wing Across Reynolds Number and Mach Number Ranges, Volume 3-Medium-Radius Leading Edge**, NASA TM-4645, Vol. 3, February 1996, pp. 37, (505KB).

Format(s): Postscript, or PDF

Keywords: Aerodynamics; Delta wing; Reynolds number; Leading-edge bluntness; Vortex flow; Cryogenic testing

Abstract: An experimental wind tunnel test of a 65-degree delta wing model with interchangeable leading edges was conducted in the Langley National Transonic Facility (NTF). The objective was to investigate the effects of Reynolds and Mach numbers on slender-wing leading-edge vortex flows with four values of wing leading-edge bluntness. Experimentally obtained pressure data are presented without analysis in tabulated and graphical formats across a Reynolds number range of $6 \times E+06$ to $120 \times E+06$ at a Mach number of 0.85 and across a Mach number range of 0.4 to 0.9 at Reynolds numbers of $6 \times E+06$, $60 \times E+06$, and $120 \times E+06$. Normal-force and pitching-moment coefficient plots for these Reynolds number and Mach number ranges are also presented.

122.

Julio Chu and James M. Luckring, **Experimental Surface Pressure Data Obtained on 65-Degree Delta Wing Across Reynolds Number and Mach Number Ranges, Volume 4-Large-Radius Leading Edge**, NASA TM-4645, Vol. 4, February 1996, (4.9MB), Appendix C [Postscript] or [PDF] Appendix D [Postscript] or [PDF] Appendix E [Postscript] or [PDF].

Format(s): Postscript, or PDF

Keywords: Aerodynamics; Delta wing; Reynolds number; Leading-edge bluntness; Vortex flow; Cryogenic testing

Abstract: An experimental wind tunnel test of a 65-degree delta wing model with interchangeable

leading edges was conducted in the Langley National Transonic Facility (NTF). The objective was to investigate the effects of Reynolds and Mach numbers on slender-wing leading-edge vortex flows with four values of wing leading-edge bluntness. Experimentally obtained pressure data are presented without analysis in tabulated and graphical formats across a Reynolds number range of 6×10^6 to 120×10^6 at a Mach number of 0.85 and across a Mach number range of 0.4 to 0.9 at Reynolds numbers of 6×10^6 and 60×10^6 . Normal-force and pitching-moment coefficient plots for these Reynolds number and Mach number ranges are also presented.

123.

Robert L. Jones III, **Dataflow Design Tool: User's Manual**, NASA TM-4672, February 1996, pp. 67, (409KB).

Format(s): Postscript, or PDF

Keywords: Multiprocessing; Real-time processing; Scheduling theory; Graph-theoretic model; Graph-search algorithms; Dataflow paradigm; Petri net; Performance metrics; Computer-aided design; Digital signal processing; Control law; Windows environment

Abstract: The Dataflow Design Tool is a software tool for selecting a multiprocessor scheduling solution for a class of computational problems. The problems of interest are those that can be described with a dataflow graph and are intended to be executed repetitively on a set of identical processors. Typical applications include signal processing and control law problems. The software tool implements graph-search algorithms and analysis techniques based on the dataflow paradigm. Dataflow analyses provided by the software are introduced and shown to effectively determine performance bounds, scheduling constraints, and resource requirements. The software tool provides performance optimization through the inclusion of artificial precedence constraints among the schedulable tasks. The user interface and tool capabilities are described. Examples are provided to demonstrate the analysis, scheduling, and optimization functions facilitated by the tool.

124.

S. Naomi McMillin, James E. Byrd, Devendra S. Parmar, Gaudy M. Bezos-O'Connor, Dana K. Forrest and Susan Bowen, **Surface-Pressure and Flow-Visualization Data at Mach Number of 1.60 for Three 65 Degree Delta Wings Varying in Leading-Edge Radius and Camber**, NASA TM-4673, December 1996, pp. 265, (31MB).

Format(s): Postscript, or PDF

Keywords: Delta wings; Supersonic; Vortical flows; Leading-edge separation; Leaside

Abstract: An experimental investigation of the effect of leading-edge radius, camber, Reynolds number, and boundary-layer state on the incipient separation of a delta wing at supersonic speeds was conducted at the Langley Unitary Plan Wind Tunnel at Mach number of 1.60 over a free-stream Reynolds number range of 1×10^6 to $5 \times 10^6 \text{ ft}^{-1}$. The three delta wing models examined had a 65 degree swept leading edge and varied in cross-sectional shape: a sharp wedge, a 20:1 ellipse, and a 20:1 ellipse with a -9.750 circular camber imposed across the

span. The wings were tested with and without transition grit applied. Surface-pressure coefficient data and flow-visualization data are electronically stored on a CD-ROM. The data indicated that by rounding the wing leading edge or cambering the wing in the spanwise direction, the onset of leading-edge separation on a delta wing can be raised to a higher angle of attack than that observed on a sharp-edged delta wing. The data also showed that the onset of leading-edge separation can be raised to a higher angle of attack by forcing boundary-layer transition to occur closer to the wing leading edge by the application of grit or the increase in free-stream Reynolds number.

125.

F. McNeil Cheatwood and Peter A. Gnoffo, **User's Manual for the Langley Aerothermodynamic Upwind Relaxation Algorithm (LAURA)**, NASA TM-4674, April 1996, pp. 223, (4.5MB).

Format(s): Postscript, or PDF

Keywords: Computational fluid dynamics; Hypersonic flow; Thermal nonequilibrium; Chemical nonequilibrium; Upwind schemes; Total variation diminishing

Abstract: This user's manual provides detailed instructions for the installation and the application of version 4.1 of the Langley Aerothermodynamic Upwind Relaxation Algorithm (LAURA) (refs. 2 and 3), which is a program for obtaining the simulations discussed above. Earlier versions of LAURA were predominantly research codes, and they had minimal (or no) documentation. This manual describes UNIX-based utilities for customizing the code for special applications that also minimize system resource requirements. The algorithm is reviewed, and the various program options are related to specific equations and variables in the theoretical development.

126.

Anna C. Trujillo, **Airline Transport Pilot Preferences for Predictive Information**, NASA TM-4702, February 1996, pp. 46, (306KB).

Format(s): Postscript, or PDF

Keywords: Predictive information; Caution and warning system; Relative time criticality of failures; Subjective utility of predictive information; Preferred form and prediction time

Abstract: This experiment assessed certain issues about the usefulness of predictive information: (1) the relative time criticality of failures, (2) the subjective utility of predictive information for different parameters or sensors, and (3) the preferred form and prediction time for displaying predictive information. To address these issues, three separate tasks were administered to 22 airline pilots. As shown by the data, these pilots preferred predictive information on parameters they considered vital to the safety of the flight. These parameters were related to the checklists performed first for alert messages. These pilots also preferred to know whether a parameter was changing abnormally and the time to a certain value being reached. Furthermore, they considered this information most useful during the cruise, the climb, and the descent phases of flight. Lastly, these pilots preferred the information to predict as far ahead as possible.

127.

C. Ranganathaiah, D. R. Sprinkle, R. H. Pater and A. Eftekhari, **A Method for Characterizing Thermoset Polyimides**, NASA TM-4707, March 1996, pp. 9, (172KB).

Format(s): Postscript, or PDF

Keywords: Thermoset polyimides; Cross-link density; Coefficient of thermal expansion; Positron lifetime; Free-volume cell size; Free-volume fraction

Abstract: Thermoset polyimides have great potential for successfully meeting tough stress and temperature challenges in the advanced aircraft development program. However, studies of structure-property relationships in these materials have not been very successful so far. Positron lifetime spectroscopy has been used to investigate free volumes and associated parameters in a series of variable, segmental molecular weight samples. The free volume correlates well with the molecular weight, the cross-link density, and the coefficient of thermal expansion of these materials. Currently, no other techniques are available for direct measurement of these parameters, particularly for polymers in solid phase. Experimental results and their interpretations are presented.

128.

John C. Wilson, Garl L. Gentry and Susan Althoff Gorton, **Wind Tunnel Test Results of a 1/8-Scale Fan-in-Wing Model**, NASA TM-4710, May 1996, pp. 83, (6MB).

Format(s): Postscript, or PDF

Keywords: Fan-in-wing; Ducted fan; Powered lift; Ground effects

Abstract: A 1/8-scale model of a fan-in-wing concept considered for development by Grumman Aerospace Corporation for the U.S. Army was tested in the Langley 14- by 22-Foot Subsonic Tunnel. Hover testing, which included height above a pressure-instrumented ground plane, angle of pitch, and angle of roll for a range of fan thrust, was conducted in a model preparation area near the tunnel. The air loads and surface pressures on the model were measured for several configurations in the model preparation area and in the tunnel. The major hover configuration change was varying the angles of the vanes attached to the exit of the fans for producing propulsive force. As the model height above the ground was decreased, there was a significant variation of thrust-removed normal force with constant fan speed. The greatest variation was generally for the height-to-fan exit diameter ratio of less than 2.5; the variation was reduced by deflecting fan exit flow outboard with the vanes. In the tunnel angles of pitch and sideslip, height above the tunnel floor, and wind speed were varied for a range of fan thrust and different vane angle configurations. Other configuration features such as flap deflections and tail incidence were evaluated as well. Though the V-tail empennage provided an increase in static longitudinal stability, the total model configuration remained unstable.

129.

S. V. Tsynkov, **Artificial Boundary Conditions for Computation of Oscillating External Flows**, NASA TM-4714, August 1996, pp. 44, (434KB).

Format(s): Postscript, or PDF

Keywords: Time-periodic flows; Artificial boundary conditions; Boundary projection operators; Difference potentials method

Abstract: In this paper, we propose a new technique for the numerical treatment of external flow problems with oscillatory behavior of the solution in time. Specifically, we consider the case of unbounded compressible viscous plane flow past a finite body (airfoil). Oscillations of the flow in time may be caused by the time-periodic injection of fluid into the boundary layer, which in accordance with experimental data, may essentially increase the performance of the airfoil. To conduct the actual computations, we have to somehow restrict the original unbounded domain, that is, to introduce an artificial (external) boundary and to further consider only a finite computational domain. Consequently, we will need to formulate some artificial boundary conditions (ABC's) at the introduced external boundary. The ABC's we are aiming to obtain must meet a fundamental requirement. One should be able to uniquely complement the solution calculated inside the finite computational domain to its infinite exterior so that the original problem is solved within the desired accuracy. Our construction of such ABC's for oscillating flows is based on an essential assumption: the Navier-Stokes equations can be linearized in the far field against the free-stream background. To actually compute the ABC's, we represent the far-field solution as a Fourier series in time and then apply the Difference Potentials Method (DPM) of V. S. Ryaben'kii. This paper contains a general theoretical description of the algorithm for setting the DPM-based ABC's for time-periodic external flows. Based on our experience in implementing analogous ABC's for steady-state problems (a simpler case), we expect that these boundary conditions will become an effective tool for constructing robust numerical methods to calculate oscillatory flows.

130.

Milton Lamb, John G. Taylor and Mark C. Frassinelli, **Static Internal Performance of a Two-Dimensional Convergent-Divergent Nozzle With External Shelf**, NASA TM-4719, September 1996, pp. 106, (5MB) The paper is missing a figure. Please see [question 16](#) of the Frequently Asked Questions (FAQ) for information on how to obtain a hardcopy of this document.

Format(s): Postscript, or PDF

Keywords: Two-dimensional; Convergent-divergent shelf nozzles; Static internal performance; Pressure distributions

Abstract: An investigation was conducted in the static test facility of the Langley 16-Foot Transonic Tunnel to determine the internal performance of a two-dimensional convergent-divergent nozzle. The nozzle design was tested with dry and afterburning throat areas, which represent different power settings and three expansion ratios. For each of these configurations, three trailing-edge geometries were tested. The baseline geometry had a straight trailing edge. Two different shaping techniques were applied to the baseline nozzle design to reduce radar observables: the scarfed design and the sawtooth design. A flat plate extended downstream of the lower divergent flap trailing edge parallel to the model centerline to form a shelflike expansion

surface. This shelf was designed to shield the plume from ground observation (infrared radiation (IR) signature suppression). The shelf represents the part of the aircraft structure that might be present in an installed configuration. These configurations were tested at nozzle pressure ratios from 2.0 to 12.0.

131.

David C. Lo, Timothy W. Coats, Charles E. Harris and David H. Allen, **Progressive Damage Analysis of Laminated Composite (PDALC)-A Computational Model Implemented in the NASA COMET Finite Element Code**, NASA TP-4724, November 1996, pp. 42, (459KB).

Format(s): Postscript, or PDF

Keywords: Composites; Graphite/epoxy; Damage; Matrix cracks; Stiffness loss; Residual strength; Internal state variables; Finite element code

Abstract: A method for analysis of progressive failure in the Computational Structural Mechanics Testbed is presented in this report. The relationship employed in this analysis describes the matrix crack damage and fiber fracture via kinematics-based volume-averaged variables. Damage accumulation during monotonic and cyclic loads is predicted by damage evolution laws for tensile load conditions. The implementation of this damage model required the development of two testbed processors. While this report concentrates on the theory and usage of these processors, a complete list of all testbed processors and inputs that are required for this analysis are included. Sample calculations for laminates subjected to monotonic and cyclic loads were performed to illustrate the damage accumulation, stress redistribution, and changes to the global response that occur during the load history. Residual strength predictions made with this information compared favorably with experimental measurements.

132.

Roger A. Lepsch, Jr., George M. Ware and Ian O. MacConochie, **Subsonic Aerodynamic Characteristics of a Circular Body Earth-to-Orbit Vehicle**, NASA TM-4726, July 1996, pp. 32, (6MB).

Format(s): Postscript, or PDF

Keywords: Aerodynamics; Subsonic; Spacecraft; Booster

Abstract: A test of a generic reusable earth-to-orbit transport was conducted in the 7- by 10-Foot high-speed tunnel at the Langley Research Center at Mach number 0.3. The model had a body with a circular cross section and a thick clipped delta wing as the major lifting surface. For directional control, three different vertical fin arrangements were investigated: a conventional aft-mounted center vertical fin, wingtip fins, and a nose-mounted vertical fin. The configuration was longitudinally stable about the estimated center-of-gravity position of 0.72 body length and had sufficient pitch-control authority for stable trim over a wide range of angle of attack, regardless of fin arrangement. The maximum trimmed lift/drag ratio for the aft center-fin configuration was less than 5, whereas the other configurations had values of above 6. The aft center-fin configuration was directionally stable for all angles of attack tested. The wingtip and nose fins were not

intended to produce directional stability but to be active controllers for artificial stabilization. Small rolling-moment values resulted from yaw control of the nose fin. Large adverse rolling-moment increments resulted from tip-fin controller deflection above 13 angle of attack. Flow visualization indicated that the adverse rolling-moment increments were probably caused by the influence of the deflected tip-fin controller on wing flow separation.

133.

Steven D. Young, Robert W. Wills and R. Marshall Smith, **Pilot Evaluation of Runway Status Light System** , NASA TM-4727, October 1996, pp. 32, (542KB).

Format(s): Postscript, or PDF

Keywords: Runway status lights; Incursions; Flight simulation

Abstract: This study focuses on use of the Transport Systems Research Vehicle (TSRV) Simulator at the Langley Research Center to obtain pilot opinion and input on the Federal Aviation Administration's Runway Status Light System (RWSL) prior to installation in an operational airport environment. The RWSL has been designed to reduce the likelihood of runway incursions by visually alerting pilots when a runway is occupied. Demonstrations of the RWSL in the TSRV Simulator allowed pilots to evaluate the system in a realistic cockpit environment.

134.

Earl R. Booth, Jr., Gary Romberg, Larry Hansen and Ron Lutz, **Acoustic Survey of a 3/8-Scale Automotive Wind Tunnel** , NASA TM-4736, October 1996, pp. 85, (13MB).

Format(s): Postscript, or PDF

Keywords: Acoustic wind tunnel; Background noise level; Noise sources; Acoustic calibration; Open jet section

Abstract: An acoustic survey that consists of insertion loss and flow noise measurements was conducted at key locations around the circuit of a 3/8-scale automotive acoustic wind tunnel. Descriptions of the test, the instrumentation, and the wind tunnel facility are included in the current report, along with data obtained in the test in the form of 1/3-octave-band insertion loss and narrowband flow noise spectral data.

135.

Charles L. Ladson, Cuyler W. Brooks, Jr., Acquilla S. Hill and Darrell W. Sproles, **Computer Program To Obtain Ordinates for NACA Airfoils** , NASA TM-4741, December 1996, pp. 23, (215KB).

Format(s): Postscript, or PDF

Keywords: NACA airfoils; 4-digit; 6-series; Platform-independent; FORTRAN

Abstract: Computer programs to produce the ordinates for airfoils of any thickness, thickness distribution, or camber in the NACA airfoil series were developed in the early 1970's and are published as NASA TM X-3069 and TM X-3284. For analytic airfoils, the ordinates are exact. For the 6-series and all but the leading edge of the 6A-series airfoils, agreement between the ordinates obtained from the program and previously published ordinates is generally within 5×10^{-5} chord. Since the publication of these programs, the use of personal computers and individual workstations has proliferated. This report describes a computer program that combines the capabilities of the previously published versions. This program is written in ANSI FORTRAN 77 and can be compiled to run on DOS, UNIX, and VMS based personal computers and workstations as well as mainframes. An effort was made to make all inputs to the program as simple as possible to use and to lead the user through the process by means of a menu.

136.

Stephen J. Katzberg and James L. Garrison, Jr., **Utilizing GPS To Determine Ionospheric Delay Over the Ocean**, NASA TM-4750, December 1996, pp. 14, [ERRATA](#) (196KB).

Format(s): [Postscript](#), or [PDF](#)

Keywords: GPS; GPS multipath; Ionosphere correction; Altimeter; Satellite; Models

Abstract: Several spaceborne altimeters have been built and flown, and others are being developed to provide measurements of ocean and ice sheet topography. Until the launch of TOPEX, altimeters were single frequency systems incapable of removing the effects of ionospheric delay on the radar pulse. With the current state of the art in satellite altimetry, the ionosphere causes the largest single error when using single frequency altimeters. Ionospheric models provide the only recourse short of adding a second frequency to the altimeter. Unfortunately, measurements of the ionosphere are lacking over the oceans or ice sheets where they are most needed. A possible solution to the lack of data density may result from an expanded use of the Global Positioning System (GPS). This paper discusses how the reflection of the GPS signal from the ocean can be used to extend ionospheric measurements by simply adding a GPS receiver and downward-pointing antenna to satellites carrying single frequency altimeters. This paper presents results of a study assessing the feasibility and effectiveness of adding a GPS receiver and downward-pointing antenna to satellites carrying single frequency altimeters.

137.

, **[Research and Technology Highlights 1995](#)**, NASA TM-4765, December 1996, pp. 147.

Keywords: Research and technology; Aeronautics; Space; Structures; Materials; Electronics; Flight systems; Technology transfer; Technology commercialization; Engineering; Aerodynamics; Wind tunnels; Facilities; Tests

Abstract: The mission of the NASA Langley Research Center is to increase the knowledge and capability of the United States in a full range of aeronautics disciplines and in selected space disciplines. This mission is accomplished by performing innovative research relevant to national needs and Agency goals, transferring technology to users in a timely manner, and providing development support to other United States Government agencies, industry, and other NASA

Centers, the educational community, and the local community. This report contains highlights of the major accomplishments and applications that have been made by Langley researchers and by our university and industry colleagues during the past year. The highlights illustrate both the broad range of research and technology (R&T) activities carried out by NASA Langley Research Center and the contributions of this work toward maintaining United States leadership in aeronautics and space research. An electronic version of the report is available at URL <http://techreports.larc.nasa.gov/RandT95>. This electronic version allows viewing, retrieving, and printing of the highlights, searching and browsing through the sections, and access to an on-line directory of Langley researchers. For further information concerning this report, contact Dennis M. Bushnell, Senior Scientist, Mail Stop 110, NASA Langley Research Center, Hampton, Virginia 23681-0001, (757) 864-8987.

138.

William B. Igoe, **Analysis of Fluctuating Static Pressure Measurements in the National Transonic Facility**, NASA TP-3475, March 1996, pp. 187, (6.9MB).

Format(s): Postscript, or PDF

Keywords: Transonic; Dynamic flow quality; Cryogenic; Pressure fluctuations; High Reynolds number

Abstract: Dynamic measurements of fluctuating static pressure levels were taken with flush-mounted, high-frequency response pressure transducers at 11 locations in the circuit of the National Transonic Facility (NTF) across the complete operating range of this wind tunnel. Measurements were taken at test-section Mach numbers from 0.1 to 1.2, at pressures from 1 to 8.6 atm, and at temperatures from ambient to -250 degrees F, which resulted in dynamic flow disturbance measurements at the highest Reynolds numbers available in a transonic ground test facility. Tests were also made by independent variation of the Mach number, the Reynolds number, or the fan drive power while the other two parameters were held constant, which for the first time resulted in a distinct separation of the effects of these three important parameters.

139.

Carey S. Buttrill, Barton J. Bacon, Jennifer Heeg, Jacob A. Houck and David V. Wood, **Aeroservoelastic Simulation of an Active Flexible Wing Wind Tunnel Model**, NASA TP-3510, April 1996, pp. 57, (1.7MB).

Format(s): Postscript, or PDF

Keywords: AFW; Active flexible wing; Aeroservoelastic simulation; Model reduction; Turbulence; Real-time simulation

Abstract: Mathematical models and implementation issues are described for simulations developed in the active flexible wing wind tunnel test program, which resulted in successful application of active flutter control. The wind tunnel test program required a truth batch simulation for off-line tests of proposed control designs and functional, hot-bench tests of digital controller hardware and software. To provide the hot-bench test environment, a real-time

simulation of the wind tunnel model and test environment was desired. Although mathematical model complexity and computing power limitations prevented attainment of real-time operation, essential test goals were met with a hot-bench simulation running at a timescale ratio no slower than 1:5. To achieve the required timescale, model reduction methods were applied to the aeroservoelastic portion of the full-order mathematical model. The reduction method was based on the internally balanced realization of a linear dynamic system. The error-bound properties of the internally balanced realization contributed to the method utility in the model reduction process. The state dimensions of the aeroservoelastic model were reduced by a factor of 2. The errors due to reduction appeared beyond the 10th bit of the analog-to-digital converters for all 560 combinations of simulation inputs and outputs.

140.

M. C. Bailey, **Closed-Form Evaluation of Mutual Coupling in a Planar Array of Circular Apertures**, NASA TP-3552, April 1996, pp. 20, (461KB).

Format(s): Postscript, or PDF

Keywords: Antennas; Mutual coupling; Phased arrays; Circular apertures

Abstract: The integral expression for the mutual admittance between circular apertures in a planar array is evaluated in closed form. Very good accuracy is realized when compared with values that were obtained by numerical integration. Utilization of this closed-form expression, for all element pairs that are separated by more than one element spacing, yields extremely accurate results and significantly reduces the computation time that is required to analyze the performance of a large electronically scanning antenna array.

141.

Harry W. Carlson, Marcus O. McElroy, Wendy B. Lessard and L. Arnold McCullers, **Improved Method for Prediction of Attainable Wing Leading-Edge Thrust**, NASA TP-3557, April 1996, pp. 63, (1.2MB).

Format(s): Postscript, or PDF

Keywords: Aerodynamics; Linearized theory; Numerical methods; Attainable thrust

Abstract: Prediction of the loss of wing leading-edge thrust and the accompanying increase in drag due to lift, when flow is not completely attached, presents a difficult but commonly encountered problem. A method (called the previous method) for the prediction of attainable leading-edge thrust and the resultant effect on airplane aerodynamic performance has been in use for more than a decade. Recently, the method has been revised to enhance its applicability to current airplane design and evaluation problems. The improved method (called the present method) provides for a greater range of airfoil shapes from very sharp to very blunt leading edges. It is also based on a wider range of Reynolds numbers than was available for the previous method. The present method, when employed in computer codes for aerodynamic analysis, generally results in improved correlation with experimental wing-body axial-force data and provides reasonable estimates of the measured drag.

142.

Charles E. Cockrell, Jr. and Lawrence D. Huebner, **Aerodynamic Characteristics of Two Waverider-Derived Hypersonic Cruise**, NASA TP-3559, July 1996, pp. 73, (16MB).

Format(s): Postscript, or PDF

Keywords: Hypersonic cruise; Waveriders; Airbreathing vehicles

Abstract: An evaluation was made on the effects of integrating the required aircraft components with hypersonic high-lift configurations known as waveriders to create hypersonic cruise vehicles. Previous studies suggest that waveriders offer advantages in aerodynamic performance and propulsion/airframe integration (PAI) characteristics over conventional non-waverider hypersonic shapes. A wind-tunnel model was developed that integrates vehicle components, including canopies, engine components, and control surfaces, with two pure waverider shapes, both conical-flow-derived waveriders for a design Mach number of 4.0. Experimental data and limited computational fluid dynamics (CFD) solutions were obtained over a Mach number range of 1.6 to 4.63. The experimental data show the component build-up effects and the aerodynamic characteristics of the fully integrated configurations, including control surface effectiveness. The aerodynamic performance of the fully integrated configurations is not comparable to that of the pure waverider shapes, but is comparable to previously tested hypersonic models. Both configurations exhibit good lateral-directional stability characteristics.

143.

Wendell R. Ricks, Jon E. Jonsson and John S. Barry, **Managing Approach Plate Information Study (MAPLIST): An Information Requirements Analysis of Approach Chart Use**, NASA TP-3561, February 1996, pp. 76, (5.8MB).

Format(s): Postscript, or PDF

Keywords: Approach information; Approach and landing tasks; Information requirements; Cognition; Mental models; Cognitive tasks; Approach charts; Approach plates

Abstract: Adequately presenting all necessary information on an approach chart represents a challenge for cartographers. Since many tasks associated with using approach charts are cognitive (e.g., planning the approach and monitoring its progress), and since the characteristic of a successful interface is one that conforms to the users' mental models, understanding pilots' underlying models of approach chart information would greatly assist cartographers. To provide such information, a new methodology was developed for this study that enhances traditional information requirements analyses by combining psychometric scaling techniques with a simulation task to provide quantifiable links between pilots' cognitive representations of approach information and their use of approach information. Results of this study should augment previous information requirements analyses by identifying what information is acquired, when it is acquired, and what presentation concepts might facilitate its efficient use by better matching the pilots' cognitive model of the information. The primary finding in this study indicated that pilots mentally organize approach chart information into ten primary categories: communications, geography, validation, obstructions; navigation, missed approach, final items, other runways,

visibility requirement, and navigation aids. These similarity categories were found to underlie the pilots' information acquisitions, other mental models, and higher level cognitive processes that are used to accomplish their approach and landing tasks.

144.

John F. Shaeffer, Kam W. Hom, R. Craig Baucke, Brett A. Cooper and Noel A. Talcott, Jr., **Bistatic k-Space Imaging for Electromagnetic Prediction Codes for Scattering and Antennas**, NASA TP-3569, July 1996, pp. 81, (277KB).

Format(s): Postscript, or PDF

Keywords: Electromagnetics; Radar cross section; Scattering; Antennas; Imaging

Abstract: A bistatic k-space image concept for frequency domain electromagnetic computer codes is presented. The concept enables images to be computed without the frequency sweep required for experimental images and results in significant reduction in computation effort. This analytical image technique uses bistatic radiation computed from a generalized radiation integral. The technique can be applied to antenna or scattering problems. One-, two-, or three-dimensional images can be computed. The theory for the method and images in 1-D, 2-D, and 3-D for selected scattering and antenna examples are presented. Electromagnetic computer codes utilized for the examples include patch and body-of-revolution method-of-moment computer codes, a physical optics computer code, and a finite element frequency domain computer code. Also, a comparison of the computational method with the experimental swept-frequency-rotation-angle approach is included. Finally, flat plate target 1-D and 2-D images measured experimentally are compared with images computed by the bistatic k-space approach.

145.

Stephen J. Katzberg and Richard B. Statham, **Performance Assessment of the Digital Array Scanned Interferometer (DASI) Concept**, NASA TP-3570, August 1996, pp. 26, (213KB).

Format(s): Postscript, or PDF

Keywords: Interferometer; Imaging; Multispectral imager throughput; Signal to noise

Abstract: Interferometers are known to have higher throughput than grating spectrometers for the same resolvance. The digital array scanned interferometer (DASI) has been proposed as an instrument that can capitalize on the superior throughput of the interferometer and, simultaneously, be adapted to imaging. The DASI is not the first implementation of the dual purpose concept, but it is one that has made several claims of major performance superiority, and it has been developed into a complete instrument. This paper reviews the DASI concept, summarizes its claims, and gives an assessment of how well the claims are justified. It is shown that the claims of signal-to-noise ratio superiority and operational simplicity are realized only modestly, if at all.

146.

Danny R. Sprinkle, Sushil K. Chaturvedi and Ali Kheireddine, **On-Line Measurement of Heat of Combustion of Gaseous Hydrocarbon Fuel Mixtures** , NASA TP-3572, March 1996, pp. 13, (1.3MB).

Format(s): Postscript, or PDF

Keywords: Natural gas; Natural gas energy content; Heat of combustion; Hydrocarbon combustion; Combustion physics; Combustion control; Enthalpy of combustion; Thermal energy measurement; Combustion calorimetry

Abstract: A method for the on-line measurement of the heat of combustion of gaseous hydrocarbon fuel mixtures has been developed and tested. The method involves combustion of a test gas with a measured quantity of air to achieve a preset concentration of oxygen in the combustion products. This method involves using a controller which maintains the fuel (gas) volumetric flow rate at a level consistent with the desired oxygen concentration in the combustion products. The heat of combustion is determined from a known correlation with the fuel flow rate. An on-line computer accesses the fuel flow data and displays the heat of combustion measurement at desired time intervals. This technique appears to be especially applicable for measuring heats of combustion of hydrocarbon mixtures of unknown composition such as natural gas.

147.

John A. Tanner, **Computational Methods for Frictional Contact With Applications to the Space Shuttle Orbiter Nose-Gear Tire---Comparisons of Experimental Measurements and Analytical Predictions** , NASA TP-3573, May 1996, pp. 55, (2MB) .

Format(s): Postscript, or PDF

Keywords: Finite elements; Frictional contact; Nose-gear; Shell theory; Shuttle; Tire modeling

Abstract: A computational procedure is presented for the solution of frictional contact problems for aircraft tires. A Space Shuttle nose-gear tire is modeled using a two-dimensional laminated anisotropic shell theory which includes the effects of variations in material and geometric parameters, transverse-shear deformation, and geometric nonlinearities. Contact conditions are incorporated into the formulation by using a perturbed Lagrangian approach with the fundamental unknowns consisting of the stress resultants, the generalized displacements, and the Lagrange multipliers associated with both contact and friction conditions. The contact-friction algorithm is based on a modified Coulomb friction law. A modified two-field, mixed-variational principle is used to obtain elemental arrays. This modification consists of augmenting the functional of that principle by two terms: the Lagrange multiplier vector associated with normal and tangential node contact-load intensities and a regularization term that is quadratic in the Lagrange multiplier vector. These capabilities and computational features are incorporated into an in-house computer code. Experimental measurements were taken to define the response of the Space Shuttle nose-gear tire to inflation-pressure loads and to inflation-pressure loads combined with normal static loads against a rigid flat plate. These experimental results describe the meridional growth of the tire cross section caused by inflation loading, the static load-deflection characteristics of the tire, the geometry of the tire footprint under static loading conditions, and the normal and tangential load-intensity distributions in the tire footprint for the various static vertical-loading conditions.

Numerical results were obtained for the Space Shuttle nose-gear tire subjected to inflation pressure loads and combined inflation pressure and contact loads against a rigid flat plate. The experimental measurements and the numerical results are compared.

148.

John A. Tanner, **Computational Methods for Frictional Contact With Applications to the Space Shuttle Orbiter Nose-Gear Tire - Development of Frictional Contact Algorithm**, NASA TP-3574, April 1996, pp. 48, (941KB).

Format(s): Postscript, or PDF

Keywords: Finite elements; Tire modeling; Frictional contact; Shuttle; Nose-gear; Shell theory

Abstract: A computational procedure is presented for the solution of frictional contact problems for aircraft tires. A Space Shuttle nose-gear tire is modeled using a two-dimensional laminated anisotropic shell theory which includes the effects of variations in material and geometric parameters, transverse-shear deformation, and geometric nonlinearities. Contact conditions are incorporated into the formulation by using a perturbed Lagrangian approach with the fundamental unknowns consisting of the stress resultants, the generalized displacements, and the Lagrange multipliers associated with both contact and friction conditions. The contact-friction algorithm is based on a modified Coulomb friction law. A modified two-field, mixed-variational principle is used to obtain elemental arrays. This modification consists of augmenting the functional of that principle by two terms: the Lagrange multiplier vector associated with normal and tangential node contact-load intensities and a regularization term that is quadratic in the Lagrange multiplier vector. These capabilities and computational features are incorporated into an in-house computer code. Experimental measurements were taken to define the response of the Space Shuttle nose-gear tire to inflation-pressure loads and to inflation-pressure loads combined with normal static loads against a rigid flat plate. These experimental results describe the meridional growth of the tire cross section caused by inflation loading, the static load-deflection characteristics of the tire, the geometry of the tire footprint under static loading conditions, and the normal and tangential load-intensity distributions in the tire footprint for the various static vertical loading conditions. Numerical results were obtained for the Space Shuttle nose-gear tire subjected to inflation pressure loads and combined inflation pressure and contact loads against a rigid flat plate. The experimental measurements and the numerical results are compared.

149.

M. D. Deshpande, C. R. Cockrell and C. J. Reddy, **Electromagnetic Scattering Analysis of Arbitrarily Shaped Material Cylinder**, NASA TP-3575, July 1996, pp. 31, (261KB).

Format(s): Postscript, PDF, or HTML

Keywords: Electromagnetic scattering; Hybrid FEM-BEM technique

Abstract: A hybrid method that combines the finite element method (FEM) and the boundary element method (BEM) is developed to analyze electromagnetic scattering from arbitrarily shaped material cylinders. By this method, the material cylinder is first enclosed by a fictitious boundary.

Maxwell's equations are then solved by FEM inside and by BEM outside the boundary. Electromagnetic scattering from several arbitrarily shaped material cylinders is computed and compared with results obtained by other numerical techniques.

150.

Dennis O. Allison and Raymond E. Mineck, **Assessment of Dual-Point Drag Reduction for an Executive-Jet Modified Airfoil Section**, NASA TP-3579, July 1996, pp. 117, (10MB).

Format(s): Postscript, or PDF

Keywords: Airfoil section; Pressure distributions; Aerodynamic characteristics; Drag reduction; Transonic conditions; Executive jet; Business jet

Abstract: This paper presents aerodynamic characteristics and pressure distributions for an executive-jet modified airfoil and discusses drag reduction relative to a baseline airfoil for two cruise design points. A modified airfoil was tested in the adaptive-wall test section of the NASA Langley 0.3-Meter Transonic Cryogenic Tunnel (0.3-m TCT) for Mach numbers from ranging 0.250 to 0.780 and chord Reynolds numbers ranging from 3.0×10^6 to 18.0×10^6 . The angle of attack was varied from -2 degrees to almost 10 degrees. Boundary-layer transition was fixed at 5 percent of chord on both the upper and lower surfaces of the model for most of the test. The two design Mach numbers were 0.654 and 0.735, chord Reynolds numbers were 4.5×10^6 and 8.9×10^6 , and normal-force coefficients were 0.98 and 0.51. Test data are presented graphically as integrated force and moment coefficients and chordwise pressure distributions. The maximum normal-force coefficient decreases with increasing Mach number. At a constant normal-force coefficient in the linear region, as Mach number increases an increase occurs in the slope of normal-force coefficient versus angle of attack, negative pitching-moment coefficient, and drag coefficient. With increasing Reynolds number at a constant normal-force coefficient, the pitching-moment coefficient becomes more negative and the drag coefficient decreases. The pressure distributions reveal that when present, separation begins at the trailing edge as angle of attack is increased. The modified airfoil, which is designed with pitching moment and geometric constraints relative to the baseline airfoil, achieved drag reductions for both design points (12 and 22 counts). The drag reductions are associated with stronger suction pressures in the first 10 percent of the upper surface and weakened shock waves.

151.

Terence A. Ghee, John D. Berry and Laith A. J. Zori, **Wake Geometry Measurements and Analytical Calculations on a Small-Scale Rotor Model**, NASA TP-3584, August 1996, (7MB).

Format(s): Postscript, or PDF

Keywords: Rotor; Wake; Vortex; Flow visualization; Helicopter; Laser; Light sheet; Wind tunnel

Abstract: An experimental investigation was conducted in the Langley 14- by 22-Foot Subsonic Tunnel to quantify the rotor wake behind a scale model helicopter rotor in forward level flight at one thrust level. The rotor system in this test consisted of a four-bladed fully articulated hub with blades of rectangular planform and an NACA 0012 airfoil section. A laser light sheet, seeded with

propylene glycol smoke, was used to visualize the vortex geometry in the flow in planes parallel and perpendicular to the free-stream flow. Quantitative measurements of wake geometric properties, such as vortex location, vertical skew angle, and vortex particle void radius, were obtained as well as convective velocities for blade tip vortices. Comparisons were made between experimental data and four computational method predictions of experimental tip vortex locations, vortex vertical skew angles, and wake geometries. The results of these comparisons highlight difficulties of accurate wake geometry predictions.

152.

Xian-He Sun and Stuti Moitra, **A Fast Parallel Tridiagonal Algorithm for a Class of CFD Applications**, NASA TP-3585, August 1996, pp. 5, (222KB).

Format(s): Postscript, or PDF

Keywords: Parallel algorithm; Parallel tridiagonal solver; CFD application; Symmetric Toeplitz tridiagonal solver

Abstract: The parallel diagonal dominant (PDD) algorithm is an efficient tridiagonal solver. This paper presents for study a variation of the PDD algorithm, the reduced PDD algorithm. The new algorithm maintains the minimum communication provided by the PDD algorithm, but has a reduced operation count. The PDD algorithm also has a smaller operation count than the conventional sequential algorithm for many applications. Accuracy analysis is provided for the reduced PDD algorithm for symmetric Toeplitz tridiagonal (STT) systems. Implementation results on Langley's Intel Paragon and IBM SP2 show that both the PDD and reduced PDD algorithms are efficient and scalable.

153.

Michael P. Nemeth, **Buckling and Postbuckling Behavior of Laminated Composite Plates With a Cutout**, NASA TP-3587, July 1996, pp. 24, This work was done under the Floyd Thompson Fellowship. This paper was previously published as a chapter in Buckling and Postbuckling of Composite Plates, G. J. Turvey and I. H. Marshall, eds., Chapman and Hall Ltd., Dec. 1994. (228KB).

Format(s): Postscript, PDF, or HTML

Keywords: Buckling; Postbuckling; Cutouts; Plates; Composites

Abstract: This paper addresses the effects of a cutout on the buckling and postbuckling behavior of rectangular plates made of advanced composite materials. An overview of past research is presented, and several key findings and behavioral characteristics are discussed. These findings include the effects of cutout size, shape, eccentricity, and orientation; plate aspect and slenderness ratios; loading and boundary conditions; and plate orthotropy and anisotropy. Some overall important findings of these studies are that plates that have a cutout can buckle at loads higher than the buckling loads for corresponding plates without a cutout and can exhibit substantial postbuckling load-carrying capability. In addition, laminate construction, coupled with cutout geometry, offers a viable means for tailoring structural response.

154.

Raymond E. Mineck and Peter M. Hartwich, **Effect of Full-Chord Porosity on Aerodynamic Characteristics of the NACA 0012 Airfoil**, NASA TP-3591, April 1996, pp. 89, (7.7MB).

Format(s): Postscript, or PDF

Keywords: Porous airfoils

Abstract: A test was conducted on a model of the NACA 0012 airfoil section with a solid upper surface or a porous upper surface with a cavity beneath for passive venting. The purposes of the test were to investigate the aerodynamic characteristics of an airfoil with full-chord porosity and to assess the ability of porosity to provide a multipoint or self-adaptive design. The tests were conducted in the Langley 8-Foot Transonic Pressure Tunnel over a Mach number range from 0.50 to 0.82 at chord Reynolds numbers of 2×10^6 , 4×10^6 , and 6×10^6 . The angle of attack was varied from -1 degree to 6 degrees. At the lower Mach numbers, porosity leads to a dependence of the drag on the normal force. At subcritical conditions, porosity tends to flatten the pressure distribution, which reduces the suction peak near the leading edge and increases the suction over the middle of the chord. At supercritical conditions, the compression region on the porous upper surface is spread over a longer portion of the chord. In all cases, the pressure coefficient in the cavity beneath the porous surface is fairly constant with a very small increase over the rear portion. For the porous upper surface, the trailing edge pressure coefficients exhibit a creep at the lower section normal force coefficients, which suggests that the boundary layer on the rear portion of the airfoil is significantly thickening with increasing normal force coefficient.

155.

William B. Compton III, **Comparison of Turbulence Models for Nozzle-Afterbody Flows With Propulsive Jets**, NASA TP-3592, September 1996, pp. 117, (11MB).

Format(s): Postscript, or PDF

Keywords: Computational fluid dynamics; Navier-Stokes; Turbulence models; Two-equation k-e; Transonic; Separated flow; Boundary layer; Afterbody; Nozzle; Convergent-divergent; Jet plume; Mixing; Drag; Skin friction

Abstract: A numerical investigation was conducted to assess the accuracy of two turbulence models when computing non-axisymmetric nozzle-afterbody flows with propulsive jets. Navier-Stokes solutions were obtained for a convergent-divergent nonaxisymmetric nozzle-afterbody and its associated jet exhaust plume at free-stream Mach numbers of 0.600 and 0.938 at an angle of attack of 0 degrees. The Reynolds number based on model length was approximately 20×10^6 . Turbulent dissipation was modeled by the algebraic Baldwin-Lomax turbulence model with the Degani-Schiff modification and by the standard Jones-Launder k-e turbulence model. At flow conditions without strong shocks and with little or no separation, both turbulence models predicted the pressures on the surfaces of the nozzle very well. When strong shocks and massive separation existed, both turbulence models were unable to predict the flow accurately. Mixing of the jet exhaust plume and the external flow was underpredicted. The differences in drag coefficients for the two turbulence models illustrate that substantial development is still required

for computing very complex flows before nozzle performance can be predicted accurately for all external flow conditions.

156.

Francis A. Cucinotta and John W. Wilson, **Study of Analytic Statistical Model for Decay of Light and Medium Mass Nuclei in Nuclear Fragmentation**, NASA TP-3594, October 1996, pp. 26, (442KB).

Format(s): Postscript, or PDF

Keywords: Heavy ions; Nuclear fragmentation; Galactic cosmic rays

Abstract: The angular momentum independent statistical decay model is often applied using a Monte-Carlo simulation to describe the decay of prefragment nuclei in heavy ion reactions. This paper presents an analytical approach to the decay problem of nuclei with mass number less than 60, which is important for galactic cosmic ray (GCR) studies. This decay problem of nuclei with mass number less than 60 incorporates well-known levels of the lightest nuclei ($A < 11$) to improve convergence and accuracy. A sensitivity study of the model level density function is used to determine the impact on mass and charge distributions in nuclear fragmentation. This angular momentum independent statistical decay model also describes the momentum and energy distribution of emitted particles (n, p, d, t, h, and a) from a prefragment nucleus.

157.

S. P. Pao and K. S. Abdol-Hamid, **Numerical Simulation of Jet Aerodynamics Using the Three-Dimensional Navier-Stokes Code PAB3D**, NASA TP-3596, September 1996, pp. 43, (2MB).

Format(s): Postscript, or PDF

Keywords: Jet; Computation; Fluid dynamics

Abstract: This report presents a unified method for subsonic and supersonic jet analysis using the three-dimensional Navier-Stokes code PAB3D. The Navier-Stokes code was used to obtain solutions for axisymmetric jets with on-design operating conditions at Mach numbers ranging from 0.6 to 3.0, supersonic jets containing weak shocks and Mach disks, and supersonic jets with nonaxisymmetric nozzle exit geometries. This report discusses computational methods, code implementation, computed results, and comparisons with available experimental data. Very good agreement is shown between the numerical solutions and available experimental data over a wide range of operating conditions. The Navier-Stokes method using the standard Jones-Launder two-equation k-e turbulence model can accurately predict jet flow, and such predictions are made without any modification to the published constants for the turbulence model.

158.

Wendy B. Lessard, **Subsonic Analysis of 0.04-Scale F-16XL Models Using an Unstructured**

Euler Code , NASA TP-3597, October 1996, pp. 78, (23MB).

Format(s): Postscript, or PDF

Keywords: Unstructured grids; Euler computations; Subsonic flow field

Abstract: The subsonic flow field about an F-16XL airplane model configuration was investigated with an inviscid unstructured grid technique. The computed surface pressures were compared to wind-tunnel test results at Mach 0.148 for a range of angles of attack from 0 to 20. To evaluate the effect of grid dependency on the solution, a grid study was performed in which fine, medium, and coarse grid meshes were generated. The off-surface vortical flow field was locally adapted and showed improved correlation to the wind-tunnel data when compared to the nonadapted flow field. Computational results are also compared to experimental five-hole pressure probe data. A detailed analysis of the off-body computed pressure contours, velocity vectors, and particle traces are presented and discussed.

159.

William R. Doggett, A Guidance Scheme for Automated Tetrahedral Truss Structure Assembly Based on Machine Vision , NASA TP-3601, November 1996, pp. 18, (3MB).

Format(s): Postscript, or PDF

Keywords: Automated construction; Guidance; Machine vision

Abstract: The Automated Structures Assembly Laboratory (ASAL) is a unique facility at Langley Research Center used to investigate robotic assembly of truss structures. An industrial robot equipped with a special purpose end-effector has been used to assemble 102 struts into an 8-m-diameter structure, as well as beam structures. Initially, robot motions required to construct the structure were developed with iterative manual procedures. However, this approach is not suitable for in-space applications because of astronaut and time and safety considerations. Thus, an off-line geometric path planner combined with a compact machine vision system has been developed. By providing position information relative to passive targets on the structure, the vision system guides the robot through a critical region, beginning approximately 12 in. from the structure and proceeding to a position where the structure is grasped prior to strut insertion. This approach offsets model uncertainties in the path planner and greatly increases operational reliability. This paper presents details of the machine-vision-based guidance algorithms used during structure assembly.

160.

M. C. Bailey, Technique for Extension of Small Antenna Array Mutual-Coupling Data to Larger Antenna Arrays , NASA TP-3603, August 1996, pp. 15, (713KB).

Format(s): Postscript, or PDF

Keywords: Antennas; Phased arrays; Mutual coupling

Abstract: A technique is presented whereby the mutual interaction between a small number of elements in a planar array can be interpolated and extrapolated to accurately predict the combined interactions in a much larger array of many elements. An approximate series expression is developed, based upon knowledge of the analytical characteristic behavior of the mutual admittance between small aperture antenna elements in a conducting ground plane. This expression is utilized to analytically extend known values for a few spacings and orientations to other element configurations, thus eliminating the need to numerically integrate a large number of highly oscillating and slowly converging functions. This paper shows that the technique can predict very accurately the mutual coupling between elements in a very large planar array with a knowledge of the self-admittance of an isolated element and the coupling between only two elements arranged in eight different pair combinations. These eight pair combinations do not necessarily have to correspond to pairs in the large array, although all of the individual elements must be identical.

161.

John D. W. Barrick, John A. Ritter, Catherine E. Watson, Mark W. Wynkoop and John K. Quinn, **Calibration of NASA Turbulent Air Motion Measurement System**, NASA TP-3610, December 1996, pp. 29, (2MB).

Format(s): Postscript, or PDF

Keywords: Aircraft air motion measurement; Static pressure position error; Turbulent air motion

Abstract: A turbulent air motion measurement system (TAMMS) was integrated onboard the Lockheed 188 Electra airplane (designated NASA 429) based at the Wallops Flight Facility in support of the NASA role in global tropospheric research. The system provides air motion and turbulence measurements from an airborne platform which is capable of sampling tropospheric and planetary boundary-layer conditions. TAMMS consists of a gust probe with free-rotating vanes mounted on a 3.7-m epoxy-graphite composite nose boom, a high-resolution inertial navigation system (INS), and data acquisition system. A variation of the tower flyby method augmented with radar tracking was implemented for the calibration of static pressure position error and air temperature probe. Additional flight calibration maneuvers were performed remote from the tower in homogeneous atmospheric conditions. System hardware and instrumentation are described and the calibration procedures discussed. Calibration and flight results are presented to illustrate the overall ability of the system to determine the three-component ambient wind fields during straight and level flight conditions.

162.

Michael P. Nemeth, Vicki O. Britt, Timothy J. Collins and James H. Starnes, Jr., **Nonlinear Analysis of the Space Shuttle Superlightweight External Fuel Tank**, NASA TP-3616, December 1996, pp. 27, (2MB) Presented at the 37th AIAA/ASME/ASCE/AHS/ASC Structures, Structural Dynamics, and Materials Conference, Salt Lake City, Utah, April 15-17, 1996.

Format(s): Postscript, or PDF

Keywords: Space Shuttle external tank; Nonlinear stability analysis; Launch vehicles; Buckling

Abstract: Results of buckling and nonlinear analyses of the Space Shuttle external tank superlightweight liquid-oxygen (LO2) tank are presented. Modeling details and results are presented for two prelaunch loading conditions and for two full-scale structural tests that were conducted on the original external tank. The results illustrate three distinctly different types of nonlinear response for thin-walled shells subjected to combined mechanical and thermal loads. The nonlinear response phenomena consist of bifurcation-type buckling, short-wavelength nonlinear bending, and nonlinear collapse associated with a limit point. For each case, the results show that accurate predictions of non-linear behavior generally require a large-scale, high-fidelity finite-element model. Results are also presented that show that a fluid-filled launch-vehicle shell can be highly sensitive to initial geometric imperfections. In addition, results presented for two full-scale structural tests of the original standard-weight external tank suggest that the finite-element modeling approach used in the present study is sufficient for representing the nonlinear behavior of the superlightweight LO2 tank.

163.

Jag J. Singh, Ruth H. Pater and Abe Eftekhari, **Microstructural Characterization of Semi-Interpenetrating Polymer Networks by Positron Lifetime Spectroscopy**, NASA TP-3617, October 1996, pp. 17, (393KB).

Format(s): Postscript, or PDF

Keywords: Polyimides (thermoset and thermoplastic); Semi-interpenetrating polymer networks; Positron lifetime spectroscopy; Free volume cell radius; Free volume fraction; Dielectric constant; Electric dipole interactions

Abstract: Thermoset and thermoplastic polyimides have complementary physical and mechanical properties. Whereas thermoset polyimides are brittle and generally easier to process, thermoplastic polyimides are tough but harder to process. A combination of these two types of polyimides may help produce polymers more suitable for aerospace applications. Semi-Interpenetrating Polymer Networks (S-IPN) of thermoset LaRCTM-RP46 and thermoplastic LaRCTM-IA polyimides were prepared in weight percent ratios ranging from 100:0 to 0:100. Positron lifetime measurements were made in these samples to correlate their free volume features with physical and mechanical properties. As expected, positronium atoms are not formed in these samples. The second lifetime component has been used to infer the positron trap dimensions. The "free volume" goes through a minimum at a ratio of about 50:50, and this suggests that S-IPN samples are not merely solid solutions of the two polymers. These data and related structural properties of the S-IPN samples are discussed.

164.

C. J. Reddy, M. D. Deshpande, D. T. Fralick, C. R. Cockrell and F. B. Beck, **A Combined FEM/MoM/GTD Technique To Analyze Elliptically Polarized Cavity-Backed Antennas With Finite Ground Plane**, NASA TP-3618, November 1996, pp. 20, (426KB).

Format(s): Postscript, or PDF

Keywords: Spiral antennas; Cavity-backed; Finite Element Method; Method of Moments;

Geometrical Theory of Diffraction

Abstract: Radiation pattern prediction analysis of elliptically polarized cavity-backed aperture antennas in a finite ground plane is performed using a combined Finite Element Method/Method of Moments/Geometrical Theory of Diffraction (FEM/MoM/GTD) technique. The magnetic current on the cavity-backed aperture in an infinite ground plane is calculated using the combined FEM/MoM analysis. GTD, including the slope diffraction contribution, is used to calculate the diffracted fields caused by both soft and hard polarizations at the edges of the finite ground plane. Explicit expressions for regular diffraction coefficients and slope diffraction coefficients are presented. The slope of the incident magnetic field at the diffraction points is derived and analytical expressions are presented. Numerical results for the radiation patterns of a cavity-backed circular spiral microstrip patch antenna excited by a coaxial probe in a finite rectangular ground plane are computed and compared with experimental results.

165.

Jag J. Singh and Abe Eftekhari, **Investigation of Oxygen-Induced Quenching of Phosphorescence in Photoexcited Aromatic Molecules by Positron Annihilation**, NASA TP-3619, October 1996, pp. 9, (236KB).

Format(s): Postscript, or PDF

Keywords: Platinum octaethyl porphyrin; Phosphorescence; Fluorescence; Quenching; Positron annihilation spectroscopy; Positronium formation; Doppler broadening spectroscopy

Abstract: Platinum octaethyl porphyrin (Pt.OEP) is an efficient phosphor under ultraviolet excitation. The phosphorescent triplet state P(T1) is readily quenched by the oxygen O₂ molecules. This phenomenon is being utilized as the basis for global air pressure measurements in aerodynamic facilities at various laboratories. The exact mechanism by which O₂ molecules quench the P(T1) \leftrightarrow P(S₀) transitions is still unknown. The diamagnetic singlet states P(S_n), which feed P(T1) states via intersystem crossings, would presumably not be affected by O₂. It must be only the magnetic P(T1) states, which can interact with the paramagnetic O₂ molecules, that are affected. However, our positron lifetime and Doppler broadening studies suggest the formation of O₂.P(S_n) complexes which can also eventually reduce the population of the P(T1) states (i.e., quench phosphorescence). This reduction is possible because higher triplet states in (Pt.OEP) are admixed with the P(S_n) states via spin orbit interactions. The experimental procedures and the results of various measurements are presented in this paper.

166.

Jessica A. Woods-Vedeler and Lucas G. Horta, **On-Orbit Application of H-Infinity to the Middeck Active Controls Experiment: Overview of Results**, *6th AAS/AIAA Space Flight Mechanics Meeting*, Austin, Texas, AAS 96-189, February 11-15, 1996, pp. 17, (143KB).

Format(s): Postscript, or PDF

Keywords: Flexible; Spacecraft; Robust control; Flight experiment

Abstract: The Middeck Active Control Experiment (MACE) was successfully completed during the flight of STS-67 in March 1995. MACE provided an on-orbit validation of modern robust control theory and system identification techniques through the testing of a flexible, multi-instrument, science platform in the micro-gravity environment of the Space Shuttle's Middeck. As part of this experiment, H-infinity control design was validated in zero gravity (0-G) environment. The control objective was to isolate a payload sensor from a 50Hz bandwidth disturbance occurring on the test article. Controllers were design with the use of finite element models developed using 1-G measurements and a measurement model obtained by applying system identification techniques to open loop data obtained on orbit. Over 50 single-input, single-output and multi-input, multi-output, single and multi-axis H-infinity control designs were evaluated on-orbit. Up to 19 dB reduction in vibration levels and 25 Hz bandwidth of control were achieved.

167.

J. G. Smith, Jr., **Chemistry and Properties of Imide Oligomers Containing Pendant and Terminal Phenylethynyl Groups**, *19th Annual Meeting of The Adhesion Society*, Myrtle Beach, South Carolina, February 18-21, 1996, pp. 4, (184KB).

Format(s): Postscript, or PDF

Keywords: Polyimide; Pendant and terminal; Imide oligomer; Phenylethynyl containing; Thermoset

Abstract: The evaluation of phenylethynyl terminated imide oligomers (PETIs) for use as structural resins for aeronautical applications has been ongoing. Upon thermal cure, the phenylethynyl group undergoes chain extension, branching and/or crosslinking to afford materials exhibiting a favorable combination of physical and mechanical properties. As a variation of work on PETIs, a series of imide oligomers containing both pendant and terminal phenylethynyl groups were prepared at a calculated average molecular weight of 5000 g/mol. By incorporating pendant phenylethynyl groups in PETIs, increases in the glass transition temperature and modulus and lower elongations to break for unoriented thin films with respect to PETIs were observed due to the increased crosslink density. Lap shear specimens processed at 350 degrees C for 1h under 200 psi for one pendant and terminal phenylethynyl imide oligomer (PTPEI) composition had strengths of 5000 psi at 23 degrees C with approximately 80 percent retention of properties at 232 degrees C. Good retention of lap shear strengths were obtained after exposure to jet fuel and hydraulic fluid. The processability of PTPEIs as moldings, adhesives, and composites was similar to PETI systems. The chemistry, physical, and mechanical properties of PTPEIs will be discussed.

168.

Willard E. Meador, Jr., Lawrence W. Townsend and Gilda A. Miner, **Effects of H₂O Vapor on Vibrational Relaxation in Contracting and Expanding Flows**, *34th AIAA Aerospace Sciences Meeting and Exhibit*, Reno, Nevada, AIAA Paper No. 96-0105, January 15-18, 1996, pp. 7, (732KB).

Format(s): Postscript, or PDF

Keywords: Hypersonics; Vibrational relaxation; Nonequilibrium mixtures; Purity effects

Abstract: As opposed to previous explanations based on the effects of anharmonicity of simple diatomic molecules, tracers of water vapor are suggested to be the most likely cause of the anomalously fast vibrational relaxation of such gases observed in supersonic and hypersonic nozzles. The mechanism is the strong V-VR coupling with H₂O molecules that dramatically facilitates the collisional transfer of vibrational energy. Slight moisture content is thus a real-world aspect of gas dynamics that must be considered in characterizations of shock tubes, reflected shock tunnels, and expansion tubes.

169.

K. S. Brentner, **An Efficient and Robust Method for Predicting Helicopter Rotor High-Speed Impulsive Noise**, *34th AIAA Aerospace Sciences Meeting and Exhibit*, Reno, Nevada, AIAA Paper No. 96-0151, January 15-18, 1996, pp. 10, (105KB).

Format(s): Postscript, or PDF

Keywords: High-speed impulsive noise; Helicopter noise prediction; Quadrupole noise; Rotor noise; Acoustic analogy

Abstract: A new formulation for the Ffowcs Williams-Hawkings quadrupole source, which is valid for a far-field in-plane observer, is presented. The far-field approximation is new and unique in that no further approximation of the quadrupole source strength is made and integrands with r to the -2 and r to the -3 dependence are retained. This paper focuses on the development of a retarded-time formulation in which time derivatives are analytically taken inside the integrals to avoid unnecessary computational work when the observer moves with the rotor. The new quadrupole formulation is similar to Farassat's thickness and loading formulation 1A. Quadrupole noise prediction is carried out in two parts: a preprocessing stage in which the previously computed flow field is integrated in the direction normal to the rotor disk, and a noise computation stage in which quadrupole surface integrals are evaluated for a particular observer position. Preliminary predictions for hover and forward flight agree well with experimental data. The method is robust and requires computer resources comparable to thickness and loading noise prediction.

170.

N. T. Frink, **Assessment of an Unstructured-Grid Method for Predicting 3-D Turbulent Viscous Flows**, *34th AIAA Aerospace Sciences Meeting and Exhibit*, Reno, Nevada, AIAA Paper No. 96-0292, January 15-18, 1996, pp. 11, (527KB).

Format(s): Postscript, or PDF

Keywords: Unstructured grid; Navier-Stokes; Viscous flow; Tetrahedral; Three-dimensional;

Abstract: A method is presented for solving turbulent flow problems on three-dimensional unstructured grids. Spatial discretization is accomplished by a cell-centered finite-volume formulation using an accurate linear reconstruction scheme and upwind flux differencing. Time is advanced by an implicit backward-Euler time-stepping scheme. Flow turbulence effects are modeled by the Spalart-Allmaras one-equation model, which is coupled with a wall function to

reduce the number of cells in the sublayer region of the boundary layer. A systematic assessment of the method is presented to devise guidelines for more strategic application of the technology to complex problems. The assessment includes the accuracy in predictions of skin-friction coefficient, law-of-the-wall behavior, and surface pressure for a flat-plate turbulent boundary layer, and for the ONERA M6 wing under a high Reynolds number, transonic, separated flow condition.

171.

Glenn S. Diskin, Walter R. Lempert and Richard B. Miles, **Observation of Vibrational Relaxation Dynamics in $X^{3}\Sigma_{g}$ Oxygen Following Stimulated Raman Excitation to the $v=1$ Level: Implications for the RELIEF Flow Tagging Technique**, *AIAA 34th Aerospace Sciences Meeting and Exhibit*, Reno, Nevada, AIAA 96-0301, January 15-18, 1996, pp. 12, (3.4MB).

Format(s): Postscript, or PDF

Keywords: Oxygen; Laser-induced fluorescence; Stimulated Raman scattering; RELIEF

Abstract: The vibrational relaxation of ground-state molecular oxygen (O_2) has been observed, following stimulated Raman excitation to the first excited vibrational level ($v=1$). Time delayed laser-induced fluorescence probing of the ro-vibrational population distribution was used to examine the temporal relaxation behavior. In the presence of water vapor, the relaxation process is rapid, and is dominated by near-resonant vibrational energy exchange between the $v=1$ level of O_2 and the (0,1,0) bending mode of H_2O . In the absence of H_2O , reequilibration proceeds via homogeneous vibrational energy transfer, in which a collision between two $v=1$ O_2 molecules leaves one molecule in the $v=2$ state and the other in the $v=0$ state. Subsequent collisions between molecules in $v=1$ and $v>1$ result in continued transfer of population up the vibrational ladder. The implications of these results for the RELIEF flow tagging technique are discussed.

172.

William A. Wood, Peter A. Gnoffo and Didier F. G. Rault, **Aerothermodynamic Analysis of Commercial Experiment Transporter (COMET) Reentry Capsule**, *AIAA 34th Aerospace Sciences Meeting and Exhibit*, Reno, NV, AIAA 96-0316, January 1996, pp. 8, (597KB).

Format(s): Postscript, or PDF

Keywords: Aerothermodynamics, COMET

Abstract: An aerothermodynamic analysis of the Commercial Experiment Transporter (COMET) reentry capsule has been performed using the laminar thin-layer Navier-Stokes solver Langley Aerothermodynamic Upwind Relaxation Algorithm. Flowfield solutions were obtained at Mach numbers 1.5, 2, 5, 10, 15, 20, 25, and ~ 27.5 . Axisymmetric and 5, 10, and 20-degree angles of attack were considered across the Mach-number range, with the Mach 25 conditions taken to 90 degrees angle of attack and the Mach 27.5 cases taken to 60 degrees angle of attack. Detailed surface heat-transfer rates were computed at Mach 20 and 25, revealing that heating rates on the heat-shield shoulder can exceed the stagnation-point heating by 230 percent. Finite-rate chemistry

solutions were performed above Mach 10, otherwise perfect gas computations were made. Drag, lift, and pitching moment coefficients are computed and details of a wake flow are presented. The effect of including the wake in the solution domain was investigated and base pressure corrections to forebody drag coefficients were numerically determined for the lower Mach numbers. Pitching moment comparisons are made with direct simulation Monte Carlo results in the more rarefied flow at the highest Mach numbers, showing agreement within two-percent. Thin-layer Navier-Stokes computations of the axial force are found to be 15 percent higher across the speed range than the empirical/Newtonian based results used during the initial trajectory analyses.

173.

David W. Witte, Kenneth E. Tatum and S. Blake Williams, **Computation of Thermally Perfect Compressible Flow Properties**, *34th Aerospace Sciences Meeting & Exhibit*, January 15-18, 1996, Reno, NV, AIAA-96-0681, January 1996, pp. 19, related paper: [NASA TP-3447](#), "Computer Code for Determination of Thermally Perfect Gas Properties", Witte, D. W., and Tatum, K. E., September 1994, (269KB).

Format(s): [Postscript](#), or [PDF](#)

Keywords: Thermally perfect gas; Calorically imperfect gas; Compressible flow relations; Tables of compressible flow properties; Thermally perfect gas computer code; Imperfect gas effects; Graphical user interface

Abstract: A set of compressible flow relations for a thermally perfect, calorically imperfect gas are derived for a value of c_p (specific heat at constant pressure) expressed as a polynomial function of temperature and developed into a computer program, referred to as the Thermally Perfect Gas (TPG) code. The code is available free from the NASA Langley Software Server at URL <http://www.larc.nasa.gov/LSS>. The code produces tables of compressible flow properties similar to those found in NACA Report 1135. Unlike the NACA Report 1135 tables which are valid only in the calorically perfect temperature regime the TPG code results are also valid in the thermally perfect, calorically imperfect temperature regime, giving the TPG code a considerably larger range of temperature application. Accuracy of the TPG code in the calorically perfect and in the thermally perfect, calorically imperfect temperature regimes are verified by comparisons with the methods of NACA Report 1135. The advantages of the TPG code compared to the thermally perfect, calorically imperfect method of NACA Report 1135 are its applicability to any type of gas (monatomic, diatomic, triatomic, or polyatomic) or any specified mixture of gases, ease-of-use, and tabulated results.

174.

Jaroslav Sobieszczanski-Sobieski and Raphael T. Haftka, **Multidisciplinary Aerospace Design Optimization: Survey of Recent Developments**, *34th AIAA Aerospace Sciences Meeting and Exhibit*, Reno, Nevada, AIAA Paper No. 96-0711, January 15-18, 1996, pp. 32, (98KB).

Format(s): [Postscript](#), or [PDF](#)

Keywords: Design; Optimization; Systems; Multidisciplinary; Survey

Abstract: The increasing complexity of engineering systems has sparked increasing interest in multidisciplinary optimization (MDO). This paper presents a survey of recent publications in the field of aerospace where interest in MDO has been particularly intense. The two main challenges of MDO are computational expense and organizational complexity. Accordingly the survey is focused on various ways different researchers use to deal with these challenges. The survey is organized by a breakdown of MDO into its conceptual components. Accordingly, the survey includes sections on Mathematical Modeling, Design- oriented Analysis, Approximation Concepts, Optimization Procedures, System Sensitivity, and Human Interface. With the authors' main expertise being in the structures area, the bulk of the references focus on the interaction of the structures discipline with other disciplines. In particular, two sections at the end focus on two such interactions that have recently been pursued with a particular vigor: Simultaneous Optimization of Structures and Aerodynamics, and Simultaneous Optimization of Structures Combined With Active Control.

175.

Jason T. Lachowicz, Ndaona Chokani and Stephen P. Wilkinson, **Hypersonic Boundary Layer Stability Over a Flared Cone in a Quiet Tunnel**, *34th AIAA Aerospace Sciences Meeting and Exhibit*, Reno, Nevada, AIAA 96-0782, January 15-18, 1996, (571KB).

Format(s): Postscript, or PDF

Keywords: Quiet tunnel; Stability and transition; Hypersonic

Abstract: Hypersonic boundary layer measurements were conducted over a flared cone in a quiet wind tunnel. The flared cone was tested at a freestream unit Reynolds number of $2.82 \times 10^6/\text{ft}$ in a Mach 6 flow. This Reynolds number provided laminar- to-transitional flow over the model in a low-disturbance environment. Point measurements with a single hot wire using a novel constant voltage anemometry system were used to measure the boundary layer disturbances. Surface temperature and schlieren measurements were also conducted to characterize the laminar-to-transitional state of the boundary layer and to identify instability modes. Results suggest that the second mode disturbances were the most unstable and scaled with the boundary layer thickness. The integrated growth rates of the second mode compared well with linear stability theory in the linear stability regime. The second mode is responsible for transition onset despite the existence of a second mode sub-harmonic. The sub-harmonic wavelength also scales with the boundary layer thickness. Furthermore, the existence of higher harmonics of the fundamental suggests that non-linear disturbances are not associated with "high" free stream disturbance levels.

176.

William L. Kleb, **Aerodynamic Characteristics of an Aerospace Vehicle During a Subsonic Pitch-Over Maneuver**, *34th Aerospace Sciences Meeting & Exhibit*, Reno, NV, AIAA Paper No. 96-0825, January 1996, pp. 11, (2.2MB).

Format(s): Postscript, or PDF

Keywords: Unsteady; Computational Fluid Dynamics; Inviscid; Unstructured grids; Flight vehicle

Abstract: Time-dependent CFD has been used to predict aerospace vehicle aerodynamics during a subsonic rotation maneuver. The inviscid 3D3U code is employed to solve the 3-D unsteady flowfield using an unstructured grid of tetrahedra. As this application represents a challenge to time-dependent CFD, observations concerning spatial and temporal resolution are included. It is shown that even for a benign rotation rate, unsteady aerodynamic effects are significant during the maneuver. Possibly more significant, however, the rotation maneuver creates flow asymmetries leading to yawing moment, rolling moment, and side force which are not present in the quasi-steady case. A series of steady solutions at discrete points in the maneuver are also computed for comparison with wind tunnel measurements and as a means of quantifying unsteady effects.

177.

Y. Y. Tang, J. H. Robinson and R. J. Silcox, **Sound Transmission Through a Cylindrical Sandwich Shell With Honeycomb Core**, *34th AIAA Aerospace Sciences Meeting and Exhibit*, Reno, Nevada, AIAA Paper No. 96-0877, January 15-18, 1996, pp. 10, (109KB).

Format(s): Postscript, or PDF

Keywords: Sound transmission; Sandwich shell; Honeycomb core; Transmission loss; Incident plane wave; Modal impedance; shear effect

Abstract: Sound transmission through an infinite cylindrical sandwich shell is studied in the context of the transmission of airborne sound into aircraft interiors. The cylindrical shell is immersed in fluid media and excited by an oblique incident plane sound wave. The internal and external fluids are different and there is uniform airflow in the external fluid medium. An explicit expression of transmission loss is derived in terms of modal impedance of the fluids and the shell. The results show the effects of (a) the incident angles of the plane wave; (b) the flight conditions of Mach number and altitude of the aircraft; (c) the ratios between the core thickness and the total thickness of the shell; and (d) the structural loss factors on the transmission loss. Comparisons of the transmission loss are made among different shell constructions and different shell theories.

178.

Prasun N. Desai, Robert D. Braun, Richard W. Powell, Walter C. Engelund and Paul V. Tartabini, **Six Degree-of-Freedom Entry Dispersion Analysis for the METEOR Recovery Module**, *34th AIAA Aerospace Sciences Meeting and Exhibit*, Reno, Nevada, AIAA Paper No. 96-0903, January 15-18, 1996, pp. 10, (754KB).

Format(s): Postscript, or PDF

Keywords: Planetary entry; Entry dispersion analysis; Six degree-of-freedom analysis

Abstract: The present study performs a six degree-of-freedom entry dispersion analysis for the Multiple Experiment Transporter to Earth Orbit and Return (METEOR) mission. METEOR offered the capability of flying a recoverable science package in a microgravity environment. However, since the Recovery Module has no active control system, an accurate determination of the splashdown position is difficult because no opportunity exists to remove any errors. Hence, uncertainties in the initial conditions prior to deorbit burn initiation, during deorbit burn and exo-

atmospheric coast phases, and during atmospheric flight impact the splashdown location. This investigation was undertaken to quantify the impact of the various exo-atmospheric and atmospheric uncertainties. Additionally, a Monte-Carlo analysis was performed to statistically assess the splashdown dispersion footprint caused by the multiple mission uncertainties. The Monte-Carlo analysis showed that a 3-sigma splashdown dispersion footprint with axes of 43.3 nm (long), -33.5 nm (short), and 10.0 nm (crossrange) can be constructed. A 58 percent probability exists that the Recovery Module will overshoot the nominal splashdown site.

179.

Donald J. Baker, **Evaluation of Thin Kevlar-Epoxy Fabric Panels Subjected to Shear Loading**, *AIAA/ASME/ASCE/AHS/ASC 37th Structures, Structural Dynamics, and Materials Conference*, Salt Lake City, Utah, AIAA Paper No. 96-1367, April 15-17, 1996, (3MB).

Format(s): Postscript, or PDF

Keywords: Shear panels; Postbuckled strength; Fatigue life; Composites; Kevlar-epoxy; Buckling

Abstract: The results of an analytical and experimental investigation of 4-ply Kevlar-49-epoxy panels loaded by in-plane shear are presented. Approximately one-half of the panels are thin-core sandwich panels and the other panels are solid-laminate panels. Selected panels were impacted with an aluminum sphere at a velocity of either 150 or 220 ft/sec. The strength of panels impacted at 150 ft/sec was not reduced when compared to the strength of the undamaged panels, but the strength of panels impacted at 220 ft/sec was reduced by 27 to 40 percent. Results are presented for panels that were cyclically loaded from a load less than the buckling load to a load in the postbuckling load range. The thin-core sandwich panels had a lower fatigue life than the solid panels. The residual strength of the solid and sandwich panels cycled more than one million cycles exceeded the baseline undamaged panel strengths. The effect of hysteresis in the response of the sandwich panels is not significant. Results of a nonlinear finite element analysis conducted for each panel design are presented.

180.

Mark S. Lake, Peter A. Warren and Lee D. Peterson, **A Revolute Joint With Linear Load-Displacement Response for Precision Deployable Structures**, *AIAA/ASME/ASCE/AHS/ASC 37th Structures, Structural Dynamics, and Materials Conference*, Salt Lake City, Utah, AIAA Paper No. 96-1500, April 15-17, 1996, (575KB).

Format(s): Postscript, or PDF

Keywords: Deployable structures; Precision; Reflector; Telescope; Revolute joint; Deployable accuracy

Abstract: NASA Langley Research Center is developing key structures and mechanisms technologies for micron-accuracy, in-space deployment of future science instruments. Achieving micron-accuracy deployment requires significant advancement in deployment mechanism design such as the revolute joint presented herein. The joint presented herein exhibits a load-cycling response that is essentially linear with less than two percent hysteresis, and the joint rotates with

less than one in.-oz. of resistance. A prototype reflector metering truss incorporating the joint exhibits only a few microns of kinematic error under repeated deployment and impulse loading. No other mechanically deployable structure found in the literature has been demonstrated to be this kinematically accurate.

181.

O. O. Storaasli, **Performance of NASA Equation Solvers on Computational Mechanics Applications**, Salt Lake City, Utah, AIAA Paper No. 96-1505, April 15-17, 1996, (1.2MB).

Keywords: Structural analysis; Equation solution; High-performance computing; Finite element; Electromagnetics; Computational mechanics

Abstract: This paper describes the performance of a new family of NASA-developed equation solvers used for large-scale (i.e. 551,705 equations) structural analysis. To minimize computer time and memory, the solvers are divided by application and matrix characteristics (sparse/dense, real/complex, symmetric/nonsymmetric, size: in-core/out of core) and exploit the hardware features of current and future computers. In this paper, the equation solvers, which are written in FORTRAN, and are therefore easily transportable, are shown to be faster than specialized computer library routines utilizing assembly code. Twenty NASA structural benchmark models with NASA solver timings reside on World Wide Web with a challenge to beat them.

182.

F. Farassat and M. K. Myers, **A Study of Wave Propagation in a Duct and Mode Radiation**, *2nd AIAA/CEAS Aeroacoustics Conference (17th AIAA Aeroacoustics Conference)*, State College, Pennsylvania, AIAA Paper No. 96-1677, May 6-8, 1996, (728KB).

Format(s): Postscript, or PDF

Keywords: Duct acoustics; Graphical approach; Mode detection; Circular microphone array; Ducted fans

Abstract: In this paper we discuss two problems of classical duct acoustics: (1) wave propagation in infinite ducts with uniform flow based on a graphical approach, and (2) detection of mode radiation from a duct by an external circular microphone array. In (1) we show that the wave number vectors for a given flow Mach number form an ellipse whose center and shape depend on the Mach number only. We construct graphically the upstream and downstream wave number vectors of modes that propagate in the duct. We then show how one can infer from this graphical approach many known results in duct propagation such as the mode cut-off concept, the direction of energy propagation, the angle of the radiation lobe at peak directivity using Rice's cut-off ratio concept, and other qualitative results. In (2) we give the mathematics behind the experimental detection of mode radiation from a duct by a circular array of microphones whose axis coincides with the engine axis. Since the external microphone array does not introduce additional noise sources inside the engine, as does a rotating rake of microphones positioned at the inlet, this measurement technique may be preferable to use of a rotating rake. The simplicity afforded by the lack of sophisticated rotating parts is an additional advantage over the rotating array.

183.

H. L. Atkins and Chi-Wang Shu, **Quadrature-Free Implementation of the Discontinuous Galerkin Method for Hyperbolic Equations**, *2nd AIAA/CEAS Aeroacoustics Conference*, State College, PA, AIAA Paper 96-1683, May 6-8, 1996, (2MB).

Format(s): Postscript, or PDF

Keywords: Aeroacoustics; High-order; Unstructured grids; Discontinuous Galerkin, Exact integrations

Abstract: A discontinuous Galerkin formulation that avoids the use of discrete quadrature formulas is described and applied to linear and nonlinear test problems in one and two space dimensions. This approach requires less computational time and storage than conventional implementations but preserves the compactness and robustness inherent to the discontinuous Galerkin method. Test problems include both linear and nonlinear one-dimensional scalar advection of both smooth and discontinuous initial value problems, two-dimensional scalar advection of smooth initial value problems discretized by using unstructured grids with varying degrees of smoothness and regularity, and two-dimensional linear Euler solutions on unstructured grids.

184.

Kenneth A. Cunefare, Scott P. Crane, Stephen P. Engelstad and Eugene A. Powell, **A Tool for Design Minimization of Aircraft Interior Noise**, *2nd AIAA/CEAS Aeroacoustics Conference (17th AIAA Aeroacoustics Conference)*, State College, Pennsylvania, AIAA Paper No. 96-1702, May 6-8, 1996, (959KB).

Format(s): Postscript, or PDF

Keywords: Structural acoustics; Optimization; Boundary elements; Noise reduction; Sensitivity; Cabin noise; Constrained minimization

Abstract: The design and development of new generations of aircraft of all classes continues apace. Increasingly, the quality of the interior acoustic environment of such new aircraft is becoming of greater importance. A need exists, then, to address the integration of acoustic considerations into the aircraft design process. To address this need, a computational design tool was developed to perform a constrained optimization of the acoustic environment within a vibrating cylinder, incorporating finite element and boundary element methods. The tool comprises a UNIX shell script that coordinates an iterative design optimization process integrating a number of programs, the key components of which are: NASTRAN for structural analyses; COMET/Acoustics for acoustic analyses; and CONMIN for nonlinear optimization. In addition to the structure and implementation of the tool, this paper presents the results of a number of trials of the tool applied to unstiffened cylinders, considering different formulations of the objective function to be optimized. The results presented here are principally directed toward tonal noise components within turbo-prop driven aircraft.

185.

F. Farassat, **Generalized Functions and Kirchhoff Formulas**, *2nd AIAA/CEAS Aeroacoustics Conference (17th AIAA Aeroacoustics Conference)*, State College, Pennsylvania, AIAA Paper No. 96-1705, May 6-8, 1996, (2.6MB).

Format(s): Postscript, or PDF

Keywords: Generalized functions; Kirchhoff formulas for moving surfaces (subsonic and supersonic); Aeroacoustics; Rotating blade noise prediction

Abstract: The theory of generalized functions was developed by L. Schwartz in the forties. It has had a major impact in many areas of mathematics, physics, and engineering. In particular, the solution of many of the problems of wave propagation in acoustics can be simplified by using generalized function theory. In this theory, mathematical objects other than ordinary functions, such as the Dirac delta function and its derivatives, are treated rigorously. One begins by thinking of a function $f(x)$ not as a table of ordered pairs $(x, f(x))$ but as a table of the action of $f(x)$ on functions in a suitable space of functions D . This action is defined by the integral of the product of f and any function in D . This integral is a functional since it maps D into scalars. After selecting D , we define generalized functions as the space of all continuous linear functionals on D . Each functional produces a generalized function by the table of the functional values on D . The operational properties of generalized functions make them very useful in applications. For our purpose in acoustics, the most important generalized functions are the Dirac delta function and its derivatives with support on $f=0$, where f is a closed or open moving surface. The theory part of this paper is based on NASA Technical Paper 3428 (May 1994) by the author. Next the derivation of the subsonic and supersonic Kirchhoff formulas are briefly discussed. This part of the paper is based on two works of Farassat and Myers (JSV, Vol. 123 (3), 1988, 451-460 and on a paper presented at the First Joint CEAS/AIAA Aeroacoustics Conference, June 12-15, 1995, Munich, Germany). These latter articles are included as an appendix to the present paper. Finally, some remarks on the development and validation of codes based on Kirchhoff formulas are made to help in the application of these results.

186.

Kenneth S. Brentner, **Numerical Algorithms for Acoustic Integrals – the Devil is in the Details**, *2nd AIAA/CEAS Aeroacoustic Conference*, State College, PA, AIAA Paper No. 96-1706, May 6-8, 1996, pp. 12, (201KB).

Format(s): Postscript, or PDF

Keywords: Acoustic analogy; Kirchhoff formulation; Acoustic algorithms; Acoustic integrals

Abstract: The accurate prediction of the aeroacoustic field generated by aerospace vehicles or nonaerospace machinery is necessary for designers to control and reduce source noise. Powerful computational aeroacoustic methods, based on various acoustic analogies (primarily the Lighthill acoustic analogy) and Kirchhoff methods, have been developed for prediction of noise from complicated sources, such as rotating blades. Both methods ultimately predict the noise through a numerical evaluation of an integral formulation. In this paper, we consider three generic acoustic formulations and several numerical algorithms that have been used to compute the solutions to

these formulations. Algorithms for retarded-time formulations are the most efficient and robust, but they are difficult to implement for supersonic-source motion. Collapsing-sphere and emission-surface formulations are good alternatives when supersonic-source motion is present, but the numerical implementations of these formulations are more computationally demanding. New algorithms - which utilize solution adaptation to provide a specified error level - are needed.

187.

Ferdinand W. Grosveld, **Numerical Comparison of Active Acoustic and Structural Noise Control in a Stiffened Double Wall Cylinder**, *2nd AIAA/CEAS Aeroacoustics Conference (17th AIAA Aeroacoustics Conference)*, State College, PA, AIAA 96-1722, May 6-8, 1996, pp. 12, (2MB).

Format(s): Postscript, or PDF

Keywords: Acoustics; Active noise control; Aeroacoustics; Sound transmission; Numerical methods; Boundary element methods

Abstract: The active acoustic and structural noise control characteristics of a double wall cylinder with and without ring stiffeners were numerically evaluated. An exterior monopole was assumed to acoustically excite the outside of the double wall cylinder at an acoustic cavity resonance frequency. Structural modal vibration properties of the inner and outer shells were analyzed by post-processing the results from a finite element analysis. A boundary element approach was used to calculate the acoustic cavity response and the coupled structural-acoustic interaction. In the frequency region of interest, below 500 Hz, all structural resonant modes were found to be acoustically slow and the nonresonant modal response to be dominant. Active sound transmission control was achieved by control forces applied to the inner or outer shell, or acoustic control monopoles placed just outside the inner or outer shell. A least mean square technique was used to minimize the interior sound pressures at the nodes of a data recovery mesh. Results showed that single acoustic control monopoles placed just outside the inner or outer shells resulted in better sound transmission control than six distributed point forces applied to either one of the shells. Adding stiffeners to the double wall structure constrained the modal vibrations of the shells, making the double wall stiffer with associated higher modal frequencies. Active noise control obtained for the stiffened double wall configurations was less than for the unstiffened cylinder. In all cases, the acoustic control monopoles controlled the sound transmission into the interior better than the structural control forces.

188.

D. L. Palumbo, S. L. Padula, K. H. Lyle, J. H. Cline and R. H. Cabell, **Performance of Optimized Actuator and Sensor Arrays in an Active Noise Control System**, *2nd AIAA/CEAS Aeroacoustics Conference (17th AIAA Aeroacoustics Conference)*, State College, Pennsylvania, AIAA Paper No. 96-1724, May 6-8, 1996, also published as NASA TM-110281. (402KB).

Format(s): Postscript, or PDF

Keywords: Active noise control; Optimization; Modal decomposition; Aircraft interior noise

Abstract: Experiments have been conducted in NASA Langley's Acoustics and Dynamics Laboratory to determine the effectiveness of optimized actuator/sensor architectures and controller algorithms for active control of harmonic interior noise. Tests were conducted in a large scale fuselage model - a composite cylinder which simulates a commuter class aircraft fuselage with three sections of trim panel and a floor. Using an optimization technique based on the component transfer functions, combinations of 4 out of 8 piezoceramic actuators and 8 out of 462 microphone locations were evaluated against predicted performance. A combinatorial optimization technique call tabu search was employed to select the optimum transducer arrays. Three test frequencies represent the cases of a strong acoustic and strong structural response, a weak acoustic and strong structural response and a strong acoustic and weak structural response. Noise reduction was obtained using a Time Averaged/Gradient Descent (TAGD) controller. Results indicate that the optimization technique successfully predicted best and worst case performance. An enhancement of the TAGD control algorithm was also evaluated. The principal components of the actuator/sensor transfer functions were used in the PC-TAGD controller. The principal components are shown to be independent of each other while providing control as effective as the standard TAGD.

189.

Christopher L. Rumsey, **Computation of Acoustic Waves Through Sliding-Zone Interfaces Using an Euler/Navier-Stokes Code**, *2nd AIAA/CEAS Aeroacoustics Conference*, State College, PA, AIAA Paper No. 96-1752, May 1996, pp. 11, (685KB).

Format(s): Postscript, or PDF

Keywords: Acoustic waves; Patched grid; Zonal interfaces; Euler

Abstract: The effect of a patched sliding-zone interface on the transmission of acoustic waves is examined for two- and three-dimensional model problems. A simple but general interpolation scheme at the patched boundary passes acoustic waves without distortion, provided that a sufficiently small time step is taken. A guideline is provided for the maximum permissible time step or zone speed that gives an acceptable error introduced by the sliding-zone interface.

190.

Yvette Y. Tang, Richard J. Silcox and Jay H. Robinson, **Sound Transmission Through Cylindrical Shell Structures Excited by Boundary Layer Pressure Fluctuations**, *2nd AIAA/CEAS Aeroacoustics Conference (17th AIAA Aeroacoustics Conference)*, State College, Pennsylvania, AIAA Paper No. 96-1760, May 6-8, 1996, (240KB).

Format(s): Postscript, or PDF

Keywords: Sound transmission; Two concentric finite cylindrical sandwich shells; Turbulent boundary layer; Cross-spectral density; Coincidences

Abstract: This paper examines sound transmission into two concentric cylindrical sandwich shells subject to turbulent flow on the exterior surface of the outer shell. The interior of the shells is filled with fluid medium and there is an airgap between the shells in the annular space. The

description of the pressure field is based on the cross-spectral density formulation of Corcos, Maestrello, and Efimtsov models of the turbulent boundary layer. The classical thin shell theory and the first-order shear deformation theory are applied for the inner and outer shells, respectively. Modal expansion and the Galerkin approach are used to obtain closed-form solutions for the shell displacements and the radiation and transmission pressures in the cavities including both the annular space and the interior. The average spectral density of the structural responses and the transmitted interior pressures are expressed explicitly in terms of the summation of the cross-spectral density of generalized force induced by the boundary layer turbulence. The effects of acoustic and hydrodynamic coincidences on the spectral density are observed. Numerical examples are presented to illustrate the method for both subsonic and supersonic flows.

191.

C. C. Fenno, Jr., A. Bayliss and L. Maestrello, **Response of a Panel Structure Forced by the Noise From a Nearly Sonic Jet**, *2nd AIAA/CEAS Aeroacoustics Conference (17th AIAA Aeroacoustics Conference)*, State College, Pennsylvania, AIAA Paper No. 96-1762, May 6-8, 1996, (865KB).

Format(s): Postscript, or PDF

Keywords: Jet acoustics; Structural acoustics; Interior noise; Computational aeroacoustics; Jet/Structure interaction

Abstract: A model of a high subsonic jet with a nearby array of flexible, aircraft-type panels is studied numerically in two dimensions. The jet is excited by a limited duration, spatially localized starter pulse in the potential core. The long time evolution of unsteady disturbances in the jet, the responses of the panels and the ensuing radiation are computed. The results show that the spectral responses of the panels and the ensuing radiation are computed. The results show that the spectral response of both the jet and the panels is concentrated in a relatively narrow frequency band centered at a Strouhal number (based on jet exit velocity) of approximately 0.25 and associated harmonics. The loading on the panels generally increases with downstream distance. Panel radiation is weakest in upstream directions. Interior zones of silence, due to destructive interference of radiation from the panels, are observed.

192.

M. H. Dunn, J. Tweed and F. Farassat, **The Prediction of Ducted Fan Engine Noise Via a Boundary Integral Equation Method**, *2nd AIAA/CEAS Aeroacoustics Conference (17th AIAA Aeroacoustics Conference)*, State College, Pennsylvania, AIAA Paper No. 96-1770, May 6-8, 1996, (1.7MB).

Format(s): Postscript, or PDF

Keywords: Ducted fan noise prediction; Boundary integral equations; Singular integral equations; Passive noise control; Boundary value problem

Abstract: A computationally efficient Boundary Integral Equation Method (BIEM) for the prediction of ducted fan engine noise is presented. The key features of the BIEM are its versatility

and the ability to compute rapidly any portion of the sound field without the need to compute the entire field. Governing equations for the BIEM are based on the assumptions that all acoustic processes are linear, generate spinning modes, and occur in a uniform flow field. An exterior boundary value problem (BVP) is defined that describes the scattering of incident sound by an engine duct with arbitrary profile. Boundary conditions on the duct walls are derived that allow for passive noise control treatment. The BVP is recast as a system of hypersingular boundary integral equations for the unknown duct surface quantities. BIEM solution methodology is demonstrated for the scattering of incident sound by a thin cylindrical duct with hard walls. Numerical studies are conducted for various engine parameters and continuous portions of the total pressure field are computed. Radiation and duct propagation results obtained are in agreement with the classical results of spinning mode theory for infinite ducts.

193.

Peter A. Gnoffo and George R. Inger, **Analytic Corrections to CFD Heating Predictions Accounting for Changes in Surface Catalysis**, *31st AIAA Thermophysics Conference*, New Orleans, Louisiana, AIAA Paper No. 96-1800, June 17-20, 1996, (169KB).

Format(s): Postscript, or PDF

Keywords: Nonequilibrium flow; Heating; Catalytic surface; Hypersonic; Analytic solution; Reusable Launch Vehicle (RLV); Computational Fluid Dynamics (CFD); LAURA; Boundary-layer theory

Abstract: Integral boundary-layer solution techniques applicable to the problem of determining aerodynamic heating rates of hypersonic vehicles in the vicinity of stagnation points and windward centerlines are briefly summarized. A new approach for combining the insight afforded by integral boundary-layer analysis with comprehensive (but time intensive) computational fluid dynamic (CFD) flowfield solutions of the thin-layer Navier-Stokes equations is described. The approach extracts CFD derived quantities at the wall and at the boundary layer edge for inclusion in a post-processing boundary-layer analysis. It allows a designer at a work-station to address two questions, given a single CFD solution. (1) How much does the heating change for a thermal protection system with different catalytic properties than was used in the original CFD solution? (2) How does the heating change at the interface of two different TPS materials with an abrupt change in catalytic efficiency? The answer to the second question is particularly important, because abrupt changes from low to high catalytic efficiency can lead to localized increase in heating which exceeds the usually conservative estimate provided by a fully catalytic wall assumption.

194.

Richard G. Wilmoth, Gerald J. LeBeau and Ann B. Carlson, **DSMC Grid Methodologies for Computing Low-Density, Hypersonic Flows About Reusable Launch Vehicles**, *31st AIAA Thermophysics Conference*, New Orleans, Louisiana, AIAA-96-1812, June 17-20, 1996, (4MB).

Format(s): Postscript, or PDF

Keywords: DSMC; Low-density flow; Rarefied flow; Hypersonic flow; Reusable launch vehicle;

Unstructured grid; Cartesian grid

Abstract: Two different grid methodologies are studied for application to DSMC simulations about reusable launch vehicles. One method uses an unstructured, tetrahedral grid while the other uses a structured, variable-resolution Cartesian grid. The relative merits of each method are discussed in terms of accuracy, computational efficiency, and overall ease of use. Both methods are applied to the computation of a low-density, hypersonic flow about a winged single-stage-to-orbit reusable launch vehicle concept at conditions corresponding to an altitude of 120 km. Both methods are shown to give comparable results for both surface and flowfield quantities as well as for the overall aerodynamic behavior. For the conditions simulated, the flowfield about the vehicle is very rarefied but the DSMC simulations show significant departure from free-molecular predictions for the surface friction and heat transfer as well as certain aerodynamic quantities.

195.

Brian R. Hollis and John N. Perkins, **Comparison of Experimental and Computational Aerothermodynamics of a 70-deg Sphere-Cone**, *31st AIAA Thermophysics Conference*, New Orleans, Louisiana, AIAA Paper No. 96-1867, June 18-20, 1996, (2MB).

Format(s): Postscript, or PDF

Keywords: Aerothermodynamics; Blunt body; Computational fluid dynamics; Heat-transfer; Hypersonics; Mars; Pathfinder; Wake

Abstract: Numerical solutions for hypersonic flows of carbon-dioxide and air around a 70-degree sphere-cone have been computed using an axisymmetric non-equilibrium Navier-Stokes solver. Freestream flow conditions for these computations were equivalent to those obtained in an experimental blunt-body heat-transfer study conducted in a high-enthalpy, hypervelocity expansion tube. Comparisons have been made between the computed and measured surface heat-transfer rates on the forebody and afterbody of the sphere-cone and on the string which supported the test model. Computed forebody heating rates were within the estimated experimental uncertainties of plus/minus 10 percent on the forebody and plus/minus 15 percent in the wake except for within the recirculating flow region of the wake.

196.

Glenn S. Diskin, Walter R. Lempert and Richard B. Miles, **A 3-level Model for Schumann-Runge O₂ Laser-Induced Fluorescence**, *27th AIAA Fluid Dynamics Conference*, New Orleans, Louisiana, AIAA 96-1991, June 17-20, 1996, (145KB).

Format(s): Postscript, or PDF

Keywords: Oxygen; Laser-induced Fluorescence; RELIEF

Abstract: A three level model has been developed for the analysis of Schumann-Runge band (B-X) laser-induced fluorescence of molecular oxygen, O₂. Such a model is required due to the severe lower state depletion which can occur when transitions having relatively large absorption cross-sections are excited. Such transitions are often utilized via ArF* or KrF* excimer or dye-

laser excitation in high temperature environments. The rapid predissociation of the upper state prevents substantial repopulation of the lower state by collisional processes, and the lower state may be largely depleted, even at laser fluences as low as 10-100 mJ/cm². The resulting LIF signal in such cases no longer varies linearly with laser pulse energy, and the extent of the sublinear behavior varies with the particular rovibrational transition of interest. Relating the measured signal to the lower state population, then, necessitates the use of exceedingly low laser fluences. These low fluences in turn lead to the need to compromise spatial resolution in order to generate sufficient signal.

197.

Stephen J. Alter and F. McNeil Cheatwood, **Elliptic Volume Grid Generation for Viscous Computations in Parametric Design Studies**, *27th AIAA Fluid Dynamics Conference*, New Orleans, Louisiana, AIAA Paper No. 96-1999, June 18, 1996, (3MB).

Format(s): Postscript, or PDF

Keywords: Grid generation; Parametric studies; Grid reusability; SSTO; SSV; Mathematics; Mesh; Elliptic partial differential equation; Design trades; MDO; 3DMAGGS

Abstract: This paper presents a robust method for the generation of zonal volume grid of design parametrics for aerodynamic configurations. The process utilizes simple algebraic techniques with parametric splines coupled with elliptic volume grid generation to perform parametric design studies. Speed of the algorithm is maximized through the algebraic methods and reduced number of grid points to be regenerated for each design parametric without sacrificing grid quality and continuity within the volume domain. The method is directly applicable to grid reusability, because it modifies existing flow adapted volume grids and enables the user to restart the CFD solution process with an established flow field. Use of this zonal approach reduces computer usage time to create new volume grids for design parametric studies by an order of magnitude, as compared to current methods which require the regeneration of an entire volume grid. A sample configuration of a proposed Single Stage-to-Orbit Vehicle is used to illustrate an application of this method.

198.

James F. Meyers, **Application of Doppler Global Velocimetry to Supersonic Flows**, *19th AIAA Advanced Measurement and Ground Testing Technology Conference*, New Orleans, Louisiana, AIAA 96-2188, June 17-20, 1996, (3MB).

Format(s): Postscript, or PDF

Keywords: Laser; Laser velocimetry; Velocity measurements; Flow measurements

Abstract: The design and implementation of Doppler Global Velocimetry (DGV) for testing in the Langley Unitary Plan Wind Tunnel is presented. The discussion begins by outlining the characteristics of the tunnel and the test environment, with potential problem areas highlighted. Modifications to the optical system design to implement solutions for these problems are described. Since this tunnel entry was the first ever use of DGV in a supersonic wind tunnel, the

test series was divided into three phases, each with its own goal. Phase I determined if condensation provided sufficient scattered light for DGV applications. Phase II studied particle lag by measuring the flow about an oblique shock above an inclined flat plate. Phase III investigated the supersonic vortical flow field above a 75-degree delta wing at 24-degrees angle of attack. Example results from these tests are presented.

199.

L. D. Huebner, K. E. Rock, R. T. Volland and A. R. Wieting, **Calibration of the Langley 8-Foot High Temperature Tunnel for Hypersonic Airbreathing Propulsion Testing**, *19th AIAA Advanced Measurement and Ground Testing Technology Conference*, New Orleans, Louisiana, AIAA 96-2197, June 17-20, 1996, (649KB) You may have a problem viewing some figures in this report. Please see [question 4](#) of the Frequently Asked Questions (FAQ) on how to view this report..

Format(s): [Postscript](#), or [PDF](#)

Keywords: High-enthalpy facility; Combustion-heated; Oxygen-enriched; Flow quality and calibration; Hypersonic airbreathing propulsion testing; Scramjet testing

Abstract: The NASA Langley 8-Foot High Temperature Tunnel has recently been modified to produce a unique testing capability for hypersonic airbreathing propulsion systems. Prior to these modifications, the facility was used primarily for aerothermal loads and structural verification testing at true flight total enthalpy conditions for Mach numbers between 6 and 7. One of the recent modifications was an oxygen replenishment system which allows operating airbreathing propulsion systems to be tested at true flight total enthalpies. Following the modifications to the facility, calibration runs were performed at total enthalpies corresponding to flight Mach numbers of 6.3 and 6.8 to establish the flow characteristics of the facility with its new capabilities. The results of this calibration, as well as modifications to tunnel combustor hardware prior to calibration to improve tunnel flow quality, are described in this paper.

200.

Brian R. Hollis and John N. Perkins, **Hypervelocity Heat-Transfer Measurements in an Expansion Tube**, *19th AIAA Advanced Measurement and Ground Testing Technology Conference*, New Orleans, LA, AIAA Paper No. 96-2240, June 18-20, 1996, (2MB).

Format(s): [Postscript](#), or [PDF](#)

Keywords: Aerothermodynamics; Blunt body; Expansion tube; Heat-transfer; Hypersonics;; Mars; Pathfinder; Thin-film; Wake

Abstract: A series of experiments has been conducted in the NASA HYPULSE Expansion Tube, in both CO/sub2 and air test gases, in order to obtain data for comparison with computational results and to assess the capability for performing hypervelocity heat-transfer studies in this facility. Heat-transfer measurements were made in both test gases on 70 degree sphere-cone models and on hemisphere models of various radii. HYPULSE freestream flow conditions in these test gases were found to be repeatable to within plus/minus 3-10 percent, and

aerothermodynamic test times of 150 μ /sec. in CO/sub2 and 125 μ /sec. in air were identified. Heat-transfer measurement uncertainty was estimated to be plus/minus 10-15 percent. Comparisons were made with computational results from the non-equilibrium Navier-Stokes solver NEQ2D. Measured and computed heat-transfer rates agreed to within 10 percent on the hemispheres and on the sphere-cone forebodies, and to within 10 percent in CO/sub2 and 25 percent in air on the afterbodies and stings of the sphere-cone models.

201.

G. M. Gatlin and R. J. McGhee, **Study of Semi-Span Model Testing Techniques**, *14th AIAA Applied Aerodynamics Conference*, New Orleans, Louisiana, AIAA Paper No. 96-2386, June 17-20, 1996, (468KB).

Format(s): Postscript, or PDF

Keywords: Semi-span; Standoff; Boundary layer; Tangential blowing; Horseshoe vortex; Flow visualization

Abstract: An investigation has been conducted in the NASA Langley 14- by 22-foot Subsonic Tunnel in order to further the development of semi-span testing capabilities. A twin engine, energy efficient transport (EET) model with a four-element wing in a takeoff configuration was used for this investigation. Initially a full span configuration was tested and force and moment data, wing and fuselage boundary layer measurements were obtained as a baseline data set. The semi-span configurations were then mounted on the wind tunnel floor, and the effects of fuselage standoff height and shape as well as the effects of the tunnel floor boundary-layer height were investigated. The effectiveness of tangential blowing at the standoff/floor juncture as an active boundary-layer control technique was also studied. Results indicate that the semi-span configuration was more sensitive to variations in standoff height than to variations in floor boundary-layer height. A standoff height equivalent to 30 percent of the fuselage radius resulted in better correlation with full span data than no standoff or the larger standoff configurations investigated. Undercut standoff leading edges or the use of tangential blowing in the standoff/floor juncture improved correlation of semi-span data with full span data in the region of maximum lift coefficient.

202.

William E. Milholen, II, N. Chokani and Robert J. McGhee, **Development of Semi-Span Model Test Techniques**, *14th AIAA Applied Aerodynamics Conference*, New Orleans, Louisiana, AIAA Paper No. 96-2412, June 17-20, 1996, (2MB).

Format(s): Postscript, or PDF

Keywords: Semi-span model; Stand-off height; Local blowing jets; Upstream blowing slot; Sidewall suction; Navier-Stokes solutions; National Transonic Facility

Abstract: A computational investigation was performed to support the development of a semi-span model test capability in the NASA Langley Research Center's National Transonic Facility. This capability is desirable for the testing of advanced subsonic transport aircraft at full-scale

Reynolds numbers. A state-of-the-art three-dimensional Navier-Stokes solver was used to examine methods to improve the flow over a semi-span configuration. First, a parametric study is conducted to examine the influence of the stand-off height on the flow over the semi-span model. It is found that decreasing the stand-off height, below the maximum fuselage radius, improves the aerodynamic characteristics of the semi-span model. Next, active sidewall boundary layer control techniques are examined. Juncture region blowing jets, upstream tangential blowing, and sidewall suction are found to improve the flow over the aft portion of the semi-span model. Both upstream blowing and suction are found to reduce the sidewall boundary layer separation. The resulting near surface streamline patterns are improved, and found to be quite similar to the full-span results. Both techniques however adversely affect the pitching moment coefficient.

203.

C. W. Mastin, R. E. Smith, I. Sadrehaghighi and M. R. Wiese, **Geometric Model for a Parametric Study of the Blended-Wing-Body Airplane**, *14th AIAA Applied Aerodynamics Conference*, New Orleans, Louisiana, AIAA Paper No. 96-2416, June 17-20, 1996, (546KB).

Format(s): Postscript, or PDF

Keywords: Parametric modeling; NURBS; Grid generation; Computational fluid dynamics

Abstract: A fully automated iterative design method has been developed by which an airfoil with a substantial amount of natural laminar flow can be designed, while maintaining other aerodynamic and geometric constraints. Drag reductions have been realized using the design method over a range of Mach numbers, Reynolds numbers and airfoil thicknesses. The thrusts of the method are its ability to calculate a target N-Factor relationship that is used to reduce the N-Factors in order to prolong transition; and its ability to design airfoils to meet lift, pitching moment, thickness and leading-edge radius constraints while also being able to meet the natural laminar flow constraint. The method uses several existing CFD codes and can design a new airfoil in only a few days using a Silicon Graphics IRIS workstation.

204.

R. C. Blanchard, R. G. Wilmoth and G. J. LeBeau, **Orbiter Aerodynamic Acceleration Flight Measurements in the Rarefied-Flow Transition Regime**, *14th AIAA Applied Aerodynamics Conference*, New Orleans, Louisiana, AIAA 96-2467, June 17-20, 1996, Also appears as "Rarefied-Flow Transition Regime Orbiter Aerodynamic Acceleration Flight Measurements" in the Journal of Spacecraft and Rockets, Volume 34, Number 1, January--February 1997. (1MB).

Format(s): Postscript, or PDF

Abstract: Acceleration data taken from the Orbital Acceleration Research Experiment (OARE) during reentry on STS-62 have been analyzed using calibration factors taken on orbit. This is the first Orbiter mission which collected OARE data during the Orbiter reentry phase. The data examined include the flight regime from orbital altitudes down to about 90 km which covers the free-molecule-flow regime and the upper altitude fringes of the rarefied-flow transition into the hypersonic continuum. Ancillary flight data on Orbiter position, orientation, velocity, and rotation rates have been used in models to transform the measured accelerations to the Orbiter center-of-

gravity, from which aerodynamic accelerations along the Orbiter body axes have been calculated. Residual offsets introduced in the measurements by unmodeled Orbiter forces are identified and discussed. Direct comparisons are made between the OARE flight data and an independent micro-gravity accelerometer experiment, the High Resolution Accelerometer Package (HiRAP), which also obtained flight data on reentry during the mission down to about 95 km. The resulting OARE aerodynamic acceleration measurements along the Orbiter's body axis, and the normal to axial acceleration ratio in the free-molecule-flow and transition-flow regimes are presented and compared with numerical simulations from three direct simulation Monte Carlo codes.

205.

Fred H. Proctor, **Numerical Simulation of Wake Vortices Measured During the Idaho Falls and Memphis Field Programs**, *14th AIAA Applied Aerodynamic Conference*, New Orleans, Louisiana, AIAA Paper 96-2496, June 17-20, 1996, (1MB).

Format(s): Postscript, or PDF

Keywords: Aircraft wake vortices; Wake turbulence; Vortex dynamics; Aircraft hazards; Numerical simulation; Terminal area productivity

Abstract: A numerical large-eddy simulation model is under modification and testing for application to aircraft wake vortices. The model, having a meteorological framework, permits the interaction of wake vortices with environments characterized by crosswind shear, stratification, and humidity. As part of the validation process, model results are compared with measured field data from the 1990 Idaho Falls and the 1994-1995 Memphis field experiments. Cases are selected that represent different aircraft and a cross section of meteorological environments. Also included is one case with wake vortex generation in ground effect. The model simulations are initialized with the appropriate meteorological conditions and a post roll-up vortex system. No ambient turbulence is assumed in our initial set of experiments, although turbulence can be self generated by the interaction of the model wakes with the ground and environment.

206.

Bradford E. Green, John L. Whitesides, Richard L. Campbell and Raymond E. Mineck, **A Method for the Constrained Design of Natural Laminar Flow Airfoils**, *14th AIAA Applied Aerodynamics Conference*, New Orleans, Louisiana, AIAA 96-2502, June 17-20, 1996, (107KB).

Format(s): Postscript, or PDF

Keywords: Aircraft design; Airfoils; Design analysis; Drag reduction; Laminar flow; Turbulent flow; Transition; Stability analysis

Abstract: A fully automated iterative design method has been developed by which an airfoil with a substantial amount of natural laminar flow can be designed, while maintaining other aerodynamic and geometric constraints. Drag reductions have been realized using the design method over a range of Mach numbers, Reynolds numbers and airfoil thicknesses. The thrusts of the method are its ability to calculate a target N-Factor distribution that forces the flow to undergo transition at the desired location; the target-pressure-N-Factor relationship that is used to reduce

the N-Factors in order to prolong transition; and its ability to design airfoils to meet lift, pitching moment, thickness and leading- edge radius constraints while also being able to meet the natural laminar flow constraint. The method uses several existing CFD codes and can design a new airfoil in only a few days using a Silicon Graphics IRIS workstation.

207.

Karen A. Deere and Scott C. Asbury, **An Experimental and Computational Investigation of a Translating Throat Single Expansion-Ramp Nozzle**, *32nd AIAA/ASME/SAE/ASEE Joint Propulsion Conference and Exhibit*, Lake Buena Vista, Florida, AIAA Paper No. 96-2540, July 1-3, 1996, (2MB).

Format(s): Postscript, or PDF

Keywords: Nozzle; High speed SERN (single expansion ramp nozzle); Variable expansion ratio; Translating throat

Abstract: A translating throat single expansion-ramp nozzle (SERN) concept was designed to improve the off-design performance of a SERN with a large, fixed expansion ratio. The concept of translating the nozzle throat provides the SERN with a variable expansion ratio. An experimental and computational study was conducted to predict and verify the internal performance of this concept. Three nozzles with expansion ratios designed for low, intermediate, and high Mach number operating conditions were tested in the Jet-Exit Test Facility at the NASA Langley Research Center. Each nozzle was tested with a concave and convex geometric expansion ramp surface design. Internal nozzle performance, paint-oil flow and focusing Schlieren flow visualization were obtained for nozzle pressure ratios (NPRs) up to 13. The Navier-Stokes code, PAB3D, with a k-epsilon turbulence model was utilized to verify experimental results at selected NPRs and to predict the performance at conditions unattainable in the test facility. Two-dimensional simulations were computed with near static free-stream conditions and at nozzle pressure ratios of 5, 9, and 13 for the concave ramp, low Mach number configuration and at the design NPR of 102 for the concave ramp, high Mach number configuration. Remarkable similarities between predicted and experimental flow characteristics, as well as performance quantities, were obtained.

208.

Scott C. Asbury, Craig A. Hunter and Christopher L. Gunther, **A Passive Cavity Concept for Improving the Off-Design Performance of Fixed Geometry Exhaust Nozzles**, *32nd AIAA/ASME/SAE/ASEE Joint Propulsion Conference and Exhibit*, Lake Buena Vista, Florida, AIAA Paper No. 96-2541, July 1-3, 1996, (2.5MB).

Format(s): Postscript, or PDF

Keywords: Exhaust nozzles; Nonaxisymmetric nozzles; Nozzles; Passive flow control; Porous; Separation control

Abstract: An investigation was conducted in the model preparation area of the Langley 16-Foot Transonic Tunnel to study a passive cavity concept for improving the off-design performance of

fixed-geometry exhaust nozzles. Passive cavity ventilation (through a porous surface) was applied to divergent flap surfaces and tested at static conditions in a sub-scale, nonaxisymmetric, convergent-divergent nozzle. As part of a comprehensive investigation, force, moment and pressure measurements were taken and focusing schlieren flow visualization was obtained for a baseline configuration and 27 passive cavity configurations. All tests were conducted with no external flow and high-pressure air was used to simulate jet-exhaust flow at nozzle pressure ratios from 1.25 to approximately 9.50. Results indicate that baseline nozzle performance was dominated by unstable shock-induced boundary-layer separation at off-design conditions, which came about through the natural tendency of overexpanded exhaust flow to satisfy conservation requirements by detaching from the nozzle divergent flaps. Passive cavity ventilation added the ability to control off-design separation in the nozzle by either alleviating separation or encouraging stable separation of the exhaust flow. Separation alleviation offers potential for installed nozzle performance benefits by reducing drag at forward flight speeds, even though it may reduce off-design static thrust efficiency as much as 3.2 percent. Encouraging stable separation of the exhaust flow offers significant performance improvements at static, low NPR and low Mach number flight conditions by improving off-design static thrust efficiency as much as 2.8 percent. By designing a fixed-geometry nozzle with fully porous divergent flaps, where both cavity location and percent open porosity of the flaps could be varied, passive flow control would make it possible to improve off-design nozzle performance across a wide operating range. In addition, the ability to encourage separation on one flap while alleviating it on the other makes it possible to generate thrust vectoring in the nozzle through passive flow control.

209.

John R. Carlson, **High Reynolds Number Analysis of Flat Plate and Separated Afterbody Flow Using Non-Linear Turbulence Models**, *32nd AIAA/ASME/SAE/ASEE Joint Propulsion Conference and Exhibit*, Lake Buena Vista, Florida, AIAA Paper No. 96-2544, July 1-3, 1996, (1.3MB).

Format(s): Postscript, or PDF

Keywords: Computational fluid dynamics; Turbulence models; Transonic flow; External aerodynamics; Nozzle/afterbody flow; High Reynolds number; Separated flow

Abstract: The ability of the three-dimensional Navier-Stokes method, PAB3D, to simulate the effect of Reynolds number variation using non-linear explicit algebraic Reynolds stress turbulence modeling was assessed. Subsonic flat plate boundary-layer flow parameters such as normalized velocity distributions, local and average skin friction, and shape factor were compared with DNS calculations and classical theory at various local Reynolds numbers up to 180 million. Additionally, surface pressure coefficient distributions and integrated drag predictions on an axisymmetric nozzle afterbody were compared with experimental data from 10 to 130 million Reynolds number. The high Reynolds data was obtained from the NASA Langley 0.3m Transonic Cryogenic Tunnel. There was generally good agreement of surface static pressure coefficients between the CFD and measurement. The change in pressure coefficient distributions with varying Reynolds number was similar to the experimental data trends, though slightly over-predicting the effect. The computational sensitivity of viscous modeling and turbulence modeling are shown. Integrated afterbody pressure drag was typically slightly lower than the experimental data. The change in afterbody pressure drag with Reynolds number was small both experimentally and computationally, even though the shape of the distribution was somewhat modified with Reynolds number.

210.

L. J. Bement, **Functional Performance of Pyrovalves**, *32nd AIAA/ASME/SAE/ASEE Joint Propulsion Conference and Exhibit*, Lake Buena Vista, Florida, AIAA Paper No. 96-2754, July 1-3, 1996, Also published in *Journal of Spacecraft and Rockets*, Vol. 34, No. 3, May--June 1997, p. 391-396. (94KB).

Format(s): Postscript, or PDF

Keywords: Pyrotechnic; Propulsion valves; Performance; Spacecraft

Abstract: Following several flight and ground test failures of spacecraft systems using single-shot, "normally closed" pyrotechnically actuated valves (pyrovalves), a Government/Industry cooperative program was initiated to assess the functional performance of five qualified designs. The goal of the program was to provide information on functional performance of pyrovalves to allow users the opportunity to improve procurement requirements. Specific objectives included the demonstration of performance test methods, the measurement of "blowby" (the passage of gasses from the pyrotechnic energy source around the activating piston into the valve's fluid path), and the quantification of functional margins for each design. Experiments were conducted at NASA Langley Research Center on several units for each of the five valve designs. The test methods used for this program measured the forces and energies required to actuate the valves, as well as the energies and the pressures (where possible) delivered by the pyrotechnic sources. Functional performance ranged widely among the designs. Blowby cannot be prevented by o-ring seals; metal-to-metal seals were effective. Functional margin was determined by dividing the energy delivered by the pyrotechnic sources in excess to that required to accomplish the function by the energy required for that function. Two of the five designs had inadequate functional margins with the pyrotechnic cartridges evaluated.

211.

R. J. Pegg, B. D. Couch and L. G. Hunter, **Pulse Detonation Engine Air Induction System Analysis**, *32nd AIAA/ASME/SAE/ASEE Joint Propulsion Conference and Exhibit*, Lake Buena Vista, Florida, AIAA Paper No. 96-2918, July 1-3, 1996, pp. 16, (1MB).

Format(s): Postscript, or PDF

Keywords: Pulse detonation engine; Air induction system; Mach 5 waverider

Abstract: A preliminary mixed-compression inlet design concept for potential pulse-detonation engine (PDE) powered supersonic aircraft was defined and analyzed. The objectives of this research were to conceptually design and integrate an inlet/PDE propulsion system into a supersonic aircraft, perform time-dependend CFD analysis of the inlet flowfield, and to estimate the installed PDE cycle performance.

212.

R. W. Guy, R. C. Rogers, R. L. Puster, K. E. Rock and G. L. Diskin, **The NASA Langley**

Scramjet Test Complex , *32nd AIAA/ASME/SAE/ASEE Joint Propulsion Conference and Exhibit*, Lake Buena Vista, FL , AIAA Paper 96-3243, July 1-3, 1996, pp. 23, (245KB).

Format(s): Postscript, or PDF

Keywords: Ground test facilities; Scramjets

Abstract: The NASA Langley Scramjet Test Complex consists of five propulsion facilities which cover a wide spectrum of supersonic combustion ramjet (scramjet) test capabilities. These facilities permit observation of the effects on scramjet performance of speed and dynamic pressure from Mach 3.5 to near-orbital speeds, engine size from Mach 4 to 7, and test gas composition from Mach 4 to 7. In the Mach 3.5 to 8 speed range, the complex includes a direct-connect combustor test facility, two small-scale complete engine test facilities, and a large-scale complete engine test facility. In the hypervelocity speed range, a shock-expansion tube is used for combustor tests from Mach 12 to Mach 17plus. This facility has recently been operated in a tunnel mode, to explore the possibility of semi-free-jet testing of complete engine modules at hypervelocity conditions. This paper presents a description of the current configurations and capabilities of the facilities of the NASA Langley Scramjet Test Complex, reviews the most recent scramjet tests in the facilities, and discusses comparative engine tests designed to gain information about ground facility effects on scramjet performance.

213.

Martin R. Waszak and Jimmy Fung, **Parameter Estimation and Analysis of Actuators for the BACT Wind-Tunnel Model** , *AIAA Atmospheric Flight Mechanics Conference, July 29-31, 1996*, San Diego, CA, AIAA Paper No. 96-3362, July 29-31, 1996, pp. 9, (869KB).

Format(s): Postscript, or PDF

Keywords: Parameter estimation; Actuator; Dynamics; Modeling

Abstract: This paper describes the development of transfer function models for the trailing edge and upper- and lower-spoiler actuators of the Benchmark Active Control Technology (BACT) wind-tunnel model for application to control system analysis and design. A simple nonlinear least squares parameter estimation approach is applied to determine transfer function parameters from frequency response data. Unconstrained quasi-Newton minimization of weighted frequency response error was employed to estimate the transfer function parameters. An analysis of the behavior of the actuators over time to assess the effects of wear and aerodynamic load using the transfer function models is also presented. The frequency responses indicate consistent actuator behavior throughout the wind-tunnel test and only slight degradation in effectiveness due to aerodynamic hinge loading. The resulting actuator models have been used in design, analysis, and simulation of controllers for the BACT. The resulting controllers have successfully suppressed flutter over a wide range of conditions.

214.

Dan D. Vicroy and Truc Nguyen, **A Numerical Simulation Study to Develop an Acceptable Wake Encounter Boundary for a B737-100 Airplane** , *AIAA Atmospheric Flight Mechanics*

Conference, San Diego, California, AIAA 96-3372, July 29-31, 1996, pp. 88-96, (1MB).

Format(s): Postscript, or PDF

Keywords: Wake vortex; Wake vortex hazard; B737-100; Simulation

Abstract: The National Aeronautics and Space Administration (NASA) is conducting research with the goal of enabling safe improvements in the capacity of the nation's air transportation system. The wake-vortex upset hazard is an important factor in establishing the minimum safe spacing between aircraft during landing and take-off operations, thus impacting airport capacity. A batch simulation study was conducted to assess the sensitivity of various safe landing criteria in the development of an acceptable wake encounter boundary. A baseline six-degree-of-freedom simulation of a B737-100 airplane was modified to include a wake model and the vortex-induced forces and moments. The guidance and control input for the airplane was provided by an auto-land system. The wake strength and encounter geometry were varied. A sensitivity study was also conducted to assess the effects of encounter modeling methods and accuracy.

215.

Martin R. Waszak, **Modeling the Benchmark Active Control Technology Wind-Tunnel Model for Application to Flutter Suppression**, *AIAA Atmospheric Flight Mechanics Conference*, San Diego, CA, AIAA Paper No. 96-3437, July 29-31, 1996, pp. 12, (944KB).

Format(s): Postscript, or PDF

Keywords: Dynamics and control; Modeling; Flutter suppression; Equations of motion; Aeroelasticity

Abstract: This paper describes the formulation of a model of the dynamic behavior of the Benchmark Active Controls Technology (BACT) wind-tunnel model for application to design and analysis of flutter suppression controllers. The model is formed by combining the equations of motion for the BACT wind-tunnel model with actuator models and a model of wind-tunnel turbulence. The primary focus of this paper is the development of the equations of motion from first principles using Lagrange's equations and the principle of virtual work. A numerical form of the model is generated using values for parameters obtained from both experiment and analysis. A unique aspect of the BACT wind-tunnel model is that it has upper- and lower-surface spoilers for active control. Comparisons with experimental frequency responses and other data show excellent agreement and suggest that simple coefficient-based aerodynamics are sufficient to accurately characterize the aeroelastic response of the BACT wind-tunnel model. The equations of motion developed herein have been used to assist the design and analysis of a number of flutter suppression controllers that have been successfully implemented.

216.

Jay M. Brandon, James S. Simon, D. Bruce Owens and Jason S. Kiddy, **Free-Flight Investigation of Forebody Blowing for Stability and Control**, *AIAA Atmospheric Flight Mechanics Conference*, San Diego, California, AIAA Paper No. 96-3444, July 29-31, 1996, (2.3MB).

Format(s): Postscript, or PDF

Keywords: Forebody blowing; Free-flight; Pneumatic controls; High-angle-of-attack stability and control

Abstract: A free-flight wind-tunnel investigation was conducted on a generic fighter model with forebody pneumatic vortex control for high-angle-of-attack directional control. This is believed to be the first flight demonstration of a forebody blowing concept integrated into a closed-loop flight control system for stability augmentation and control. The investigation showed that the static wind tunnel estimates of the yaw control available generally agreed with flight results. The control scheme for the blowing nozzles consisted of an on/off control with a deadband. Controlled flight was obtained for the model using forebody blowing for directional control to beyond 45 degree angle of attack.

217.

I. M. Gregory and J. E. Tierno, **A New Approach to Aircraft Robust Performance Analysis**, *AIAA 1996 Guidance, Navigation and Control Conference*, San Diego, California, AIAA 96-3860, July 29-31, 1996, (77KB).

Format(s): Postscript, or PDF

Keywords: Aircraft performance; Uncertain system; Nonlinear performance

Abstract: A recently developed algorithm for nonlinear system performance analysis has been applied to an F16 aircraft to begin evaluating the suitability of the method for aerospace problems. The algorithm has a potential to be much more efficient than the current methods in performance analysis for aircraft. This paper is the initial step in evaluating this potential.

218.

Jamshid A. Samareh, **Use OF CAD Geometry in MDO**, *6th AIAA/USAF/NASA/ISSMO Symposium on Multidisciplinary Analysis and Optimization*, Bellevue, WA, AIAA-96-3991, September, 1996, pp. 12, (769KB).

Format(s): Postscript, or PDF

Keywords: MDO; Geometry; CAD; Grid generation; NURBS; Sensitivity; Aeroelastic

Abstract: The purpose of this paper is to discuss the use of Computer-Aided Design (CAD) geometry in a Multi-Disciplinary Design Optimization (MDO) environment. Two techniques are presented to facilitate the use of CAD geometry by different disciplines, such as Computational Fluid Dynamics (CFD) and Computational Structural Mechanics (CSM). One method is to transfer the load from a CFD grid to a CSM grid. The second method is to update the CAD geometry for CSM deflection.

219.

R. D. Braun, P. J. Gage, I. M. Kroo and I. Sobieski, **Implementation and Performance Issues in Collaborative Optimization**, *Sixth AIAA/USAF/NASA/ISSMO Symposium on Multidisciplinary Analysis and Optimization*, Bellevue, Washington, AIAA Paper No. 96-4017, September 4-6, 1996, (1MB).

Format(s): Postscript, or PDF

Keywords: Design optimization; Distributed design; Large-scale optimization

Abstract: Collaborative optimization is a multidisciplinary design architecture that is well-suited to large-scale multidisciplinary optimization problems. This paper compares this approach with other architectures, examines the details of the formulation, and some aspects of its performance. A particular version of the architecture is proposed to better accommodate the occurrence of multiple feasible regions. The use of system level inequality constraints is shown to increase the convergence rate. A series of simple test problems, demonstrated to challenge related optimization architectures, is successfully solved with collaborative optimization.

220.

R. D. Braun, A. A. Moore and I. M. Kroo, **Use of the Collaborative Optimization Architecture for Launch Vehicle Design**, *Sixth AIAA/USAF/NASA/ISSMO Symposium on Multidisciplinary Analysis and Optimization*, Bellevue, Washington, AIAA Paper No. 96-4018, September 4-6, 1996, (439KB).

Format(s): Postscript, or PDF

Keywords: Single-stage-to-orbit; Launch vehicle design; Design optimization

Abstract: Collaborative optimization is a new design architecture specifically created for large-scale distributed-analysis applications. In this approach, a problem is decomposed into a user-defined number of subspace optimization problems that are driven towards interdisciplinary compatibility and the appropriate solution by a system-level coordination process. This decentralized design strategy allows domain-specific issues to be accommodated by disciplinary analysts, while requiring interdisciplinary decisions to be reached by consensus. The present investigation focuses on application of the collaborative optimization architecture to the multidisciplinary design of a single-stage-to-orbit launch vehicle. Vehicle design, trajectory, and cost issues are directly modeled. Posed to suit the collaborative architecture, the design problem is characterized by 95 design variables and 16 constraints. Numerous collaborative solutions are obtained. Comparison of these solutions demonstrates the influence which an a priori ascent-abort criterion has on development cost. Similarly, objective-function selection is discussed, demonstrating the difference between minimum weight and minimum cost concepts. The operational advantages of the collaborative optimization architecture in a multidisciplinary design environment are also discussed.

221.

Sharon L. Padula, Natalia Alexandrov and Lawrence L. Green, **MDO Test Suite at NASA**

Langley Research Center , *Sixth AIAA/NASA/ISSMO Symposium on Multidisciplinary Analysis and Optimization*, Bellevue, Washington, AIAA 96-4028, September 1996, pp. 13, (4MB).

Format(s): Postscript, or PDF

Keywords: Multidisciplinary; Benchmarking; Optimization

Abstract: NASA Langley Research Center supports a wide variety of multidisciplinary design optimization (MDO) research and requires a set of standard MDO test problems for evaluating and comparing the products of this research. This paper proposes a World-Wide-Web based test suite for collecting, distributing and maintaining the standard test problems. A prototype suite of 10 problems, including written problem descriptions, benchmark solution methods, sample input and output files, and source code is available from the Langley internet site. Here, design of the MDO test suite is discussed; typical test problems are described; and sample web pages are illustrated.

222.

A. G. Striz and J. Sobieszczanski-Sobieski, **Displacement Based Multilevel Structural Optimization** , *Sixth AIAA/NASA/ISSMO Symposium on Multidisciplinary Analysis and Optimization*, Bellevue, Washington, AIAA 96-4098, September 4-6, 1996, (743KB).

Format(s): Postscript, or PDF

Keywords: Optimization; Structural optimization; Multilevel optimization

Abstract: In the complex environment of true multidisciplinary design optimization (MDO), efficiency is one of the most desirable attributes of any approach. In the present research, a new and highly efficient methodology for the MDO subset of structural optimization is proposed and detailed, i.e., for the weight minimization of a given structure under size, strength, and displacement constraints. Specifically, finite element based multilevel optimization of structures is performed. In the system level optimization, the design variables are the coefficients of assumed polynomially based global displacement functions, and the load unbalance resulting from the solution of the global stiffness equations is minimized. In the subsystems level optimizations, the weight of each element is minimized under the action of stress constraints, with the cross sectional dimensions as design variables. The approach is expected to prove very efficient since the design task is broken down into a large number of small and efficient subtasks, each with a small number of variables, which are amenable to parallel computing.

223.

John C. Otto, Drew Landman and Anthony T. Patera, **A Surrogate Approach to the Experimental Optimization of Multielement Airfoils** , *Sixth AIAA/NASA/ISSMO Symposium on Multidisciplinary Analysis and Optimization*, Bellevue Washington, AIAA 96-4138 CP, September 4-6, 1996, pp. 11, (209KB).

Format(s): Postscript, or PDF

Keywords: Highlift; Multielement airfoils; Approximation; Optimization

Abstract: The incorporation of experimental test data into the optimization process is accomplished through the use of Bayesian-validated surrogates. In the surrogate approach, a surrogate for the experiment (e.g., a response surface) serves in the optimization process. The validation step of the framework provides a qualitative assessment of the surrogate quality, and bounds the surrogate-for-experiment error on designs ``near'' surrogate-predicted optimal designs. The utility of the framework is demonstrated through its application to the experimental selection of the trailing edge flap position to achieve a design lift coefficient for a three-element airfoil.

224.

J. L. Rogers, **DeMAID/GA an Enhanced Design Manager's Aid for Intelligent Decomposition**, *Sixth AIAA/USAF/NASA/ISSMO Symposium on Multidisciplinary Analysis and Optimization*, Bellevue, Washington, AIAA Paper No. 96-4157, September 4-6, 1996, (562KB).

Format(s): Postscript, or PDF

Keywords: Decomposition; Process management; Knowledge-based system; genetic algorithm; Reducing design cycle time and cost; Parallel processing

Abstract: Many companies are looking for new tools and techniques to aid a design manager in making decisions that can reduce the time and cost of a design cycle. One tool is the Design Manager's Aid for Intelligent Decomposition (DeMAID). Since the initial public release of DeMAID in 1989, much research has been done in the areas of decomposition, concurrent engineering, parallel processing, and process management; many new tools and techniques have emerged. Based on these recent research and development efforts, numerous enhancements have been added to DeMAID to further aid the design manager in saving both cost and time in a design cycle. The key enhancement, a genetic algorithm (GA), will be available in the next public release called DeMAID/GA. The GA sequences the design processes to minimize the cost and time in converging a solution. The major enhancements in the upgrade of DeMAID to DeMAID/GA are discussed in this paper. A sample conceptual design project is used to show how these enhancements can be applied to improve the design cycle.

225.

B. Joshi, D. Morris, N. White and R. Unal, **Optimization of Operations Resources via Discrete Event Simulation Modeling**, *6th AIAA/USAF/NASA/ISSMO Symposium on Multidisciplinary Analysis and Optimization*, Bellevue, WA, AIAA 96-4181, September 4-6, 1996, pp. 6, (45KB).

Format(s): Postscript, or PDF

Keywords: Optimization; Genetic algorithm; Discrete-event; Simulation; Stochastic

Abstract: The resource levels required for operation and support of reusable launch vehicles are typically defined through discrete event simulation modeling. Minimizing these resources constitutes an optimization problem involving discrete variables and simulation. Conventional approaches to solve such optimization problems involving integer valued decision variables are

the pattern search and statistical methods. However, in a simulation environment that is characterized by search spaces of unknown topology and stochastic measures, these optimization approaches often prove inadequate. In this paper, we have explored the applicability of genetic algorithms to the simulation domain. Genetic algorithms provide a robust search strategy that does not require continuity and differentiability of the problem domain. The genetic algorithm successfully minimized the operation and support activities for a space vehicle, through a discrete event simulation model. The practical issues associated with simulation optimization, such as stochastic variables and constraints, were also taken into consideration.

226.

W. D. Morris, N. H. White and C. E. Ebeling, **Analysis of Shuttle Orbiter Reliability and Maintainability Data for Conceptual Studies**, *1996 AIAA Space Programs and Technologies Conference*, Huntsville, AL, AIAA 96-4245, September, 1996, pp. 10, (242KB).

Format(s): Postscript, or PDF

Keywords: Reliability; Maintainability; Conceptual design; Operations; Support; Simulation

Abstract: In order to provide a basis for estimating the expected support required of new systems during their conceptual design phase, Langley Research Center has recently collected Shuttle Orbiter reliability and maintainability data from the various data base sources at Kennedy Space Center. This information was analyzed to provide benchmarks, trends, and distributions to aid in the analysis of new designs. This paper presents a summation of those results and an initial interpretation of the findings.

227.

C. McClinton, A. Roudakov, V. Semenov and V. Kopehenov, **Comparative Flow Path Analysis and Design Assessment of an Axisymmetric Hydrogen Fueled Scramjet Flight Test Engine at a Mach Number of 6.5**, *AIAA 7th International Spaceplanes and Hypersonic Systems and Technologies Conference*, Norfolk, Virginia, AIAA 96-4571, November 18-22, 1996, (2MB).

Format(s): Postscript, or PDF

Abstract: NASA has contracted with the Central Institute of Aviation Motors CIAM to perform a flight test and ground test and provide a scramjet engine for ground test in the United States. The objective of this contract is to obtain ground to flight correlation for a supersonic combustion ramjet (scramjet) engine operating point at a Mach number of 6.5. This paper presents results from a flow path performance and thermal evaluation performed on the design proposed by the CIAM. This study shows that the engine will perform in the scramjet mode for stoichiometric operation at a flight Mach number of 6.5. Thermal assessment of the structure indicates that the combustor cooling liner will provide adequate cooling for a Mach number of 6.5 test condition and that optional material proposed by CIAM for the cowl leading-edge design are required to allow operation with or without a type IV shock-shock interaction.

228.

Peter A. Gnoffo and George R. Inger, **Analytic Corrections to CFD Heating Predictions Accounting for Changes in Surface Catalysis, Part II**, *AIAA 7th International Space Planes and Hypersonic Systems and Technologies Conference*, Norfolk, Va, AIAA 96-4589, November 18-22, 1996, pp. 12, (234KB).

Format(s): Postscript, or PDF

Keywords: Catalysis; Hypersonic; Boundary layer; X33; LAURA; Reusable Launch Vehicle, RLV

Abstract: A new approach for combining the insight afforded by integral boundary-layer analysis with comprehensive (but time intensive) computational fluid dynamic (CFD) flowfield solutions of the thin-layer Navier-Stokes equations is described. The approach extracts CFD derived quantities at the wall and at the boundary layer edge for inclusion in a post-processing boundary-layer analysis. It allows a designer at a workstation to address two questions, given a single CFD solution. (1) How much does the heating change for a thermal protection system (TPS) with different catalytic properties than was used in the original CFD solution? (2) How does the heating change at the interface of two different TPS materials with an abrupt change in catalytic efficiency? The answer to the second question is particularly important, because abrupt changes from low to high catalytic efficiency can lead to localized increase in heating which exceeds the usually conservative estimate provided by a fully catalytic wall assumption. Capabilities of this approach for application to Reusable Launch Vehicle (RLV) design are demonstrated. If the definition of surface catalysis is uncertain early in the design process, results show that fully catalytic wall boundary conditions provide the best baseline for CFD design points.

229.

James L. Hunt and Edward A. Eisswirth, **NASA's Dual-Fuel Airbreathing Hypersonic Vehicle Study**, *7th International Space Planes and Hypersonics Systems & Technology Conference*, Norfolk, Virginia, AIAA-96-4591, November 18-22, 1996, (822KB).

Format(s): Postscript, or PDF

Keywords: Scramjet; Hypersonic flight; Dual-fuel; Mach 10 cruise; Global reach

Abstract: Hypersonic airbreathing, horizontal takeoff and landing (HTOL), vehicles are highly integrated systems involving many advanced technologies. The design environment is variable rich, intricately networked, and sensitivity intensive; as such, it represents a tremendous challenge. Creating a viable design requires addressing three main elements: (1) an understanding of the "figures of merit" and their relationship, (2) the development of sophisticated configuration discipline prediction methods and a synthesis procedure, and (3) the synergistic integration of advanced technologies across the discipline spectrum.

230.

Mark S. Lake, Peter A. Warren and Lee D. Peterson, **A Revolute Joint With Linear Load-Displacement Response for a Deployable Lidar Telescope**, *30th Aerospace Mechanism*

Symposium, Hampton, Virginia, May 15-17, 1996, pp. 16, (881KB).

Format(s): Postscript, or PDF

Keywords: Deployable structures; Precision; Reflector; Telescope; Revolute joint; Deployment accuracy

Abstract: NASA Langley Research Center is developing concepts for an advanced spacecraft called LidarTechSat to demonstrate key structures and mechanisms technologies necessary to deploy a segmented telescope reflector. Achieving micron-accuracy deployment requires significant advancements in deployment mechanism design such as the revolute joint presented herein. The joint exhibits load-cycling response that is essentially linear with less than two percent hysteresis, and the joint rotates with less than one in-oz. of resistance. A prototype reflector metering truss incorporating the joint exhibits only a few microns of kinematic error under repeated deployment and impulse loading. No other mechanically deployable structure found in the literature has been demonstrated to be this kinematically accurate.

231.

Ben L. Di Vito, **Formalizing New Navigation Requirements for NASA's Space Shuttle**, *Formal Methods Europe (FME '96)*, Oxford, England, March 18-22, 1996, pp. 19, (68KB).

Format(s): Postscript, or PDF

Keywords: Formal methods; Requirements analysis; Space Shuttle; Flight software; Space applications; GPS (Global Positioning System)

Abstract: We describe a recent NASA-sponsored pilot project intended to gauge the effectiveness of using formal methods in Space Shuttle software requirements analysis. Several Change Requests (CRs) were selected as promising targets to demonstrate the utility of formal methods in this demanding application domain. A CR to add new navigation capabilities to the Shuttle, based on Global Positioning System (GPS) technology, is the focus of this industrial usage report. Portions of the GPS CR were modeled using the language of SRI's Prototype Verification System (PVS). During a limited analysis conducted on the formal specifications, numerous requirements issues were discovered. We present a summary of these encouraging results and conclusions we have drawn from the pilot project.

232.

Judith Crow and Ben L. Di Vito, **Formalizing Space Shuttle Software Requirements**, *Workshop on Formal Methods in Software Practice (FMSP'96)*, San Diego, CA, January 10-11, 1996, pp. 9, (88KB).

Format(s): Postscript, or PDF

Keywords: Formal methods; Requirements analysis; Space Shuttle; Flight software; Space

Abstract: This paper describes two case studies in which requirements for new flight-software

subsystems on NASA's Space Shuttle were analyzed, one using standard formal specification techniques, the other using state exploration. These applications serve to illustrate three main theses: (1) formal methods can complement conventional requirements analysis processes effectively, (2) formal methods confer benefits regardless of how extensively they are adopted and applied, and (3) formal methods are most effective when they are judiciously tailored to the application.

233.

Y. Y. Tang, R. J. Silcox and J. H. Robinson, **Sound Transmission Through Two Concentric Cylindrical Sandwich Shells**, *14th International Modal Analysis Conference*, Dearborn, Michigan, February 12-15, 1996, pp. 8, (165KB).

Format(s): Postscript, or PDF

Keywords: Sound transmission; Two concentric cylindrical sandwich shells; Honeycomb core; Transmission loss; Incident plane wave; Modal impedance; Shear effect

Abstract: The paper solves the problem of sound transmission through a system of two infinite concentric cylindrical sandwich shells. The shells are surrounded by external and internal fluid media and there is fluid (air) in the annular space between them. An oblique plane sound wave is incident upon the surface of the outer shell. A uniform flow is moving with a constant velocity in the external fluid medium. Classical thin shell theory is applied to the inner shell and first-order shear deformation theory is applied to the outer shell. A closed form for transmission loss is derived based on modal analysis. Investigations have been made for the impedance of both shells and the transmission loss through the shells from the exterior into the interior. Results are compared for double sandwich shells and single sandwich shells. This study shows that (1) the impedance of the inner shell is much smaller than that of the outer shell so that the transmission loss is almost the same in both the annular space and the interior cavity of the shells; (2) the two concentric sandwich shells can produce an appreciable increase of transmission loss over single sandwich shells especially in the high frequency range; and (3) design guidelines may be derived with respect to the noise reduction requirement and the pressure in the annular space at a mid-frequency range.

234.

V. Mukhopadhyay, **Structural Concepts Study of Non-Circular Fuselage Configurations**, *First AIAA/SAE World Aviation Congress and Exposition*, Los Angeles, California, SAE/AIAA Report No. WAC-67, October 22-24, 1996, (582KB).

Format(s): Postscript, or PDF

Keywords: Computer aided interactive design; Conceptual flutter analysis; Blended wing body; Flutter instability; Torsional frequency; Regier number; MathCad; Wing flutter

Abstract: A Preliminary study of structural concepts for non-circular fuselage configurations is presented. For an unconventional flying-wing type aircraft, in which the fuselage is inside the wing, multiple fuselage bays with non-circular sections need to be considered. In a conventional

circular fuselage section, internal pressure is carried efficiently by a thin skin via hoop tension. If the section is non-circular, internal pressure loads also induce large bending stresses. The structure must also withstand additional bending and compression loads from aerodynamic and gravitational forces. Flat and vaulted shell structural configurations for such an unconventional, non-circular pressurized fuselage of a large flying-wing were studied. A deep honeycomb sandwich-shell and a ribbed double-wall shell construction were considered. Combinations of these structural concepts were analyzed using both analytical and simple finite element models of isolated sections for a comparative conceptual study. Weight, stress, and deflection results were compared to identify a suitable configuration for detailed analyses. The flat sandwich-shell concept was found preferable to the vaulted shell concept due to its superior buckling stiffness. Vaulted double-skin ribbed shell configurations were found to be superior due to their weight savings, load diffusion, and fail-safe features. The vaulted double-skin ribbed shell structure concept was also analyzed for an integrated wing-fuselage finite element model. Additional problem areas such as wing-fuselage junction and pressure-bearing spar were identified.

This file was generated by trsbib v1.2 on 22.10.98.
Langley Technical Report Server

[Sign in](#)



[Web](#) [Images](#) [Groups](#) [News](#) [Froogle](#) [Local](#)^{New!} [more »](#)

+"~simulation ~domain" +"~simulation ~task" +

[Search](#)

[Advanced Search](#)
[Preferences](#)

Web Results 1 - 10 of about 46 for +"~simulation ~domain" +"~simulation ~task" +~aspect +~matching. (0

[PDF] [Learning by Observation in a Tactical Air Combat Domain](#)

File Format: PDF/Adobe Acrobat - [View as HTML](#)

aspects of behavioral cloning is its effectiveness in a complex domain. ...
simulation domain similar to the domains used in behavioral cloning and ...

ai.eecs.umich.edu/people/laird/papers/ML99-2.pdf - [Similar pages](#)

[PDF] [XUEQIN HUANG XML-Based Messaging in the JSIM Simulation ...](#)

File Format: PDF/Adobe Acrobat - [View as HTML](#)

the reuse and interoperability problems in the **simulation domain**. ... more challenging
simulation task, such as the design of a spacecraft, would require ...

chief.cs.uga.edu/~jam/home/theses/huang_thesis/writeup/xhuangms.pdf - [Similar pages](#)

[DOC] [ACKNOWLEDGEMENTS](#)

File Format: Microsoft Word 2000 - [View as HTML](#)

A far more challenging **simulation task**, such as the design of a spacecraft, would
require even ... <xsl:template **match**="/message/agentInfo/replicationSize"> ...

chief.cs.uga.edu/~jam/home/theses/huang_thesis/writeup/xhuangms.doc - [Similar pages](#)

[Paper: Learning by Observation in a Tactical Air Combat Domain ...](#)

OBSERVER learns many **aspects** of performance knowledge, ... At the top level of
the hierarchy, the operator with **matching** selection conditions is selected. ...

computing.breainestorm.net/ knowledge+performance+task+author+acquisition/ - 55k - [Cached](#) - [Similar pages](#)

[PDF] [Cluster Simulation in Time-Triggered Real-Time Systems](#)

File Format: PDF/Adobe Acrobat - [View as HTML](#)

simulation task states and annihilating of already sent messages. ... to the
simulation domain, by simulation distribution and by the simulation type. Ad- ...

www.decomsys.com/publications/tg_Dissertation.pdf - [Similar pages](#)

[PS] [To appear in Computer Generated Forces and Behavioral ...](#)

File Format: Adobe PostScript - [View as Text](#)

o owncomputation of "target **aspect**" from its ownsubstantial overhead. ...
as describedpilot for the air-combat **simulation domain** is provided in Section 3.2. ...

teamcore.usc.edu/papers/95/agents/PRfinal.ps - [Similar pages](#)

[PDF] [www.csafe.utah.edu/documents/FY99AnnualReport.pdf](#)

File Format: PDF/Adobe Acrobat - [View as HTML](#)

Supplemental Result - [Similar pages](#)

[PDF] [Enabling interactive and collaborative oil reservoir simulations ...](#)

File Format: PDF/Adobe Acrobat - [View as HTML](#)

These models are coupled across interfaces by a set of **matching** or ... To construct
the set of Grid elements constituting the **simulation domain**, ...

www.caip.rutgers.edu/TASSL/Papers/discover-ipars-ccpe-si-05.pdf - [Similar pages](#)

[PDF] [Enabling interactive and collaborative oil reservoir simulations ...](#)

File Format: PDF/Adobe Acrobat

may co-exist for one reservoir **simulation task** [9]. ... and track the **simulation domain**. Furthermore, it provides interactive steering capabilities that ...
dx.doi.org/10.1002/cpe.899 - [Similar pages](#)

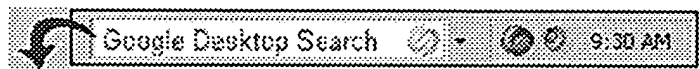
LABORATOIRE DE MECANIQUE DES FLUIDES - UMR CNRS 2698

Since spatial resolution and **simulation domain** extent are two antagonist factors in the ... Here follow some elements proposed to the **Simulation Task Group**. ...
www.ec-nantes.fr/Fr/Recherche/DEE/Dah/urbcap.htm - 141k - [Cached](#) - [Similar pages](#)

Try your search again on [Google Book Search](#)

Google

Result Page: 1 2 [Next](#)



Free! Instantly find your email, files, media and web history. [Download now.](#)

[Search within results](#) | [Language Tools](#) | [Search Tips](#) | [Dissatisfied? Help us improve](#)

[Google Home](#) - [Advertising Programs](#) - [Business Solutions](#) - [About Google](#)

©2005 Google

le Format: Adobe PostScript - [View as HTML](#)

problem spaces and a local portion that is local combat **simulation task**. ...
owncomputation of "target **aspect**" from its ownsubstantial overhead. ...

www.isi.edu/soar/papers/cgf/94/Event/PRfinal.ps - [Similar pages](#)

[PDF](#) [Enabling interactive and collaborative oil reservoir simulations ...](#)

File Format: PDF/Adobe Acrobat - [View as HTML](#)

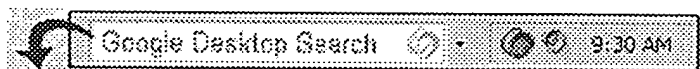
may co-exist for one reservoir **simulation task** [9]. ... To construct the set of
Grid elements constituting the **simulation domain**, we used a rectangular Grid ...

www.caip.rutgers.edu/TASSL/Papers/discover-ipars-ccpe-si-05.pdf - [Similar pages](#)

Try your search again on [Google Book Search](#)

Google

Result Page: 1 2 3 4 [Next](#)



Free! Instantly find your email, files, media and web history. [Download now.](#)

[Search within results](#) | [Language Tools](#) | [Search Tips](#) | [Dissatisfied? Help us improve](#)

[Google Home](#) - [Advertising Programs](#) - [Business Solutions](#) - [About Google](#)

©2005 Google



USPTO

[Subscribe \(Full Service\)](#) [Register \(Limited Service, Free\)](#) [Login](#)

Search: ☒ The ACM Digital Library ☐ The Guide

+"~simulation ~domain" +"~simulation ~task" +~aspect

THE ACM DIGITAL LIBRARY



[Feedback](#) [Report a problem](#) [Satisfaction survey](#)

Terms used ~simulation ~domain ~simulation ~task ~aspect

Found 2 of 167,655

Sort results by

relevance



[Save results to a Binder](#)

Try an [Advanced Search](#)

Try this search in [The ACM Guide](#)

Display results

expanded form



[Search Tips](#)

☐ Open results in a new window

Results 1 - 2 of 2

Relevance scale ☐ ☐ ☐ ☐ ☐

1 [Traffic simulation based on the high level architecture](#)

Ulrich Kelin, Thomas Schulze, Steffen Straßburger

December 1998 **Proceedings of the 30th conference on Winter simulation**

Publisher: IEEE Computer Society Press

Full text available: [pdf\(487.63 KB\)](#) Additional Information: [full citation](#), [references](#), [citations](#), [index terms](#)



2 [Parallel logic simulation of VLSI systems](#)

Mary L. Bailey, Jack V. Briner, Roger D. Chamberlain

September 1994 **ACM Computing Surveys (CSUR)**, Volume 26 Issue 3

Publisher: ACM Press

Full text available: [pdf\(3.74 MB\)](#) Additional Information: [full citation](#), [abstract](#), [references](#), [citations](#), [index terms](#)



Fast, efficient logic simulators are an essential tool in modern VLSI system design. Logic simulation is used extensively for design verification prior to fabrication, and as VLSI systems grow in size, the execution time required by simulation is becoming more and more significant. Faster logic simulators will have an appreciable economic impact, speeding time to market while ensuring more thorough system design testing. One approach to this problem is to utilize parallel processing, taking ...

Keywords: circuit structure, parallel architecture, parallelism, partitioning, synchronization algorithm, timing granularity

Results 1 - 2 of 2

The ACM Portal is published by the Association for Computing Machinery. Copyright © 2005 ACM, Inc.

[Terms of Usage](#) [Privacy Policy](#) [Code of Ethics](#) [Contact Us](#)

Useful downloads: [Adobe Acrobat](#) [QuickTime](#) [Windows Media Player](#) [Real Player](#)

12/12/05